Distribution Agreement

In presenting this dissertation as a partial fulfillment of the requirements for an advanced degree from Emory University, I hereby grant to Emory University and its agents the non-exclusive license to archive, make accessible, and display my dissertation in whole or in part in all forms of media, now or hereafter known, including display on the world wide web. I understand that I may select some access restrictions as part of the online submission of this dissertation. I retain all ownership rights to the copyright of the dissertation. I also retain the right to use in future works (such as articles or books) all or part of this dissertation.

_____   _____
Joseph Lichter   Date

A Type-II Thymidine Kinase from *Thermotoga maritima*:

Kinetic Characterization, Substrate Binding, and Oligomerization

By

Joseph Lichter
Doctor of Philosophy

Chemistry

_____
Dr. Stefan Lutz
Advisor

_____
Dr. Dale Edmondson
Committee Member

_____
Dr. David Lynn
Committee Member

Accepted:

_____
Lisa A. Tedesco, Ph.D.
Dean of the Graduate School

_____
Date

A Type-II Thymidine Kinase from *Thermotoga maritima*:

Kinetic Characterization, Substrate Binding, and Oligomerization

By

Joseph Lichter

B.S., Florida State University, 2003

Advisor: Stefan Lutz, Ph.D.

An abstract of

A dissertation submitted to the

Faculty of the Graduate School of Emory University

in partial fulfillment of the requirements for the degree of

Doctor of Philosophy

in Chemistry

2009

Abstract

A Type-II Thymidine Kinase from *Thermotoga maritima*:

Kinetic Characterization, Substrate Binding, and Oligomerization

By: Joseph Lichter

Thymidine kinases (TKs) catalyze the phosphorylation of thymidine to form thymidylate. TKs also activate nucleoside analog (NA) pro-drugs used in anti-cancer and anti-viral therapies. In this dissertation, the characterization of a novel TK from the hyperthermophilic eubacterium *Thermotoga maritima* is described, with focus on the kinetics, substrate binding, and protein oligomerization.

Due to amino acid sequence, structure and substrate specificity, TmTK is characterized as a type-II TK. Catalysis at 37 °C is suboptimal compared to the activity at 82 °C yet the kinetic parameters change at the elevated temperature, demonstrating a greater specificity for thymidine (as compared to AZT) and positive cooperativity with ATP. Analysis of activation of other NAs at 37 °C, suggests the possibility for a common structural intermediate in the reaction pathway, potentially as a result of protein conformational changes. Fluorescence experiments further suggest temperature dependent conformational changes in TmTK.

A systematic study of substrate binding on protein conformation identifies a thymidine dependent formation of the C-terminal lasso region, while ATP binding changes both the tertiary and quaternary structure. Single tryptophan mutants engineered in the $\beta c1/\beta 3$ region of the protein confirm ATP-dependent conformational changes.

Engineering of disulfide bridges between the two α1 helices at the presumed dimer II interface disabled ATP binding and catalytic competency. From the substrate binding experiments, a two-state model is proposed whereby an expansion along the dimer II interface will turn a closed/inactive protein into an open/active state.

The crux of the two-state model is the presumption that TmTK exists as a tetramer in solution. Inconsistencies between predicted tetramer molecular weight (MW) and size exclusion chromatography (SEC) estimated MW led to an investigation of the oligomeric state. Mutagenesis studies suggest the dimer I ("strong") interface is part of the solution state structure. Crosslinking studies conducted on wild type and mutants were conducted and conclusions are drawn for potential monomer-dimer and monomer-dimer-tetramer equilibriums.

A Type-II Thymidine Kinase from *Thermotoga maritima*:

Kinetic Characterization, Substrate Binding, and Oligomerization

By

Joseph Lichter

B.S., Florida State University, 2003

Advisor: Stefan Lutz, Ph.D.

A dissertation submitted to the

Faculty of the Graduate School of Emory University

in partial fulfillment of the requirements for the degree of

Doctor of Philosophy

in Chemistry

2009

Acknowledgements

I would like to first acknowledge my advisor Dr. Stefan Lutz, for giving me the opportunity to work in his lab and assisting in my growth as a scientist. For his guidance in terms of experimental design, critical thinking, and scientific maturation as well as his support for my interests in university teaching, I am extremely appreciative.

Secondly, I extend my gratitude to my committee members Dr. Dale Edmondson and Dr. David Lynn for providing insightful and critical suggestions for my project, and for also supporting my interests in teaching and research.

I owe a lot of thanks to the many scientists with whom I had the pleasure to collaborate. Many thanks to Dr. Dario Segura-Pena and Dr. Arnon Lavie for their contributions of crystal structures of TmTK, and the many great emails and discussions about the project. To the past and present members of the Lutz lab, I am grateful for the time I spent working with them. A very special thanks goes to Lingfeng "Kitty" Liu not only for her assistance with fluorescence experiments but for being a great officemate and source of good scientific conversation. Thanks also goes to Dr. Manuela Trani for work done with the tryptophan fluorescence and Dr. Ziad Eletr, for his effort in the oligomerization studies.

Finally, I want to thank my friends and family. To the many friends in Atlanta and around the globe, whom I met and shared a laugh or a tear with, I am grateful for the time we spent. To my girlfriend Debbie, thank you for being my rock of love. Your caring and understanding has helped me get through many tough days. And last but not least my parents, thank you for your endless support and for always being there to listen and provide unconditional love. No words can describe the appreciation I have for you both.

Table of Contents

List of Figures

List of Tables

Chapter 1: Introduction

1.1 Deoxyribonucleic acid (DNA)

DNA is the biomolecule containing instructions for cellular function and development. It's also the "transforming principle" responsible for transferring genetic information from generation to generation (Avery 1944). The double helical structure of DNA consists of two complementary nucleic acid strands built up of 2'-deoxyribonucleotides (dNs) linked through phosphodiester bonds along a sugar backbone (Watson and Crick 1953). Each sequence of 3 dNs is transcribed through a genetic code to form amino acids, the building blocks of proteins. The three structural components of dNs are the 2'-deoxyribose, phosphate groups, and the nucleobase (figure 1-1). The 2'-deoxyribose contains a C-5' and a C-3' hydroxyl group on the ribose portion. While present in a DNA strand, dNs are linked by phosphodiester bonds attaching the 3'-OH of one dN to the 5'-OH of its neighboring dN. As a precursor molecule to DNA, dNs can either have one (α), two (β), or three (γ) phosphates on the 5'-hydroxyl (without a phosphate the molecule is called a 2'-deoxyribonucleo*side*). The nucleobase is attached at C-1' and can either be a purine (adenine or guanine) or a pyrimidine (cytosine, thymine, uracil). In DNA replication, DNA polymerase catalyzes the addition of a deoxyribonucleotide triphosphate (dNTP) to an existing strand of DNA creating the dN linkage and releasing inorganic pyrophosphate. The success and fidelity of DNA replication and DNA repair is therefore regulated by the cellular availability of dNTPs.
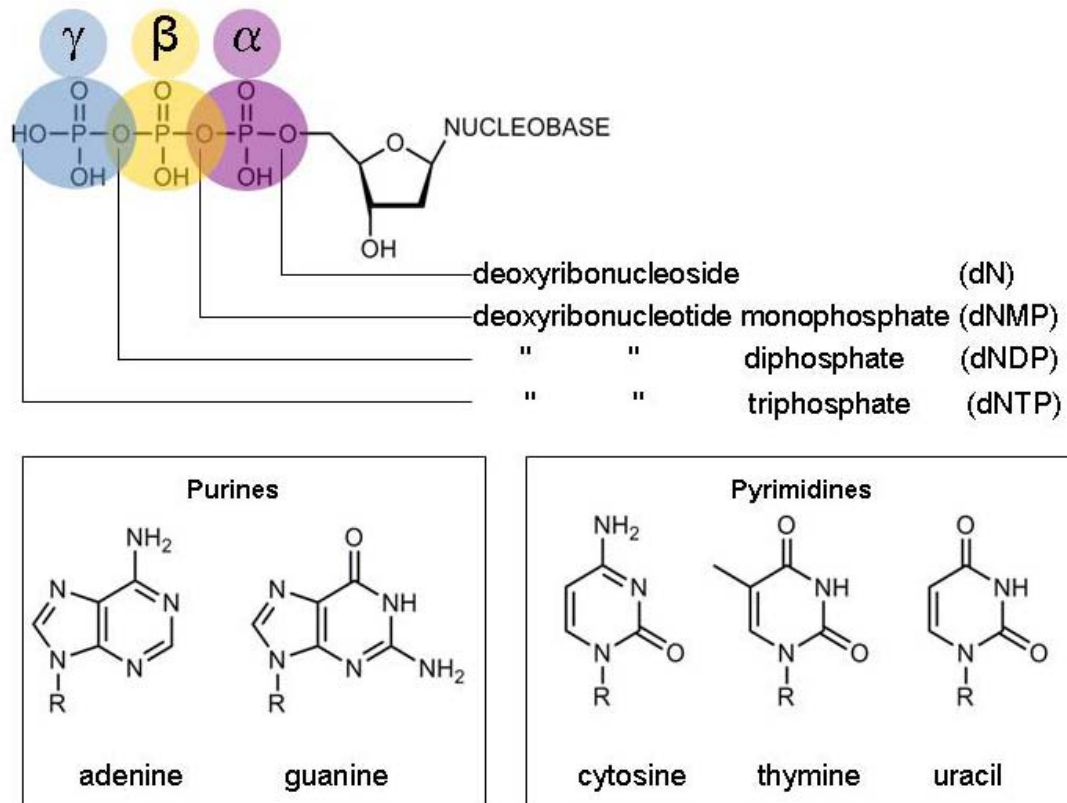
Figure 1-1: Structure of deoxyribonucleo(s/t)ides. Top: 2'-deoxyribose and phosphate groups. Bottom: Nucleobases (The R is the attachment point at the C-1' of the 2'-deoxyribose).

1.2 Biosynthesis of deoxyribonucleotide triphosphates

For most organisms (excluding fungi and some bacteria), there exist two

pathways for the synthesis of dNTPs: the *de novo* and salvage pathways (figure 1-2).

1.2.3 *De novo* pathway

As the name implies the *de novo* pathway is the process of building up

nucleotides "from scratch," using ribose-5-phosphate, some amino acids, ATP, CO_2, and

NH_3 as initial reactants. For purines, *de novo* biosynthesis begins with the formation of

5-phosphoribosyl-pyrophosphate (PRPP) from ribose-5-phosphate and ATP, followed

by a series of condensation reactions and ring closures to form the purine nucleobase at

the C-1' position of the ribose [for a full review of each reaction involved refer to

(Kornberg 1980)]. For pyrimidines, the nucleobase is first assembled and then attached

to ribose-5-phosphate. The product in both cases is the ribonucleotide monophosphate

(rNMP). The fate of the rNMP is either two subsequent phosphorylations to make the

ribonucleoside triphosphate (rNTP) or a reduction of the ribonucleotide diphosphate

(rNDP) to form the 2'-deoxyribonucleotide diphosphate (dNDP). Once the dNDP is

formed, phosphorylation via nucleoside diphosphate kinase (NDPK) is necessary to

prepare the dNTP.

1.2.3 Salvage pathway

The salvage pathway complements the *de novo* synthesis, by recycling free

nucleobases, ribonucleosides (rNs) and 2'-deoxyribonucleosides (dNs) and

reincorporating them back into dNTP biosynthesis either as rNMPs or dNMPs. These

available nucleobases and nucleosides are products of DNA, RNA, or food degradation,

either inside the cell or transported from outside the cell through nucleoside transporters

(Plagemann, Wohlhueter et al. 1988; Cass, Young et al. 1999). Nucleobases can be

reincorporated into rNs via phosphoribosyl transferases (PRT) or can be reincorporated

into a rN or dN by nucleoside phosphorylases (Kornberg 1980). Nucleoside kinases

(NK) and deoxynucleoside kinases (dNK) catalyze the phosphorylation of rNs and dNs,

respectively. By introducing a negatively charged phosphate to the nucleoside, the NKs

or dNKs essentially trap the resultant rNMP or dNMP inside the cell, preparing the precursor for synthesis of rNTPs or dNTPs. This step is thus often considered the commitment step in the salvage pathway Upon formation of the NMP or dNMP further phosphorylation is carried out by the nucleoside monophosphate kinases (NMPK) and non specific nucleoside diphosphate kinase (NDPK) used in formation of both rNTPs and dNTPs.
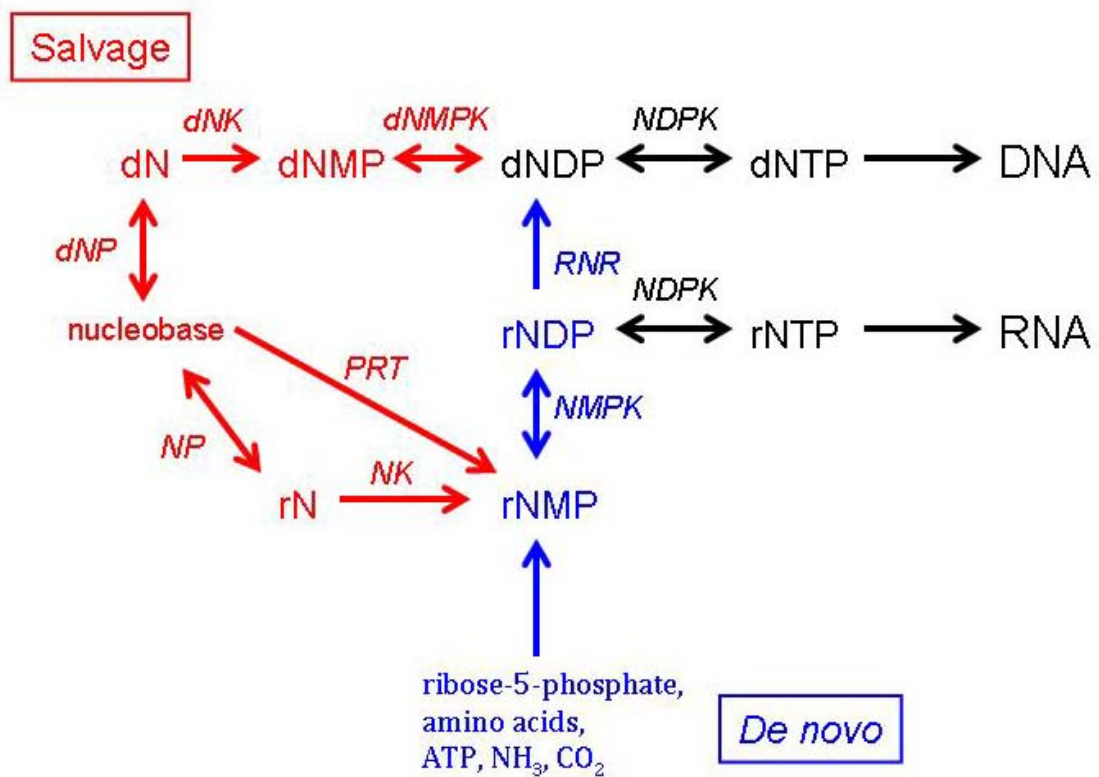
Figure 1-2: Simplified overview of the two biosynthetic pathways for nucleotide synthesis.

1.2.3 Regulation of dNTP levels and disease associated with dNTP imbalance

In maintaining a balanced dNTP pool, nucleotide biosynthesis pathways are primarily regulated by feedback inhibition. In purine *de novo* biosynthesis, the phosphorylated products AMP, ADP, and ATP inhibit amidophosphoribosyl transferase, which catalyzes the first step in purine nucleobase arrangement on the PRPP (Roth and Deuel 1974). Ribonucleotide reductase (RNR) is regulated through dNTP feedback inhibition and cell cycle regulation (Eriksson, Uhlin et al. 1997; Chabes and Thelander 2000). The salvage pathway is regulated similarly with many of the dNKs inhibited by dNTPs including both isoforms of thymidine kinase inhibited by TTP (Lee and Cheng 1976) and deoxycytidine kinase competitively inhibited by dCTP and dUTP (Cheng, Domin et al. 1977).

In the case of imbalanced dNTP pools, disease occurs. Irregularities in dNTP pools in the mitochondria have been linked to mitochondrial neurogastrointestinal encephalomyopathy (MNGIE) and mitochondrial DNA-depletion syndromes (MDS). MNGIE is an eye disease whose main symptoms include ptosis (drooping eyelids), ophthalmoplegia (weakness of eye muscles), cachexia (loss of weight), and severe gastrointestinal dysmotility (Lara, Valentino et al. 2007). The cause for MNGIE are mutations in the gene for thymidine phosphorylase disabling its activity (or depleting its expression) and leading to an increase in thymidine (T) and deoxyruridine (dU) in the mitochondria (Nishino, Spinazzola et al. 1999). The increase in circulating T and dU affects mitochondrial nucleotide pools and depletes available ATP, thus causing malfunctions in cellular processes, leading to the disease (Pontarin, Ferraro et al. 2006).

MDS are a class of mitochondrial diseases linked to gene defects in the *de novo* pathway (RNR), and the salvage pathway dNKs (human thymidine kinase 2, and human deoxyguanosine kinase) [full review on MDS syndromes found here (Spinazzola, Invernizzi et al. 2008)]. Risk of kidney disease and abnormalities in the immune system have been reported for thymidine kinase deficient mice, suggesting a crucial physiological need for this salvage pathway enzyme in higher organisms (Dobrovolsky, Bucci et al. 2003). The following section will highlight more about dNKs.

1.2   Deoxynucleoside kinase (dNK)

The first step in the salvage pathway of dNTP synthesis is catalyzed by dNKs. This bisubstrate reaction transfers a phosphate group from an rNTP to a dN to form the dNMP and rNDP. Each organism has different sets of dNKs with unique substrate specificities. Humans have four dNKs: a deoxycytidine kinase (hdCK), a deoxyguanosine kinase (hdGK), and 2 thymidine kinases: the cytosolic thymidine kinase 1 (hTK1) and mitochondrial thymidine kinase 2 (hTK2). The substrate specificities for the four dNKs overlap, providing a cell's capability of salvaging all four 2'-deoxyribonucleosides (figure 1-3). The cytosolic hdCK can phosphorylate deoxycytidine (dC), deoxyadenosine (dA) and deoxyguanosine (dG), albeit with different efficiencies (Cheng, Domin et al. 1977). Located in the mitochondria, hdGK phosphorylates dG with the highest efficiency, yet also has activity for the other purine dA and minimal activity for dC (Wang, Choudhury et al. 1999). Phosphorylation of thymidine (T) is catalyzed by either of the two thymidine kinases, with hTK1 being specific for activating T and 2'-deoxyuridine (dU) (Eriksson, Kierdaszuk et al. 1991),

while hTK2 can phosphorylate all the pyrimidines (T, dU, and dC) (Wang, Munch-

Petersen et al. 1999).
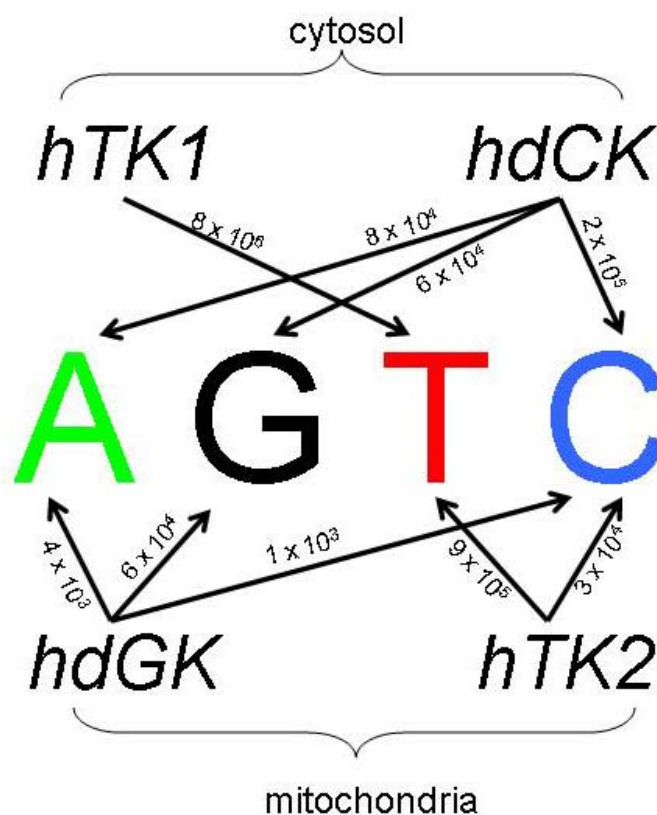
Figure 1-3: Overlapping catalytic specificities for human dNKs. k_{cat}/K_M values (in $M^{-1}s^{-1}$) are reported along the arrows. If no arrow exists between deoxyribonucleoside and dNK pair, the catalytic specificity is lower than 10^2 $M^{-1}s^{-1}$.

While there are four types of dNKs for humans, there exists different sets of

dNKs for other organisms. Some organisms, such as the fruitfly *Drosophila*

melanogaster and the silk worm *Bombyx mori* contain one dNK which can phosphorylate

all four of the natural 2'-deoxynucleosides (Munch-Petersen, Piskur et al. 1998; Knecht,

Petersen et al. 2002). Other organisms such as the bacterium *E. coli* and the roundworm *C. elegans* utilize a TK as the organism's sole dNK (Karlstrom 1970; Skovgaard and Munch-Petersen 2006). The yeast *Saccharomyces cerevisiae* completely lacks the salvage dNKs and relies completely on the *de novo* pathway (Vernis, Piskur et al. 2003). In contrast, some organisms like the bacteria *Lactobacillus acidophilus* lack the necessary *de novo* pathway enzyme RNR and therefore depend on the salvage pathway to maintain dNTP production (Ives and Ikeda 1998).

The scope of this research project is focused on thymidine kinase (TK), the specific dNK that salvages thymidine.

1.3   Thymidine Kinases (TK)

TKs catalyze the phosphorylation of thymidine and 2'-deoxyuridine to form TMP and dUMP, respectively. The enzyme was first discovered in rat tissue in 1958 (Bollum and Potter 1958), shortly thereafter isolated and characterized from *E. coli* (Okazaki and Kornberg 1964) and from humans (Lee and Cheng 1976), and found to be ubiquitous in nature. The following section discusses the two TKs present in humans (hTK1 and hTK2), TKs from other organisms, and the utility of TKs in medical and biotechnological applications.

1.3.1   Human thymidine kinase 1

The cytosolic human thymidine kinase 1 (hTK1) catalyzes the transfer of the γ-phosphate of an NTP donor to the 5'-OH of a thymidine acceptor. hTK1 has a strict preference for natural 2'-deoxyribonucleosides with a thymine or uracil nucleobase

(thymidine and deoxyuridine) as the phosphate acceptor, but little restriction on the NTP donor (even accepting dATP as a donor) (Lee and Cheng 1976). hTK1 uses a general base mechanism to catalyze the phosphorylation, whereby Glu98 abstracts a proton from the 5'-OH of the acceptor nucleoside, activating the oxygen for nucleophilic attack on the γ-phosphate of ATP (Welin, Kosinska et al. 2004). Unlike the other human dNKs, hTK1 is cell cycle regulated, with high expression levels during DNA replication in the G_1/S-phase and degradation during late mitosis (Bello 1974; Coppock and Pardee 1987). The molecular mechanism for degradation has been linked to the anaphase-promoting complex/cyclosome (APC/C) binding to a KEN motif at the C-terminus of hTK1 in early G1 phase, promoting ubiquitinylation and subsequent elimination (Ke and Chang 2004).

The gene for hTK1 is found on chromosome 17 (McDougall, Kucherlapati et al. 1973) and codes for a polypeptide with 234 amino acids and a monomeric molecular weight of 25.5 kDa (Bradshaw and Deininger 1984). There exists some dispute over the true native oligomeric state for hTK1. Early reports of hTK1 purified from human lymphocytes reported it to be a low activity dimer which is transformed to a highly active tetramer in the presence of ATP (Munch-Petersen, Tyrsted et al. 1993). Crystal structures and gel filtration experiments of recombinant hTK1 expressed and purified in *E. coli* have shown it to be a tetramer with or without the presence of ATP, with dimers only seen when hTK1 is truncated at the N-terminus (Welin, Kosinska et al. 2004; Birringer, Perozzo et al. 2006). More on the oligomeric state of hTK1 will be discussed in chapters 3 and 4.

The first two crystal structures for hTK1 were published nearly simultaneously, both presenting structures that differed from previously identified dNKs (Welin,

Kosinska et al. 2004; Birringer, Claus et al. 2005). The hTK1 monomer consists of a core N-terminal α/β domain and a C-terminal region containing a zinc binding domain and a lasso loop positioned on top of the nucleobase portion of the bound feedback inhibitor, dTTP (Fig. 1-4). Hydrogen bonding interactions between main chain atoms of the lasso loop and the O2 and N3 atoms on the nucleobase are the main factors involved in positioning the nucleobase. The specificity for dNs with thymine or uracil nucleobases was suggested to be a result of these main chain interactions and a tight binding pocket. Further analysis of substrate specificity towards the 2'-deoxyribose is a result of a tight interaction between the 2'-carbon and neighboring residues (Gly176). The mode of substrate binding by hTK1 is strikingly different to other dNKs, that utilize side chain interactions to stabilize and form hydrogen bonds.
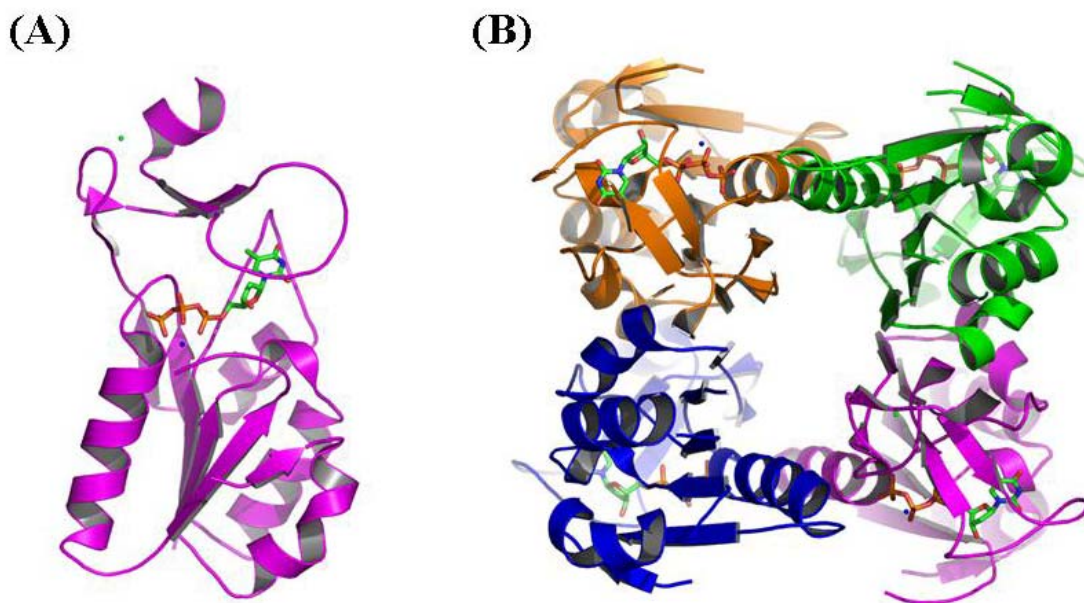
Figure 1-4: Structure of human thymidine kinase in complex with dTTP, Mg^{2+}, and Zn^{2+} (A) Monomer (B) Tetramer (pdb # 1xbt) (Welin, Kosinska et al. 2004)

1.3.2 Human thymidine kinase 2

The mitochondrial human thymidine kinase 2 (hTK2) catalyzes the same phosphoryl transfer as hTK1 but shows a broader substrate specificity, phosphorylating dC with slightly lowered efficiency than for thymidine (Lee and Cheng 1976). hTK2 is constitutively expressed in the mitochondria of non-proliferating cells, yet with lower expression levels than for hTK1 in proliferating cells. Experiments done with isotopic labeling of thymidine in cells has shown a dynamic exchange between the cytosol and mitochondria allowing for the two enzymes to provide the entire cell with a balanced level of TMP (Pontarin, Gallinaro et al. 2003) .

The gene for hTK2 is found on chromosome 16 locus q22 (Willecke, Teber et al. 1977) and encodes a 232 amino acid protein, with a significantly different sequence as to compared to hTK1. Due to difficulties in the solubility of hTK2, no crystal structures have been solved as of yet, however a homology model with DmdNK has been proposed due to their high sequence similarities (Gerth and Lutz 2007; Perez-Perez, Priego et al. 2008).

1.3.3 Other eukaryotic, bacterial, and viral TKs

Fig. 1-5 shows a phylogeny tree of a sample of eukaryotic, bacterial, and viral TKs (assembled based on sequence alignment created using ClustalW). Included in the tree are the aforementioned two human forms of TK. The other eukaryotic TKs shown in the tree include two thymidine kinases found in mice (MmTK1, MmTK2) and chicken (GgTK1, GgTK2), which are expressed in the cytosol and mitochondria respective to
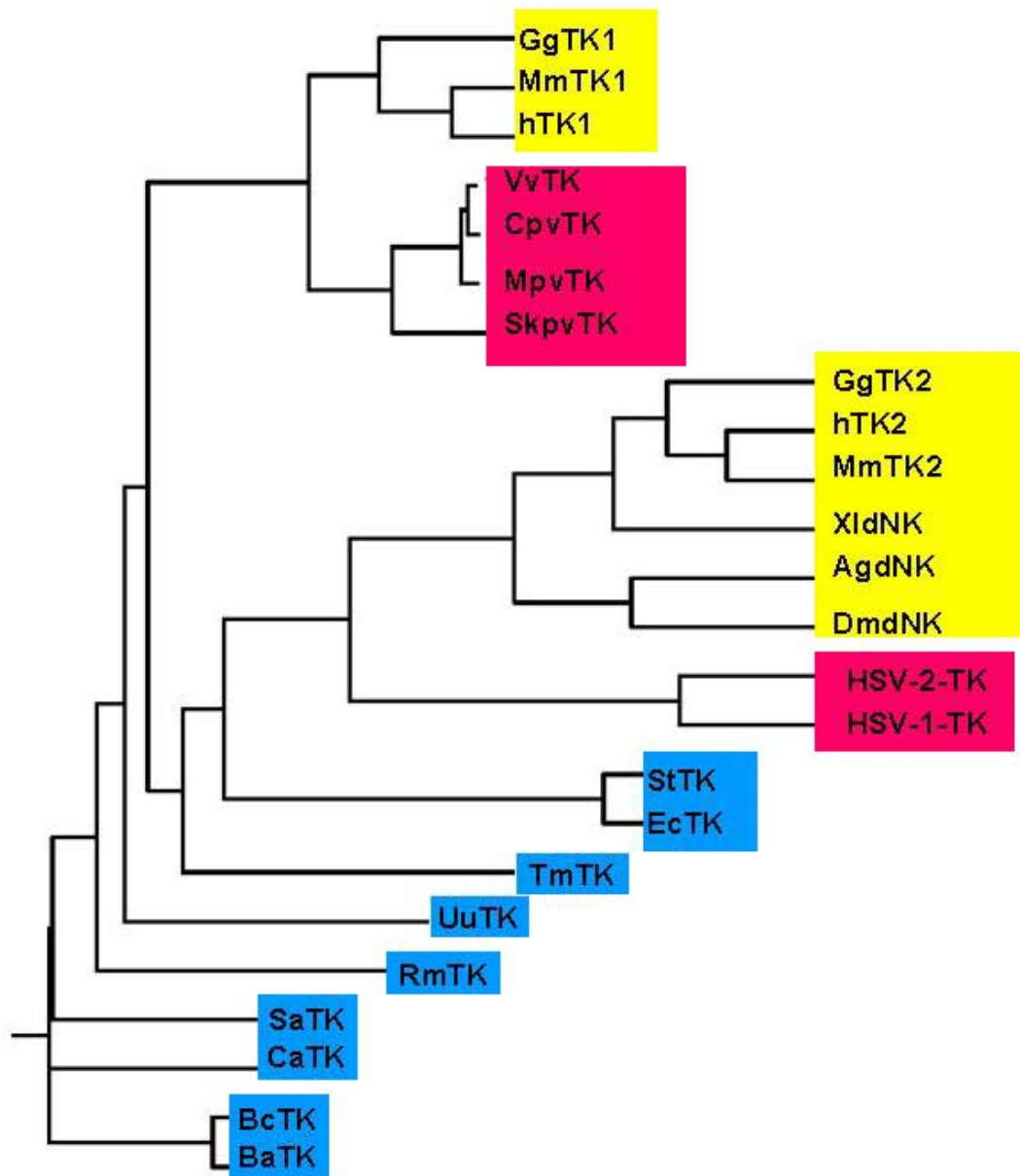
Figure 1-5: Phylogeny tree of TKs from various organisms (yellow – eukaryotes; blue – prokaryotes; pink – viral) Abbreviations: Gg, *Gal gallus*; Mm, *Mus musculus*; Vv, *Vaccinia* virus; Cpv, *Cowpox* virus; Mpv, *Monkeypox* virus, Skpv, *Skunkpox* virus; Xl, *Xenopus laevis*; Ag, *Anopheles gambiae*; Dm, *Drosophila melanogaster*; HSV, Herpes simplex virus; St, *Salmonella typhimurium*; Ec, *Escherichia coli*; Tm, *Thermotoga maritima*; Uu, *Ureaplasma urealiticum*; Rm, *Rhodothermus marinus*; Sa, *Staphylococcus aureus*; Ca, *Clostridium acetobutylicum*; Bc, *Bacillus cereus*; Ba, *Bacillus anthracis* . Tree designed using ClustalW (BioWorkbench 3.2)

their human TK homologs (McBreen, Orkwiszewski et al. 1977; Merrill, Harland et al. 1984). Aligned closely with the hTK2 are the eukaryotic multisubstrate dNKs from *Xenopus laevis, Anopheles gambiae,* and *Drosophila melanogaster* (Knecht, Petersen et al. 2002; Sandrini and Piskur 2005).

With regards to prokaryotes, one of the first extensively studied TKs was from *E. coli* (Okazaki and Kornberg 1964; Okazaki and Kornberg 1964). The only dNK present in *E. coli*, EcTK can phosphorylate thymidine, deoxyuridine and is feedback regulated by TTP. Its sequence is most closely similar to that of the TK from the pathogenic *Salmonella typhimurium*. Recent genome analyses has showed that many other gram-negative bacteria (including *Ureaplasma urealiticium*) contain a single dNK (Sandrini, Clausen et al. 2006). In the last 5 years there has been increase in the number of solved crystal structures for thymidine kinases, with many of them originating from bacteria sources such as the TKs from *Bacillus anthracis* and *Bacillus cereus* (Kosinska, Carnrot et al. 2007), and *Clostridium acetobutylicum* (Kuzin 2005).

Finally, viral genomes contain TK genes as well. The most extensively studied viral TK comes from the Herpes simplex virus (type 1). HSV-1-TK is unique in its ability to phosphorylate a broad range of substrates including the acyclic guanine analogs, acyclovir and ganciclovir (Keller, Fyfe et al. 1981). As well, HSV-1-TK is the only TK that is known to have dual activity for phosphorylating both thymidine and thymidylate (Chen and Prusoff 1978). Other viral TKs shown in the phylogeny tree include the vaccinia, cowpox, monkeypox, and skunkpox viruses.

1.3.4 Two types of TKs (type I and type II)

Early hypotheses based on amino acid sequence comparisons and substrate specificities, suggested that there might be two separately evolved classes of thymidine kinases (Black and Hruby 1990). Shown in Fig. 1-6 is the structure for HSV-1 TK in complex with ADP and TMP. Compared to the structure for hTK1 (Fig. 1-4), it is clear that there is little to no structural homology. HSV-1-TK belongs to the type-I family of TKs. Other members of the type-I family include hTK2, GgTK2, MmTK2, and DmdNK, Besides showing amino acid similarities within this sub-family, type-I TKs also tend to be homodimers, and have a broader substrate specificity. hTK2 can phosphorylate dC (Lee and Cheng 1976), and HSV-1-TK can phosphorylate acyclovir and ganciclovir, both acyclic guanosine derivatives (Keller, Fyfe et al. 1981).

Type-II TKs differ from the type-I in both amino acid sequence and structure. Substrate specificity for type-II TKs are relatively stringent for 2'-deoxyribonucleosides with thymine and uracil bases. Some modifications on C-3' of the sugar portion and the C-5 of the nucleobase tend to be tolerated (Eriksson, Munch-Petersen et al. 1991; Munch-Petersen, Cloos et al. 1991). Type-II TKs include the human thymidine kinase 1, *Ureaplasma urealyticum* TK (Welin, Kosinska et al. 2004), *Bacillus anthracis* and *Bacillus cereus* TKs (Kosinska, Carnrot et al. 2007), and *Clostridium acetobutylicum* TK (Kuzin 2004). Type-II TKs have also generally been isolated as homotetramers (Black and Hruby 1990; Welin, Kosinska et al. 2004)
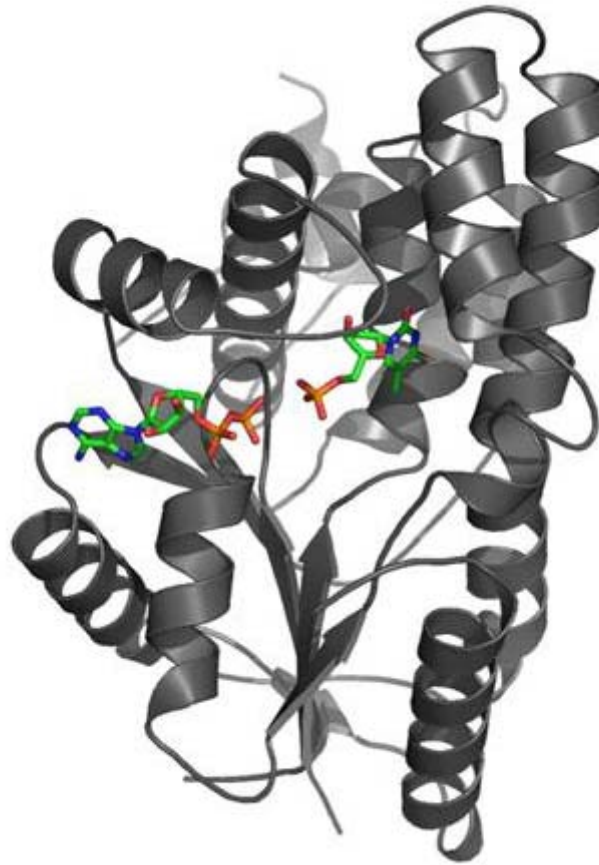
Figure 1-6: HSV-1-TK monomer in complex with ADP and TMP. Note the structural difference with the structure for hTK1 in Fig 1-4. HSV-1-TK belongs to a different subfamily of TKs (type-I) exhibiting different structure, catalytic properties, and amino acid sequence.

1.4 Medical significance and applications

Due to the significant role in dNTP synthesis, TKs have been targets for medical and therapeutic applications. Three specific applications include the use as an enzymatic marker for cancer, an activator for nucleoside analog pro-drugs, and the use in suicide gene therapy.

1.4.1 Cancer marker

Cancer is a class of diseases associated with uncontrolled cell proliferation. In detecting cancerous cells, TKs have been indirectly used as a marker due to high expression levels of hTK1 in proliferating cells. In the 1960s, Johnson and colleagues described the use of [^{3}H]-thymidine supplemented in growth medium whereby tumour cells can incorporate the radiolabeled nucleotide and be visualized using autoradiography and/or scintillation (Johnson, Haymaker et al. 1960). Another indirect use of TKs is positron emission tomography (PET). PET is a nuclear imaging technique which uses a radioisotope tracer molecule introduced into the body to image a particular organ (Ter-Pogossian, Phelps et al. 1975). Once the tracer molecule decays, the emission of a positron can collide with an electron and form photons measurable by a detector. This technique is used to image cells for oncological, neurological, and cardiological purposes. Due to the presence of high levels of hTK1 in proliferative cells, the radionuclide 3'-deoxy-3'-[^{18}F]fluorothymidine is currently used for investigating active tumors (Barthel, Cleij et al. 2003).

1.4.2 Nucleoside analog pro-drug activation

Modified nucleosides which disrupt DNA replication and are used in anti-cancer and anti-viral therapies are called nucleoside analog (NA) pro-drugs. NA pro-drugs utilize a variety of structural modifications to inhibit DNA polymerases or disrupt newly formed DNA strands. Nucleoside analogs lacking a 3'-OH group incorporated into a DNA strand will act to terminate chain elongation (Ichikawa and Kato 2001). Some nucleoside analogs contain modifications to the nucleobase that can interfere with

polymerase incorporation or with stability of a newly formed DNA strand. The ultimate desired affect is interference with DNA replication, either viral replication and/or uncontrolled cellular growth as in cancerous tumors (Galmarini, Jordheim et al. 2003).

Due to the negative charge of the active triphosphate form of NA drugs, the active drug can not be given directly. NAs are therefore administered as the inactive nucleoside pro-drug form. For nucleoside analogs containing a thymine or uracil base, activation is catalyzed by TKs. A set of nucleoside analogs activated by TKs are shown in Fig. 1-6. Floxuridine is an anticancer agent first approved by the FDA in 1970 and currently used in chemotherapy towards colorectal cancer (Gill, Thomas et al. 2003). The activation of the pro-drug to its monophosphate is catalyzed by both hTK1 and hTK2, though the overall efficiency is greater for hTK1 (Munch-Petersen, Cloos et al. 1991). Brivudin is an anti-herpetic agent which acts as a chain terminator, functioning to inhibit viral replication. Brivudin is activated by both human thymidine kinases with equal efficiency (Munch-Petersen, Cloos et al. 1991). AZT and D4T are two thymidine analogs used in HIV therapies (Mitsuya, Weinhold et al. 1985; Lin, Schinazi et al. 1987). Both drugs function similarly to brivudin, as chain terminators in viral DNA replication. The deoxyguanosine analog, ganciclovir (GCV) is a highly specific herpes drug, which takes advantage of the broader specificity of the HSV-1-TK, targeting cells that have been infected with the virus (Keller, Fyfe et al. 1981). Upon two subsequent phosphorylations, GCV-TP can act as a chain terminator (similarly to other anti-viral drugs).
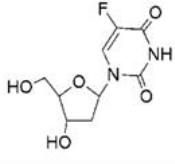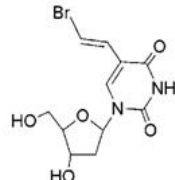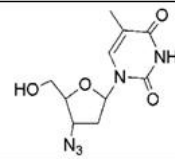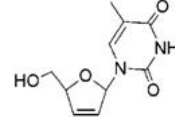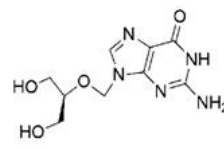
Chemical Structure	Chemical name (common names)	Disease/ Therapy	Activating enzyme
	5-fluoro-2'-deoxyuridine (Floxuridine, FUDR)	Colorectal cancer	hTK1 > hTK2
	5-(2-bromovinyl)-2'-deoxyuridine, (Brivudin, BvdU)	Herpes virus	hTK1 ≈ hTK2
	3'-azido-thymidine (Retrovir™, Zidovudine, AZT)	HIV	hTK1 > hTK2
	2',3'-didehydro-2',3'-dideoxythymidine (Stavir™, Stavudine, D4T)	HIV	hTK1
	2-amino-9-{[(1,3-dihydroxypropan-2-yl)oxy]methyl}-6,9-dihydro-3H-purin-6-one (Cytovene™, Ganciclovir, GCV)	Herpes	HSVTK

Figure 1-7: FDA approved NA drugs activated by TKs

1.4.3 Suicide gene therapy

Suicide gene therapy is a two step approach to cancer therapy where a gene for a highly active drug-activating enzyme is expressed in a tumor cell which is subsequently fed with the corresponding pro-drug. Upon pro-drug administration, only transfected cells with the gene of interest can activate the drug and the pharmacological effect is achieved. The first potential suicide gene therapy system identified combines the gene for the HSV-

1-TK with the pro-drug GCV. Experiments have proven that even though GCV-TP has a higher affinity for HSV-1 DNA polymerase, enough GCV-TP is formed in HSV-1-TK/GCV gene therapy to inhibit mammalian DNA polymerases (Moolten and Wells 1990). While not FDA approved yet, this system has been studied extensively over the last 15 years at the *in-vitro* and *in vivo* levels including phase I and II clinical trials [a review can be found here (Fillat, Carrio et al. 2003)].

1.7 Many mesophilic TKs, Few thermophilic TKs

As mentioned earlier TKs are ubiquitous, existing in virtually all organisms spanning the prokaryotic and eukaryotic kingdoms and viral genomes. Yet, the majority of the TKs studied, originate from mesophilic organisms (living at 15 - 40 ºC). Very little research has been conducted on TKs from extremophiles. At the onset of this research project, only one thymidine kinase from a thermophilic (40 – 80 ºC) organism had been reported. The TK from *Rhodothermus marinus* was cloned, expressed, and tested for thymidine kinase activity. RmTK showed optimal catalytic activity at 65 °C, and measured to be a tetramer by size exclusion chromatography (SEC) (Blöndal, Thorbjarnardóttir et al. 1999). No other nucleoside substrates were tested, nor were any structural investigation done to compare with its mesophilic homologs. To date, no psychrophilic TKs (living at < 15ºC) have been investigated, and up until this research, no hyperthermophilic (living at >80 ºC) TK had been studied

Why are we interested in studying extremophile TKs? Firstly, the investigation of an as of yet uncharacterized TK might open the possibilities for identifying new catalytic properties, for both substrate specificity and overall catalytic efficiency.

Secondly, extremophiles live in harsh conditions and therefore their survival is contingent upon the ability to catalyze essential biochemical reactions in such an environment. For thermophiles, this means catalyzing reactions at high temperatures. As a result, some thermophilic proteins have been used in industrial and biotechnological applications. Probably the best known example is the use of the DNA polymerase from the thermophilic *Thermus aquaticus* (Taq DNA polymerase) in polymerase chain reaction (PCR). Due to *T. aquaticus* growth at 70 °C, its DNA polymerase can withstand temperatures as high as 95 °C without denaturing, and therefore has been used in the cyclic process of DNA amplification (Saiki, Gelfand et al. 1988). An example of a hyperthermophilic protein with an industrial application is the L-aminoacylase from *Thermococcus litoralis* reported to be used in microfluidic bioreactors for the efficient large scale conversion of *N*-benzoyl-L-phenylalanine to L-phenylalanine (Hickey, Marle et al. 2007). A list of thermophilic enzymes and their applications (or potential) are described in table 1-1

Table 1-1: Industrial applications for particular enzymes derived from thermophiles

Enzyme	Applications	Reference
DNA polymerase	Polymerase chain reaction polymerase	(Zhou, Zhang et al. 1991; Liang, Jensen et al. 2004)
xylanase	Bleaching of pulp (papermaking), Biodiesel	(Samain, Debeire et al. 1997; Yang, Yan et al. 2006)
lipase	Production of detergent, oils and fats, paper industry	(Palomo, Segura et al. 2004)
glucosidase	conversion of dextrin to glucoses	(Giuliano, Schiraldi et al. 2004)
galactosidase	removal of raffinose from sugar beet syrup	(Ganter 1988)
amylomaltase	production of starch gels for food applications	(Kaper, Talik et al. 2005)

Following in this rationale, characterizing a thermophilic or hyperthermophilic TK might provide for potential utility in biotechnological or medical applications. For biotechnological purposes, perhaps the production of a particular rNMP or dNMP at high concentrations is desirable. In such a scenario, biocatalysis using the precursor rN/dN and a thermophilic TK might be a more green and/or efficient technique than chemical synthesis of the rNMP/dNMP. For medical applications, reports of immune responses against the viral HSV-1-TK in gene therapy (Warren, Song et al. 2002) have led groups to consider using other TKs. A thermostable human TK with broadened specificity might provide an alternative to HSV-1-TK for suicide gene therapy. Learning about the forces conferring for thermostability in the hyperthermophilic TK could allow for engineering of hTK1 to be more thermostable [two good reviews of engineering proteins for thermostability can be found here (Russell and Taylor 1995; Lehmann and Wyss 2001)]. Based on the interest in extremophile TKs, a discussion of the hyperthermophilic eubacterium *Thermotoga maritima* follows, leading into the goals of the project.

1.7 Thermotoga maritima

T. maritima is an anaerobic bacteria, originally isolated from geothermal marine sediment found in Vulcano, Italy (Huber, Langworthy et al. 1986). The genus name *Thermotoga* is derived from the ancient Greek word *therma* ("hot") and the *toga* refers to the cell envelope, a key characteristic of this branch of eubacteria. The species name *maritima* refers to "maritime" (or "related to the sea") referring to its native marine environment. *T. maritima* is a borderline hyperthermophile living at an optimal growth temperature of ~80 °C . Besides its extremely high growth temperature, *T. maritima* is

peculiar in that its believed to be one of the oldest and slowest evolving bacteria known,

consistently occupying a position within phylogenetic trees closest to archaea, a

presumed ancestral domain (Achenbach-Richter, Gupta et al. 1987).

1.6.1 *T. maritima* genome

In 1999, Karen Nelson and colleagues at the Institute for Genomic Research

decoded the 1.8 million basepair genome for *T. maritima* strain MSB8 (Nelson, Clayton

et al. 1999). They identified 1,877 open reading frames, 54% of which they assigned

functionalities and 46% of unknown function. Interestingly, the authors noted that 24% of

the *T. maritima* predicted genes were most similar to genes from archaea species

providing evidence for lateral gene transfer between these two separate domains.

Genome analysis indicates nucleotide biosynthesis in *T. maritima* functions with

both the *de novo* and salvage pathways. RNR, a key *de novo* pathway enzyme, had been

investigated previous to the genome publication and shown to be homologous to the *E.*

coli RNR (Jordan, Torrents et al. 1997). As for thymidylate synthesis, only a putative

thymidine kinase was predicted at the time of genome publication. However,

investigation of the unknown gene TM0449 showed the protein (ThyX) to function as a

thymidylate synthetase while possessing a different sequence to known thymidylate

synthetases (ThyA) (Mathews, Deacon et al. 2003; Leduc, Graziani et al. 2004). While

the characterization of ThyX led to the distinction of a flavin-dependent *de novo*

synthesis for TMP, no characterizations of the salvage pathway for *T. maritima* had been

undertaken.

1.7 Dissertation project aims and goals

This PhD dissertation sets out to characterize the thymidine kinase for *Thermotoga maritima* (TmTK). Initially the putative gene is tested for *in vivo* TK activity, and upon that distinction the focus will shift on testing how the enzyme functions with natural and unnatural substrates, at varied temperatures, and comparatively with its mesophilic homolog hTK1. A collaboration with a crystallography group at the University of Illinois-Chicago (Dr. Arnon Lavie and Dr. Dario Segura-Pena) provides some additional insight which leads to investigations of substrate binding and oligomeric state. Through researching this novel thermophilic TK, the anticipated outcome is an expansion of knowledge about TKs with potential for engineering existing TKs to function with desired properties such as thermostability and higher catalytic efficiency.

In chapter 2, the expression, purification and kinetic characterization for TmTK is described. Chapter 3 follows with an investigation of substrate binding (thymidine and ATP) and the subsequent affect on tertiary and quaternary conformational changes in the protein. Chapter 4 investigates the true native oligomeric state of TmTK. A short summary chapter concludes this dissertation.

Chapter 2: Expression and Kinetic Characterization of a Thymidine Kinase from *Thermotoga maritima*

2.1 Introduction

Thymidine kinases (TKs) catalyze the phosphorylation of thymidine to form thymidylate as part of the salvage pathway for TTP biosynthesis. TKs are critical enzymes in maintaining the cellular concentration of dNTPs and are also responsible for activating nucleoside analog (NA) pro-drugs such as the HIV reverse transcriptase inhibitors (NRTIs) 3'-azidothymidine (AZT) and 2',3'-didehydro-2',3'-dideoxythymidine (D4T) (Mitsuya, Weinhold et al. 1985; Lin, Schinazi et al. 1987). Understanding how TKs function towards natural substrates and NA pro-drugs is important for drug design and potentially for other biotechnological and medical applications.

Following the publication of the *T. maritima* genome, a hypothetical thymidine kinase had been posited (Nelson, Clayton et al. 1999). Our interest in this putative protein was driven by the following reasons (also mentioned in chapter 1). Firstly, identifying a new TK expands the existing databank of TKs, allowing for the potential for finding novel substrate specificities and structural insight. Secondly, a thermophilic TK could have potential in the biotechnological arena and for such medical applications as suicide gene therapy. Currently, the HSV-1-TK/GCV suicide gene therapy pair has been successful in early phase research trials. However, reports of immunogenic responses due

to the use of a viral TK has led to an increased interest in engineering highly active and specific TKs from non-viral sources.

In this chapter, the expression and characterization of the thymidine kinase from *T. maritima* is described. It will be shown that TmTK is a type-II TK, conferring an elevated level of thermostability and having interesting catalytic properties including substantial catalytic activity at suboptimal temperatures and temperature-dependent substrate promiscuity. An investigation for the changes in substrate specificity as a function of temperatures suggests a protein conformational change near 70 °C.

2.2 Materials and methods

2.2.1 Isolation of thymidine kinase gene

The putative *T. maritima* thymidine kinase gene (*tmtk*) was isolated and amplified from *T. maritima* genomic DNA (ATCC # 43589D) using primers including flanking restrictions sites (a 5' *Nde*I and 3' *Spe*I site). The primers used were Tm_Fwd (5'-CGC<u>CATATG</u>TCGGGAAAATTGACCGTAATCACGGG-3') and Tm_Rev (5'-GCG<u>ACTAGT</u>TCAAACTCGTTTTTTGAGGGTGTTGTAACAGTCTC-3'), (restrictions sequences underlined). The PCR product was digested with *Nde*I and *Spe*I for ligation into pDIM (Lutz, Ostermeier et al. 2001) for *in vivo* complementation assays and pET14b (Novagen, Madison, WI) for protein overexpression. The purpose for the pDIM-*tmtk* construct was for use in a genetic complementation assay described in more detail below. In addition, a vector for the overexpression of native untagged protein without His-tag (pET-*tmtk*) was engineered. All constructs were confirmed by DNA sequencing.

2.2.2 Genetic complementation test

An *in vivo* complementation assay was employed with a TK-deficient *E. coli* strain KY895 (Hiraga, Igarashi et al. 1967). pDIM-*tmtk* was transformed into KY895 via electroporation. Transformed cells were grown overnight at 37 °C on LB plates containing ampicillin (100 μg/ml). Single colonies from LB plates were restreaked on plates containing selective media (20 mg/ml bacto-peptone, 5 mg/ml NaCl, 0.8 % noble agar, 0.2 % glucose, 100 μg/ml ampicillin, 12.5 μg/ml uridine, 2 μg/ml thymidine, 10 μg/ml 5-fluoro-2-deoxyuridine). Plates were grown overnight at room temperature, 30 °C and 37 °C. As a negative control, human deoxycytidine kinase (pDIM-*hdck*) was run in parallel.

2.2.3 Protein Overexpression of His-tagged protein

E. coli BL21(DE3)pLysS cells were transformed with pET-*tmtk* and plated on LB plates. Following 8h growth at 37 °C, a single colony was picked and grown in a 2 ml starter culture [LB media supplemented with ampicillin (100 μg/ml) and chloramphenicol (50 μg/ml)] and allowed to grow to saturation. Starter culture (1 ml) was used to inoculate 400 ml LB media containing ampicillin (100 μg/ml). Cells were grown for 3 - 4 h at 37 °C until an OD_{600} of ~0.8. Protein expression was induced with 1 mM IPTG for 4 h at 37 °C. Cells were centrifuged and the cell pellets were either stored at -20 °C or directly used for protein purification.

2.2.4 Purification of His-tagged protein

Cell pellet (from 50 ml of culture) was resuspended in 1 ml lysis buffer (50 mM Tris-HCl, pH 8.0; 500 mM NaCl; 10 mM imidazole) and supplemented with protease inhibitor cocktail (Sigma). Cells were then lysed by sonication (6 x 10 sec bursts at 15 W) while on ice, and subsequently treated with benzonase (12.5 units per ml) for 30 min on ice. The cell suspension was heat treated at 80 °C for 20 min, then cooled back on ice and centrifuged (15 min; 5000 g at 4 °C). Cleared supernatant was decanted and mixed with Ni-NTA agarose (Qiagen) pre-equilibrated with lysis buffer. The Ni-NTA agarose and lysate were mixed on an orbital shaker at 4 °C for 4 h to allow for sufficient binding of protein to the Ni-NTA. Upon completion of 4 h, the Ni-NTA lysate mix was centrifuged (5 min, 3000 g at 4 °C) and the unbound lysate fraction was decanted off. Four column volumes (CV) of lysis buffer were mixed with the Ni-NTA agarose and added to a poly-propylene column (Bio-Rad). After loading the sample, 2 CV of lysis buffer containing 4 mM $MgCl_2$ and 5 mM ATP was added, and left on bench top for 20 min. Following the Mg-ATP treatment, 2 CV of wash buffer (50 mM Tris-HCl pH 8.0, 500 mM NaCl, 50 mM imidazole) was added to column and flowed through. Lastly the protein was eluted using 4 CV of elution buffer (50 mM Tris-HCl pH 8.0, 500 mM NaCl, 250 mM imidazole). Protein fractions were analyzed using 12% SDS PAGE gels and fractions containing protein were pooled and buffer exchanged via ultra-filtration (Amicon Ultra-15, MWCO: 10 kDa, 4000 g at 4 °C) into storage buffer (50 mM Tris pH 8.0; 500 mM NaCl, 5 mM $MgCl_2$, and 2 mM DTT). The protein concentration was determined using A_{280} measurements [with a molar extinction coefficient = 8960 $M^{-1}cm^{-1}$

(BioWorkBench 3.2)]. Aliquots were stored at -80°C after flash freezing in liquid nitrogen.

2.2.5 Overexpression and purification of native, untagged protein

Protein overexpression of the untagged material was done by transforming pET-*tmtk* into *E. coli* BL21(DE3)pLysS cells. Cell cultures were grown under the same conditions as for the His-tagged material. Initial purification methods were similarly employed. The clear supernatant was mixed with an equal volume of 2 M $(NH_4)_2SO_4$ and the sample was loaded on a HiTrap ButylFF column (GE Healthcare). The column was washed with 5 CV of sample buffer (50 mM Tris-HCl pH 8.0, 500 mM NaCl), followed by a linear gradient over 2 CV to 25 mM Tris-HCl (pH 8.0). TmTK activity eluted as a single peak during the gradient run. The purification was completed by gel filtration (HiLoad Sephacryl HR100 16/60; buffer: 50 mM Tris-HCl, pH 8.0; 300 mM KCl, 5 mM $MgCl_2$, 2 mM DTT). The protein was visualized using SDS-PAGE and its concentration was determined as described above. Samples were sent to Dr. Dario Segura-Pena and Dr. Arnon Lavie at the University of Illinois-Chicago for crystallization experiments (Segura-Pena, Lutz et al. 2007).

2.2.6 Secondary structure and thermal denaturation

The secondary structure composition and thermal stability of TmTK was assessed by far UV circular dichroism (CD) spectroscopy using a J-810 spectropolarimeter (Jasco, Easton, MD). TmTK samples were buffer exchanged into CD buffer (50 mM KP_i pH 8.6; 400 µM DTT) via ultrafiltration (Amicon Ultra-15, MWCO: 10 kDa, 4000 g at 4 °C).

Protein sample (~1 mg/ml) was added to a 0.1 mm pathlength cell and scanned from 260

nm to 190 nm at room temperature (22 °C) using the following conditions: 50 nm/min

scan rate, 2 nm bandwidth, 4 s response time, and 5 accumulations. A buffer-only run

was used to correct for background ellipticity. CD scans set at the global minima 209 nm

were taken from 20 - 95 °C at 5 °C increments. A buffer-only run was again used to

subtract background ellipticity. Full scans (260-190 nm) were also measured from 20 –

90 °C at 10 °C intervals. To generate chemical stability experiments, buffer exchanged

protein was mixed with CD buffer containing 8 M urea to set up protein solutions

containing 0 - 6 M urea . Samples were incubated 16 hours at room temperature before

CD scans were taken from 260 – 210 nm.

2.2.7 Spectrophotometric enzyme activity assay

Kinase activity was measured using a pyruvate kinase-lactate dehydrogenase

coupled enzyme assay (Munch-Petersen, Knecht et al. 2000; Schelling, Folkers et al.

2001). For phosphoryl acceptor experiments, substrates (natural nucleoside and NAs)

were prepared at concentrations from 1 to 2000 μM in reaction buffer containing 50 mM

Tris-HCl pH 8.0, 2.5 mM MgCl$_2$, 1 mM ATP, 0.2 mM phosphoenolpyruvate, 0.18 mM

NADH, and 2 units/ml of both pyruvate kinase and lactate dehydrogenase (Roche

Diagnostics). Reactions were initiated by the addition of TmTK (100 – 200 nM) and

monitored for absorbance changes at 340 nm. Experiments were performed at 37 °C and

done in triplicate. For phosphoryl donor reactions, nucleoside triphosphate substrates

(CTP, GTP, ATP, UTP) were varied from 10 to 500 μM and a reaction buffer was

modified to include 10 μM thymidine.

2.2.8 Radiometric enzyme activity assay

Kinase activity at varied temperatures was measured using a filter-binding assay (Gerber and Folkers 1996). The substrates [^{3}H-methyl]-thymidine or [^{3}H-methyl]-3'-azidothymidine (Moravek Biochemicals, Brea CA) were prepared at 0.3 – 35 μM in reaction buffer containing 50 mM Tris-HCl (pH 8.0), 2.5 mM MgCl$_2$, 2 mM ATP, and 1 mM DTT. For experiments above 37 °C, Tris buffers of higher pH were used to maintain pH 8.0 at the respective temperatures (T_{assay}). Corrected pH values were calculated using the following equation: pH (T_{assay}) = pH (25 °C) – 0.031*[T_{assay} – 25 °C] (CRC Handbook of Chemistry and Physics; 83rd ed.; Lide and Raton). Reactions were incubated at varying temperatures (37 – 90 °C) and initiated by the addition of 0.1 – 1 ng enzyme. At varying time points, aliquots were taken out of reaction mixture and quenched in 10 mM thymidine (at 4 °C) then spotted on Whatman DE-81 filter paper (Millipore). Filters were air dried for 30 minutes and then washed with 7 mM ammonium acetate solution followed by a methanol wash and one wash with diethylether, then left to dry for 5 minutes. Filters were placed in 24 well plates, mixed with Microscint PS scintillation cocktail (Perkin Elmer), and measured for radioactivity using a liquid scintillation counter (TopCount NXT, Perkin Elmer). All experiments were performed in duplicates and kinetic data were determined using the Michaelis-Menten equation in the non-linear regression analysis in Origin $^®$7 (OriginLab, Northampton, MA).

2.2.9 Fluorescence spectroscopy

Fluorescence experiments were conducted by colleague Lingfeng Liu. Experiments were done using a FluoroMax-3 spectrophotometer (Horbia Jobin Yvon,

Edison, NJ) with a thermostatted cell holder and a NESLAB RTE7 water bath (Thermo Electron Cooperation, Waltham, MA). A sample cuvette containing 0.1 μM methylanthraniloyl ADP (Jena Biosciences, Jena) in 50 mM Tris-HCl (pH 9.3), 2.5 mM MgCl$_2$, 1 mM DTT and 10 μM thymidine was incubated at 65 °C for 15 minutes before the addition of enzyme (0.5 μM). Raising the temperature in one-degree increments, the sample was left to equilibrate for 5 minutes before each measurement. When thymidine was substituted with TMP (50 μM), the TmTK concentration was raised to 2 μM. The molar ratios of enzyme and substrates were determined by fluorescence anisotropy, maximizing the fraction of bound substrate analog. Samples were excited at 360 ± 0.5 nm and their emission spectra were acquired with 0.5 nm bandwidth resolution at wavelengths between 420 and 465 nm. All data were analyzed in Origin$^{®}$ to determine maximum peak intensity and emission wavelength.

2.3 Results and discussion

2.3.1 TmTK has in-vivo thymidine kinase activity

The hypothetical thymidine kinase from *T. maritima* shows 36% sequence identity to the human thymidine kinase 1 (hTK1), including high conservation of characteristic motifs such as the ATP-binding P-loop, the magnesium binding site, and potential zinc binding sites (Fig. 2-1). Based on these similarities, we speculated that TmTK is a TK and began our genetic and biochemical analysis.

Figure 2-1: Sequence alignment of TmTK with hTK1. Alignment created using ClustalW (BioWorkbench 3.2)

Upon successful amplification of the ~600 base pair PCR product from genomic DNA (Fig. 2-2A), pDIM-*tmtk* was cloned and tested for in-vivo TK activity using a genetic complementation assay with the *E. coli* TK auxotroph strain KY895 (Munir, French et al. 1992). Both plasmids, pDIM-*tmtk* and our negative control pDIM-*hdck*, promoted cell growth of KY895 on standard LB media (Fig. 2-2B, control plate). In contrast, under the selective media (with the *de novo* thymidylate synthesis inhibited) only cells transformed with pDIM-*tmtk* grew (Fig 2-2B, selection plate) indicating the presence of an exogenous TK.

Figure 2-2: Genetic complementation assay. (A) 1% agarose gel of amplified *tmtk* PCR product. lane 1-size marker; lane 2- PCR product (B) left plate- LB media + Amp (100 µg/ml); right plate- TK selection media. Top half of plates: cells transformed with pDIM-*tmtk*; Lower half of plates: cells transformed with pDIM-*hdck*. Plates shown were both grown at 37 °C overnight.

2.3.2 TmTK is a highly thermostable type-II thymidine kinase

Protein secondary structure information was investigated using circular dichroism (Fig. 2-3A). The predicted percentage of secondary structural elements (solved using K2d algorithm) for TmTK is 17% α-helix, 30% β-sheet, and 50% random (Andrade, Chacon et al. 1993). As compared to the known structure for hTK1 (20% α-helix; 21% β-sheet), TmTK shows potential for structural homology (Welin, Kosinska et al. 2004). Crystallization experiments run in parallel between TmTK and hTK1 shows the two proteins to be structurally homologous as type-II TKs (Segura-Pena, Lutz et al. 2007). A discussion about the structure with respect to kinetic and biophysical characterizations is included in the conclusion.

With the TmTK CD signature identified, the thermal stability of TmTK was evaluated by monitoring changes in molar ellipticity at the global minimum of 209 nm as

a function of temperature. As shown in Fig 2-3B, there is minimal change in the ellipticity up to 90 °C at which point the phosphate buffer used was beginning to reach boiling point and no longer could be reliable. The little change in ellipticity indicates no conformational transitions or denaturation. To verify that little change in the protein structure occurs over that range of temperature, full scans from 190 -260 nm taken were taken in 10 °C increments. The overall CD signature was unchanged up to 90 °C transition temperature (T_M) of >90 °C. Similar thermal denaturation experiments have shown the mesophilic hTK1 to have a T_M as high as 84 °C (Birringer, Perozzo et al. 2006). The high T_M for the mesophile homolog suggests the likelihood of a higher T_M for the thermophilic TmTK. Chemical denaturation of TmTK using 0 - 6 M urea were attempted as well, showing very little change to the structure over those concentrations. We conclude that TmTK exhibits a high level of stability to both heat and chemical denaturants.
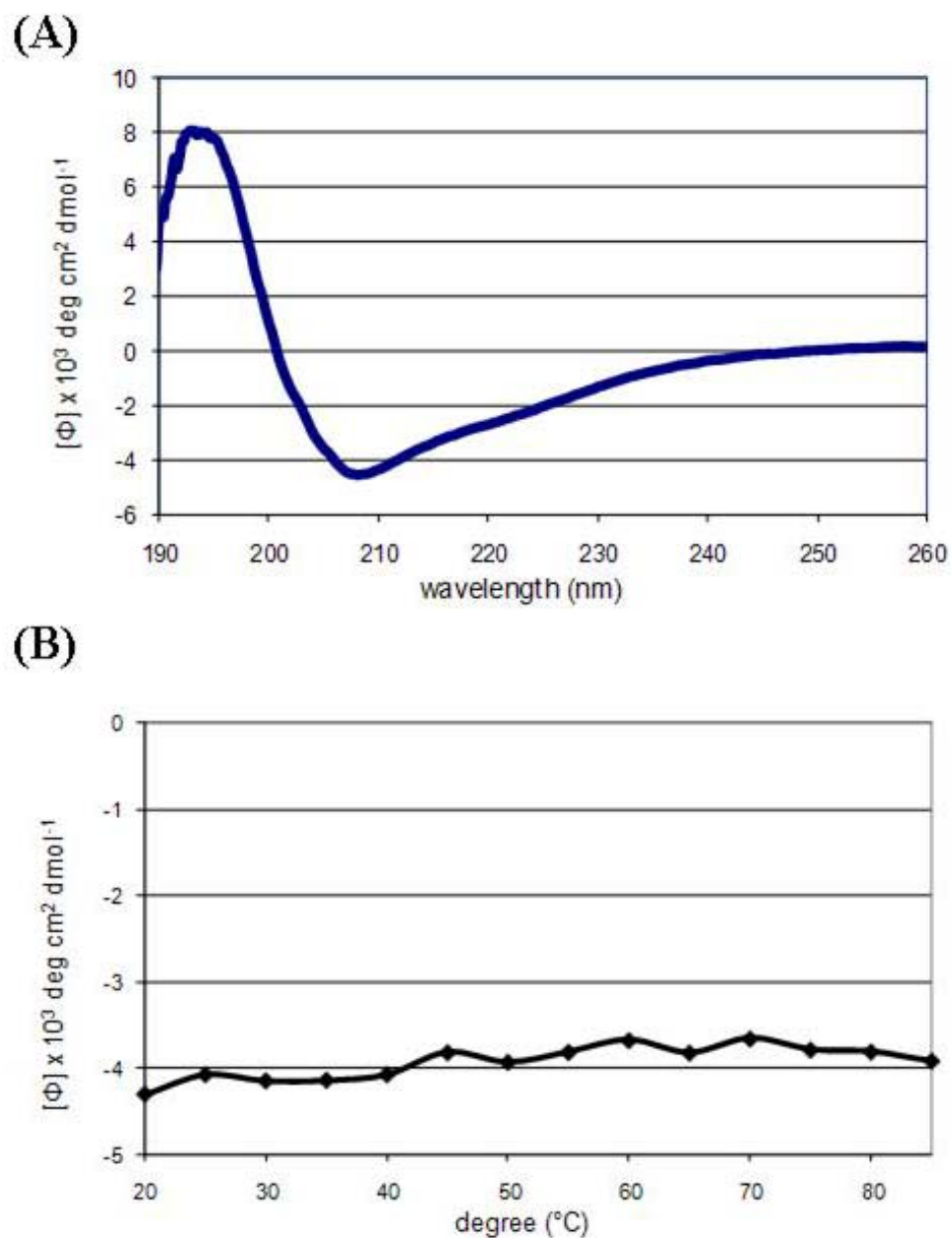
Figure 2-3: Circular dichroism spectroscopy of TmTK (A) Mean residue ellipticity from 190 - 260 nm. Data shown is average of 5 scans at ambient temperature (B) Thermal denaturation scan measured at 209 nm from 20 – 90 °C in 5 °C intervals

2.3.3 TmTK in-vitro catalytic performance

2.3.3.1 Natural catalytic activity at 37°C (Spectrophotometric assay)

To investigate the kinetic properties for TmTK, an assay was employed at 37 °C where kinase activity is coupled to the dephosphorylation of phosphoenolpyruvate by pyruvate kinase (PK) to form pyruvate, which can be further reduced to lactate via lactate dehydrogenase (LDH) (Fig 2-4). The oxidation of NADH (by LDH) is monitored at 340 nm with UV-Vis spectrophotometry.
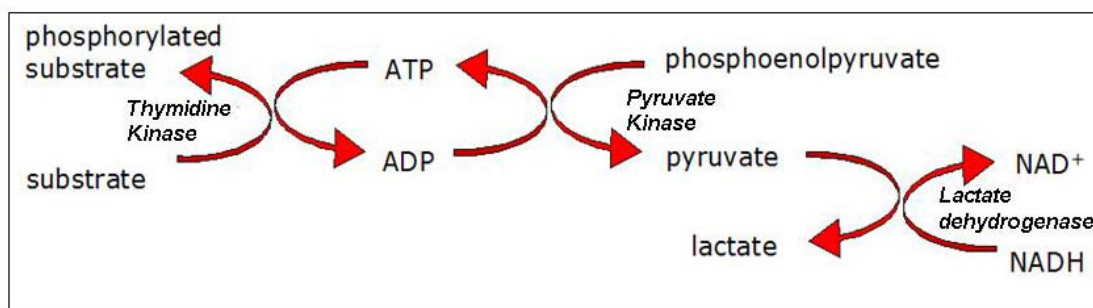
Figure 2-4: Outline of the coupled enzyme assay.

The first set of experiments was designed to study the phosphorylation of naturally occurring substrates (2'-deoxyribonucleoside acceptors and ribonucleotide triphosphate donors). An investigation of natural nucleoside acceptors showed TmTK to be highly specific in respect to the nucleobase portion of the substrate, activating only those carrying either thymine and uracil (Table 2-1). No measurable activity was seen for the purine nucleosides (2'-deoxyadenosine and 2'-deoxyguanosine) or with 2'-deoxycytidine when measured up to 3 mM concentration. The strict preference for the thymine base likely results from specific hydrogen bonding between the nucleobase and

the lasso loop (more on the structure in the discussion). With regards to phosphoryl donor, TmTK shows more tolerance, effectively catalyzing phosphoryl transfer with all four ribonucleoside triphosphates, but showing slight favor towards ATP.

Table 2-1: Kinetic parameters for natural substrates at 37 °C

	substrate	K_M (μM)	k_{cat} (s^{-1})	k_{cat}/K_M (10^4 M^{-1} s^{-1})	relative specificity
acceptors	thymidine	0.5 ± 0.2	0.3 ± 0.08	60	1
	2'-deoxycytidine	n.d.	n.d.	-	-
	2'-deoxyadenosine	n.d.	n.d.	-	-
	2'-deoxyguanosine	n.d.	n.d.	-	-
	2'- deoxyuridine	1.5 ± 1	0.7 ± 0.1	48	0.8
donors	ATP	40 ± 12	0.4 ± 0.04	1	1
	GTP	120 ± 15	0.79 ± 0.05	0.66	0.66
	UTP	194 ± 30	0.97 ± 0.06	0.5	0.5
	CTP	176 ± 21	0.91 ± 0.05	0.52	0.52

Relative specificity for *acceptors* compared to thymidine: k_{cat}/K_M (substrate) / k_{cat}/K_M (thymidine)
Relative specificity for *donors* compared to ATP: k_{cat}/K_M (substrate) / k_{cat}/K_M (ATP)
n.d. = not detectable up to 3 mM

2.3.3.2 Natural substrate specific at 82°C

The hyperthermophilic *T. maritima* lives at temperatures around 80 - 85°C (Huber, Langworthy et al. 1986). Therefore we sought to investigate TmTK activity around its physiological temperature. For these experiments, a filter binding assay was employed. The experiment is done in two parts: (1) mix the substrates ([³H]-thymidine and ATP) with enzyme and quench reaction volumes at various time points, then (2) spot an aliquot of the quenched reaction on the weak anion exchange resin, diethylaminoethyl (DEAE), coated cellulose filter paper and measure the bound [³H]-thymidylate using a scintillation counter. Due to the two part nature of the assay, the first part of the reaction can be incubated at any temperature and cooled down when quenched. We examined

TmTK activity at 82°C for both natural substrates thymidine and ATP, as well as the analog AZT.

At first, a validation that the filter binding assay provides comparable results with the coupled enzyme assay was done by implementing the assay at 37 °C. Results suggested the filter binding assay to have a 15x reduction in reaction velocity as compared to the spec assay. This observation agreed with earlier reports that during scintillation counting the DEAE cellulose filter paper has strong internal self-absorption of the weak β-radiation leading to a reported 12x reduction in actual counts (Gerber and Folkers 1996). A 15x correction factor was incorporated into the filter binding assay to normalize with data recorded from the spectrophotometric assay.

We investigated the kinetic parameters for thymidine at 37 °C (mesophilic physiological temperature) and 82 °C (thermophilic physiological temperature). TmTK is ~6x more efficient for catalyzing the phosphorylation of thymidine than at 82 °C (Table 2-2). The change is due in large part to an 11 fold increase in k_{cat}. The efficiency towards ATP is also increased at elevated temperature, with an unexpected change in the Hill coefficient from 1.1 (at 37 °C) to 2.4 (at 82 °C). When the Hill coefficient is greater than 1, it is indicative that the binding of a ligand will increase the affinity for other ligand molecules (Perutz 1970) and therefore described as positive cooperativity. In the case of TmTK, positive cooperativity is seen at its physiological but not at the suboptimal temperature. Previous reports have indicated cooperativity for TmTK's mesophilic homolog hTK1 (Munch-Petersen, Tyrsted et al. 1993). Interestingly, at both of their physiological temperatures they seem to utilize ATP as a positive effector. More discussion on ATP binding will be discussed in Chapter 3.

Table 2-2: Kinetic parameters for thymidine, ATP, and AZT at 37 and 82 °C

substrate	K_M (µM)	k_{cat} (s^{-1})	k_{cat}/K_M (10^4 M^{-1}s^{-1})	relative efficiency	h
Thymidine (37°C)	0.7 ± 0.2	0.3± 0.08	60	1	0.98
Thymidine (82°C)	1.0 ± 0.15	3.5 ± 0.3	350	5.8	1.1
ATP (37°C)	40 ± 12	0.4 ± 0.04	1	1	1.13
ATP (82°C)	187 ± 21 ($K_{0.5}$)	3.5 ± 0.3	1.8	1.8	2.4
AZT (37°C)	0.65 ± 0.2	0.41 ± 0.02	45	1	-
AZT (82°C)	8.7 ± 3	1.6 ± 0.29	18	0.4	-

Relative efficiency for substrates: k_{cat}/K_M (substrate @ 82°C) / k_{cat}/K_M (substrate @ 37°C)

Hill coefficient (h) derived from hill equation: $v = v_{max}[\text{substrate}]^h / K_{0.5}{}^h + [\text{substrate}]^h$

Intuitively it makes sense that the enzyme would function better at temperatures near its organism's optimal growth temperature. Yet, it is still interesting that contrary to other hyperthermophilic enzymes, TmTK maintains significant activity at suboptimal temperatures (Hansen, Schlichting et al. 2002; Morsomme, Chami et al. 2002; Ying, Grunden et al. 2008). More surprisingly, the kinetic parameters measured for AZT showed the opposite trend to thymidine. While AZT is phosphorylated with nearly similar efficiency as thymidine at 37 °C, the analog shows 20 times lower efficiency at 82 °C. An examination of other NAs at elevated temperature was limited by availability of radiolabeled reactants. To further investigate the temperature-dependent substrate specificity, we expanded our kinetic investigation to other NAs at 37 °C.

2.3.3.3 Broad nucleoside analog activation at 37 °C

An investigation of NA activation at 37 °C found TmTK can phosphorylate a broad range of analogs maintaining the thymine/uracil base yet modified at the ribose moiety and the C-5 position of the nucleobase (Table 2-3). The differences in catalytic efficiency for these NAs are a result in variation of the K_M values. The binding could therefore be the major determinant for the catalytic efficiency. Crystallography, NMR spectroscopy, and research on nucleosides covalently locked in particular conformations have established the preferred $C_{2'}$-endo ribose pucker for nucleosides bound to dNKs (Maltseva, Usova et al. 2001; Sabini, Ort et al. 2003; Marquez, Ben-Kasus et al. 2004). TmTK follows the same trend, favoring substrates with $C_{2'}$-endo (and $C_{3'}$-exo) over nucleosides with a $C_{3'}$-endo conformation. For instance, 5-fluoro-2'-deoxyuridine (5-FdUrd), which adopts a $C_{2'}$-endo conformation, has a catalytic efficiency (74 x 10^4 $M^{-1}s^{-1}$) even greater than that of thymidine (60 x 10^4 $M^{-1}s^{-1}$). Other analogs such as ddT and AZT show similar activity to thymidine. Analogs with the $C_{3'}$-endo conformation such as ddU and DOT, show relatively poor catalytic efficiency. Besides sugar puckering, steric effects might also play a role in the effect on substrate binding, in particular with the L-isomer nucleosides (i.e. L-FMAU, and L-T). Additionally, the lack of hydrogen bonding in the 2',3'-dideoxynucleosides might contribute to the weak binding affinity. Summarizing the analog kinetics, TmTK shows a broad tolerance for a variety of thymine based nucleoside analogs at 37 °C, and with varying catalytic efficiencies but very similar turnover rates.

The turnover rate homogeneity displayed by TmTK towards the nucleoside analogs at 37 °C might provide some explanation for the temperature-dependent

specificity change. Firstly, when TmTK's mesophilic homolog hTK1 was tested with similar substrates as tested here, rates differing up to 2 orders of magnitude were measured (Eriksson, Kierdaszuk et al. 1991). Therefore the homogeneity seems specific for TmTK. Others have rationalized rate homogeneity by a common chemical intermediate preceding the rate limiting step in an enzyme's reaction pathway (Hollaway and Hardman 1973). While the direct phosphoryl transfer mechanism makes a chemical intermediate impossible, a structural intermediate resulting from a substrate-independent change of protein conformation might be plausible. Evidence supporting this hypothesis comes from an analysis of enzyme reaction rates at different temperatures.

Table 2-3: Kinetic parameters for nucleoside analog acceptors at 37 °C

substrate	K_M (μM)	k_{cat} (s^{-1})	k_{cat}/K_M (10^4 M^{-1} s^{-1})	relative activity	preferred ribose pucker conformation
5-fluoro-2'-deoxyuridine (5-FdUrd)	1 ± 0.1	0.74 ± 0.05	74	2.5	$C_{2'}$-endo
2',3'-dideoxythymidine (ddT)	30 ± 5	0.33 ± 0.04	1.1	1.1	$C_{2'}$-endo
2',3'-dideoxyuridine (ddU)	>1000	n.d.	-	-	$C_{3'}$-endo
AZT	0.65 ± 0.2	0.29 ± 0.03	45	1	$C_{3'}$-exo
2',3'-dideoxy-2',3'-didehydrothymidine (D4T)	75 ± 5	0.41 ± 0.02	0.54	1.4	planar
dioxolane thymidine (DOT)	114 ± 15	0.29 ± 0.02	0.25	1	$C_{3'}$-endo
2'-fluoro-5-methyl-β-L-arabinofuranosyluracil (L-FMAU)	132 ± 4	0.5 ± 0.02	0.38	1.7	$C_{2'}$-endo
L-Thymidine (L-T)	>1000	n.d.	-	-	$C_{2'}$-endo

Relative activity for nucleoside analogs compared to thymidine: k_{cat} (substrate) / k_{cat} (thymidine)

2.3.3.4 Temperature-activity profile reveals change in activation energy

In an effort to evaluate the changes in activity seen as a result of temperature, maximal enzyme reaction rates (v_{max}) for thymidine/ATP were measured over a range of different temperatures from 37 – 90 °C. The reaction rates increased over the temperature range (Fig. 2-5). The inset to figure 2-5 shows an Arrhenius plot of the enzymatic activity. The data indicate a discontinuity in reaction rate at 70 °C. Above this transition temperature the slope corresponds to an activation energy of ~ 4 kcal/mol while below 70 °C the energy barrier increases to 16 kcal/mol. A conformational change as the enzyme's slowest step in the reaction pathway could explain this change in rate, and the homogeneous turnover rates seen in the NA kinetics at the lower temperatures. An investigation for conformational changes is discussed next.
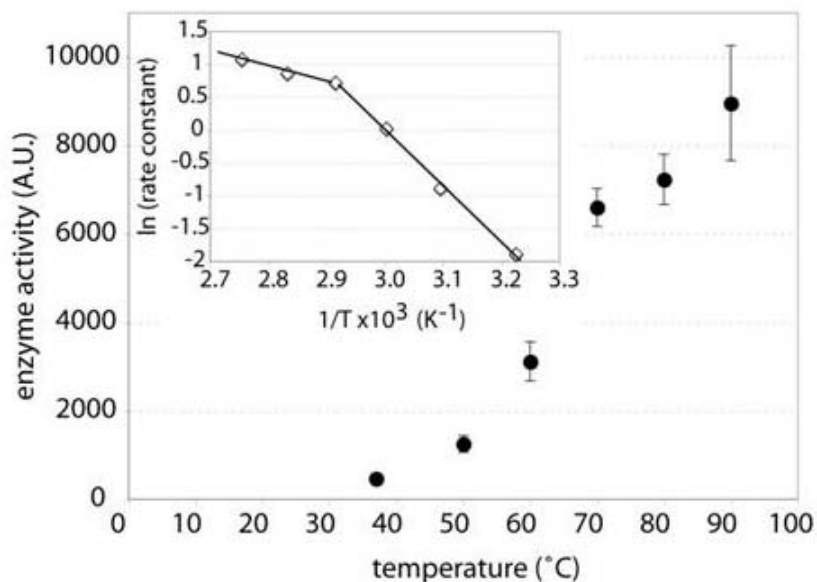
Figure 2-5: Maximal reaction rates (v_{max}) of TmTK for thymidine/ATP as a function of temperature. Concentrations used: [Thy] = 10 µM, [ATP] = 1 mM. Graph inset: Arrhenius plot of maximal reaction rate data.

2.3.4 Fluorescence spectroscopy suggest protein conformational changes

Two ways to investigate protein conformational changes are by measuring intrinsic fluorescence of a protein (through the fluorescent amino acids tryptophan, tyrosine, or phenylalanine) or by measuring fluorescence of a fluorophore labeled substrate interacting with a protein as a function of the desired variable (i.e. temperature, substrate binding). Both techniques were used to investigate potential protein conformational changes in TmTK.

Of the three fluorescent amino acids, the highly conjugated tryptophan has the greatest fluorescence and is commonly investigated in proteins as a function of temperature or substrate (Yengo, Chrin et al. 1999; Wang, Liu et al. 2008). In the case of TmTK, the absence of tryptophans in the primary sequence eliminates the possibility for looking at intrinsic tryptophan fluorescence without engineering a mutant. We therefore decided to try and use the next strongest fluorescent amino acid tyrosine. Unlike tryptophan, tyrosine has a lower quantum yield and weak fluorescence emission, but with 7 residues in the sequence it could contribute significantly to TmTK intrinsic fluorescence. Tyrosine fluorescence measured as a function of increasing temperature, showed very little change in emission maximum or intensity (Fig. 2-6A).

To investigate TmTK protein changes in a different manner, the fluorescent *N*-methylanthraniloyl (MANT) coupled to ADP (MANT-ADP) was used as a probe for changes in structure (Fig. 2-6B) Upon investigation of MANT-ADP and thymidine mixed with TmTK at varied temperatures, little change to the fluorescence intensity was noted yet a transition point in the fluorophore's emission wavelength maximum (λ_{em}) was detected at 70 °C (Fig. 2-6C). The λ_{em} plot shows biphasic behavior with a change from

an emission maximum of 439 – 440 nm from 64 - 70 °C, to a significant blue shift

dropping to 436.5 nm at 74 °C. This observed shift is consistent with the fluorophore

sensing a more hydrophobic environment, possibly due to a repositioning of protein

residues contacting the MANT-ADP. Interestingly the shift occurs at the same transition

temperature noted in the kinetic characterization. Further speculation on what potential

conformational changes occur are discussed in the conclusion.
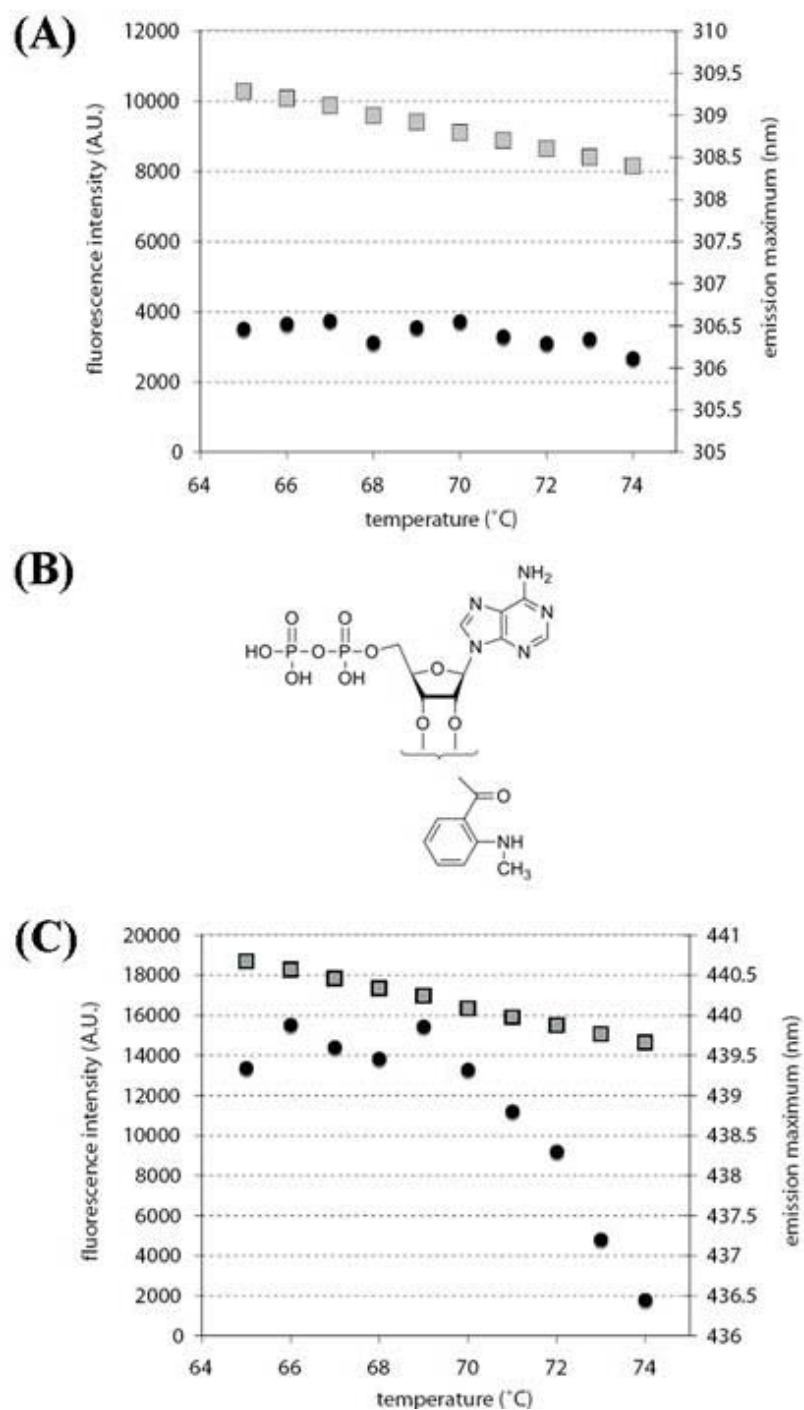
Figure 2-6: Fluorescence experiments. Gray squares – fluorescence intensity; Black circles- emission maximum (A) Intrinsic tyrosine fluorescence measured as a function of temperature. (B) MANT-ADP structure (C) MANT-ADP fluorescence as a function of temperature. Experiments were performed in the presence of thymidine

2.4 Conclusion

The first hyperthermophilic thymidine kinase has been isolated, expressed, and characterized. Following an initial *in vivo* assay validating that TmTK is TK active, an *in vitro* analysis of enzyme catalysis was undertaken. From its strict preference for phosphorylating natural nucleosides (and NAs) with thymine and uracil nucleobases, we characterize TmTK as a type-II TK. The crystal structure for TmTK supports this hypothesis, identifying the protein as a structural homolog to hTK1 (Fig. 2-7A) [(Segura-Pena, Lutz et al. 2007)]. Both proteins, co-crystallized with the bisubstrate mimic P^1-(5'-adenosyl)P^4-(5'-(2'-deoxythymidyl)) tetraphosphate (TP4A), show nearly identical structures at the monomer level. Both are comprised of a core N-terminal α/β domain and a C-terminal domain built with a 15 residue zinc binding loop, followed by a "lasso" region anchored by two β-strands. In both TKs, the thymine portion of TP4A hydrogen bonds with main chain carbonyl oxygens and nitrogen atoms from the lasso loop. The strict preference for thymine and uracil is explained by these interactions along with a tight binding pocket. In contrast, the ribose moiety is accommodated with a larger cavity, allowing for broader acceptance of sugar modifications, as evidenced by NA activation by TmTK. The quaternary structure for both proteins is also similar (Fig 2-7B). The two proteins crystallized as a dimer in the asymmetric unit, but using crystallographic 2-fold symmetry they form tetramers (dimer of dimers). A full investigation of the oligomeric state of TmTK will be pursued in chapter 4.
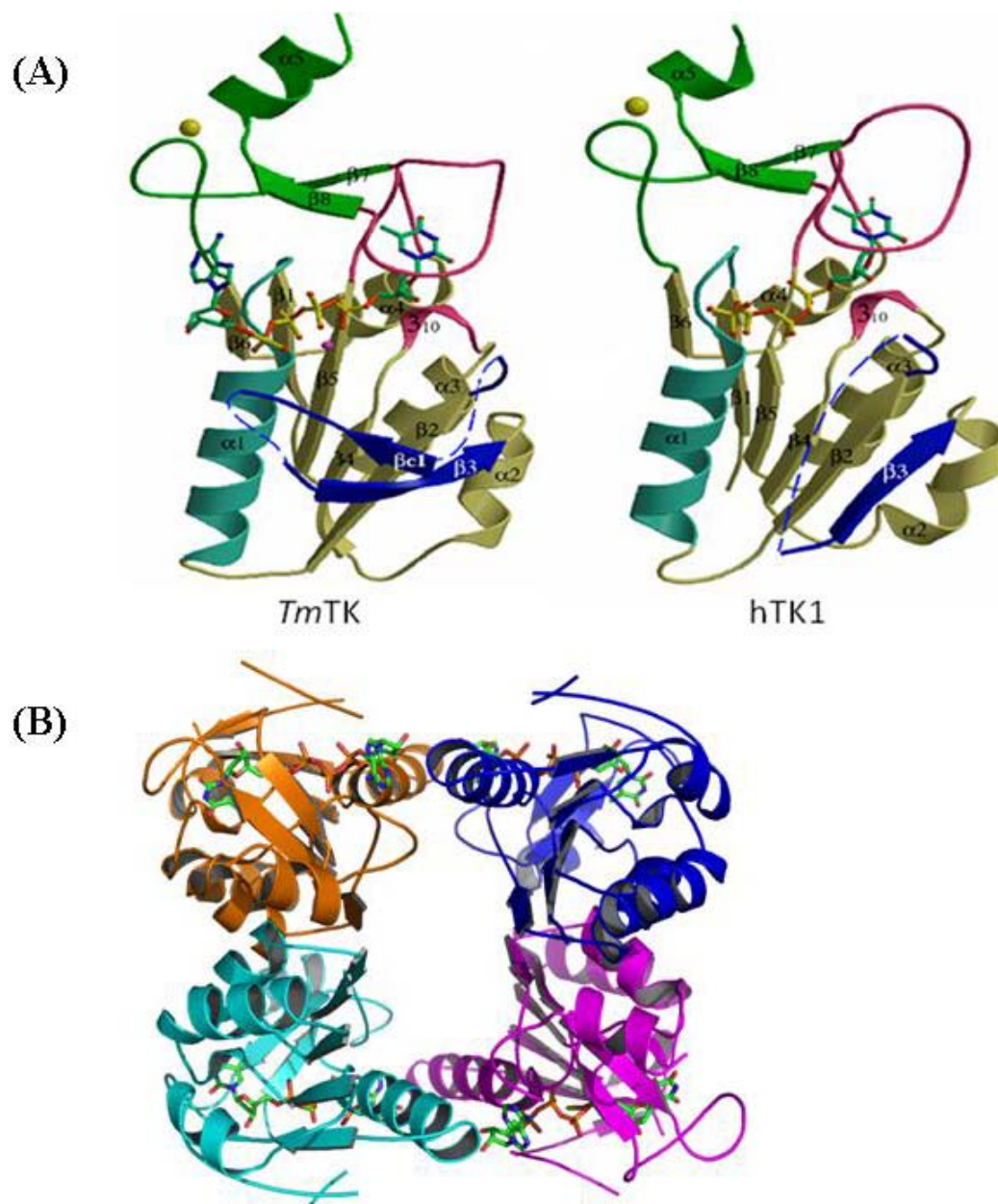
Figure 2-7: (A) Representation of TmTK (pdb # 2orw) and hTK1 (pdb # 2orv) crystal structures of the monomer units (Segura-Pena, Lutz et al. 2007). Regions are labeled by color: Green- C-terminal; Pink- Lasso region; Dark yellow- N terminal α/β core; Cyan-α1; Dark Blue- βc1 region (B) TmTK tetramer. Dimer interfaces are indicated by dotted lines.

An interesting finding from our in vitro analysis of TmTK is the difference in kinetic properties at differing temperatures. At the suboptimal temperature of 37 °C, the catalytic efficiency for TmTK towards thymidine (6×10^5 M^{-1} s^{-1}) is equal to that of the reported catalytic efficiency for its mesophilic homolog hTK1 (8×10^6 M^{-1} s^{-1}) (Birringer, Perozzo et al. 2006). As the reaction temperature is raised, TmTK catalytic efficiency increases reaching 3.5×10^7 M^{-1} s^{-1} at 82 °C. Similarly the efficiency towards ATP increases, yet changes in the Hill coefficient indicate positive cooperativity. This change in phosphoryl donor activation might signify a change in the protein catalytic cycle at elevated temperatures. One hypothesis is that the protein dynamics are greater at elevated temperatures and binding of one ATP provides structural integrity to the interface, promoting the effective binding of a second ATP molecule in that interface. The structure shows 2 ATP molecules bound in between two α1 helices at one interface. The first ATP that binds could "prop" the interface open, accommodating the second ATP. At lower temperature, a more rigid protein might not be as flexible to allow for the interface opening by just one ATP, and therefore each bind without cooperativity. More of an investigation of ATP and cooperativity is discussed in chapter 3.

An investigation of TmTK activation of the anti-HIV drug AZT showed that at elevated temperatures the catalytic efficiency is decreased three-fold. While we have investigated only AZT at elevated temperatures, an investigation of other nucleoside analogs at 82 °C was hindered by the availability of radiolabeled compounds. An investigation of other NAs at 37 °C, showed relatively similar catalytic efficiencies as for thymidine with similar turnover rates for all the substrates tested (Table 2-3).

Evidence for a conformational change in the protein occurring as a function of temperature was seen through the maximal reaction velocities measured over the range of 37 – 90 °C. The results showed a change in the reaction rate from 16 kcal/mol below 70 °C, to ~4 kcal/mol. As well, fluorescence measurements with MANT-ADP suggests some conformational changes in the protein structure at 70 °C. Looking closely at the quaternary structure, the adenosine portions of the TP4A are sandwiched by two α-helices at the dimer II interface (Fig. 2-8). The nucleobase of the adenosine moiety is flanked by Val139, Tyr13, and Leu29 while the ribose moiety is hydrogen bonding with Glu25 and a network of water molecules (hydrogen bonding with Ser22 and Thr18). The 2' and 3' position of the ribose face into the crevice between the two helices. The blue shift seen in the MANT-ADP fluorescence as a function of temperature is suggestive of a more hydrophobic environment. We hypothesize that the MANT group repositions itself from outside the interface (more solvent contacts) to inside the interface (more protein side chain interactions) at higher temperatures. The effect of increased temperature specifically at 70 °C could be to facilitate the opening of this interface and thereby allow the MANT to position itself between the two helices.

Concurrent with the structural data, we hypothesize a two state model for TmTK, where a thermodynamically preferred, yet inactive closed state and a catalytically active open state exist. We hypothesize that the conformational change from closed to open is the rate determining step below 70 °C, while above this transition temperature the protein is in rapid equilibrium between open and closed states, leading to change in the reaction's limiting step.
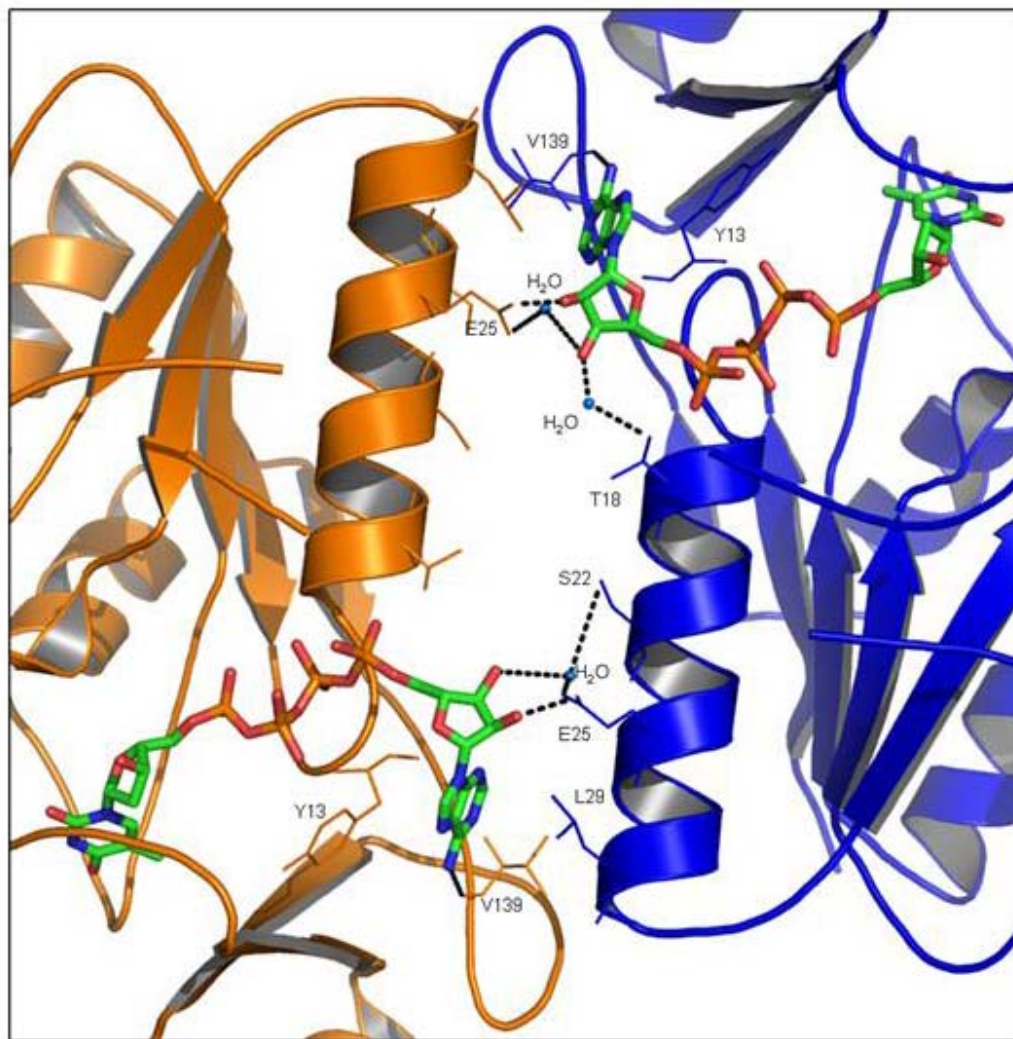
Figure 2-8: Dimer II interface. Contacts shown are made between the adenosine portion of TP4A and TmTK. The adenosine nucleobase is packed by Tyr13 of one monomer and Leu29 of the other, while being flanked by a hydrogen bond to the main chain oxygen on Val139. The ribose portion makes hydrogen bonding contacts with Glu25 and water molecules. (pdb # 2orw) (Segura-Pena, Lutz et al. 2007)

Chapter 3: Tertiary and quaternary conformational changes in TmTK as a function of substrate binding

3.1 Introduction

As discussed in chapters 1 and 2, type-II TK monomers consist of 2 domains (the large N-terminal α/β domain and the smaller C-terminal lasso region) and the proteins generally assemble as homotetramers. Kinetic and structural characterizations of the TK from *T. maritima* identify it as a member of the type-II TK family (Lutz, Lichter et al. 2007; Segura-Pena, Lutz et al. 2007). In the structure of TmTK co-crystallized with TP4A (pdb # 2orw), a hydrogen bonding network formed by protein side chains and water molecules stabilizes the adenosine portion between α1 helices at the dimer II interface. This conformation appears critical for proper orientation of the phosphoryl donor. In contrast, the structure of hTK1 with TP4A (pdb # 2orv) shows a smaller space between these same two helices, adopting a conformation that could not orient the adenosine moiety, rendering it absent from the structure.

The two structures suggested that ATP binding might induce the opening at the dimer II interface. A two-state model was proposed where the homotetramer preferentially exists in a closed inactive state as observed in the structures of hTK1, *Ureaplasma urealyticum* TK (Welin, Kosinska et al. 2004), and *Bacillus cereus* TK (Kosinska, Carnrot et al. 2007). Upon ATP binding, a conformational change leads to an open conformation as is seen in the structures for TmTK, *Clostridium acetobutylicum* TK (Kuzin 2004), and *Bacillus anthracis* TK (Kosinska, Carnrot et al. 2007). With proper

positioning of the phosphoryl donor, the open conformation is catalytically active. An ambiguity in this model derives from comparing TKs from different organisms, bound with different substrates. One can not discount the possibility that the former set of enzymes in the closed state remain closed upon ATP binding or that the group of enzymes in the open state stay open without ATP. None of the type-II TKs had been singularly examined for changes in structure due to substrate binding.

In the following chapter, an investigation on the affect of binding of natural substrates (thymidine and ATP) to TmTK is described. Crystallization experiments with TmTK in different substrate bound states were conducted by our collaborators Dr. Dario Segura-Pena and Dr. Arnon Lavie at the University of Chicago-Illinois. TmTK formed diffraction crystals in the nucleotide-free (apo form), thymidine bound (binary form) and with thymidine and an ATP analog, AppNHp. Conformational changes at both the tertiary and quaternary levels are identified as a result of addition of substrate. To verify the structural findings, single tryptophan mutations were engineered into TmTK to investigate fluorescence properties in the absence and presence of substrates. Distinct changes in tryptophan fluorescence were seen for Trp mutants placed in the $\beta c1/\beta3$ region, corroborating the structural changes induced by ATP binding. To further investigate the role of the weak dimer interface in the proposed open conformation, a double cysteine mutant was engineered. Under oxidizing conditions, disulfide bond formation across this interface locks the tetramer in the closed, inactive state. This process is reversible upon the addition of a strong reducing agent, unlocking the closed state and allowing for TmTK to regain activity. The two-state model for an open/active and closed/inactive protein is discussed in terms of substrate binding.

3.2 Materials and methods

3.2.1 Crystallization and structure determination

The crystallization studies were conducted by Dr. Dario Segura-Pena and Dr. Arnon Lavie at the University of Illinois – Chicago. Experimental procedures for crystallization and structure determination can be found in the published manuscript (Segura-Pena, Lichter et al. 2007).

3.2.2 Site-directed mutagenesis

Site directed mutagenesis was done using primer overlap extension PCR (Higuchi, Krummel et al. 1988). Mutants designed were H53A, V34W, V51W, G55W, V58W, L129W, T18C/S22C, T18A/S22A. For the first round of amplification, pET-His*mtk* was used as the DNA template and the following primer pairs were used: T7$_{fwd}$ and mut_primer_b, and T7$_{term}$ and mut_primer_a. Mutant primers used are listed in table 3-1. The second round of amplification used the two newly formed gene fragments as DNA templates and T7$_{fwd}$ and T7$_{term}$ for primer pairs.

Following the production of the mutant genes, restriction endonuclease digestion using *Nde*I and *Spe*I was performed on the PCR products and a pET14b vector. Digested PCR products and vector were ligated overnight at 16 °C. Ligations were transformed into *E. coli* DH5α cells and plated on LB agar plates ([Amp] = 100 μg/ml). Colonies were picked and clones were confirmed using DNA sequencing. Protein overexpression was done using *E. coli* BL21(DE3) cells for all mutants. Purification of the H53A and

tryptophan mutants was performed using Ni-NTA agarose chromatography as described

in chapter 1 (Lutz, Lichter et al. 2007).

Table 3-1: Primers for site directed mutagenesis

$T7_{fwd}$	5'	TAATACGACTCACTATAGGG	3'
$T7_{term}$	5'	GCTAGTTATTGCTCAGCGG	3'
H53_a	5'	CCATGATCGTCTCTGCGTCTGGAAACGG	3'
H53_b	5'	CCGTTTCCAGACGCAGAGACGATCATGG	3'
V34W_a	5'	CTGGGAAAGAAAAAATGGGCTGTTTTTAAACC	3'
V34W_b	5'	GGTTTAAAAACAGCCCATTTTTTCTTTCCCAG	3'
V51W_a	5'	CCACCATGATCTGGTCTCATTCTGG	3'
V51W_b	5'	CCAGAATGAGACCAGATCATGGTGG	3'
G55W_a	5'	GTCTCTCATTCTTGGAACGGTGTTGAAGC	3'
G55W_b	5'	GCTTCAACACCGTTCCAAGAATGAGAGAC	3'
V58W_a	5'	GGAAACGGTTGGGAAGCACACGTGATAGAACG	3'
V58W_b	5'	CGTTCTATCACGTGTGCTTCCCAACCGTTTCC	3'
L129W_a	5'	GCTCTGCTCCTCAGTTGGGCCGACACC	3'
L129W_b	5'	GGTGTCGGCCCAACTGAGGAGCAGAGC	3'
T18C/S22C_a	5'	CCGGAAAGACATGCGAGCTTCTCTGCTTTGTGG	3'
T18C/S22C_b	5'	CCACAAAGCAGAGAAGCTCGCATGTCTTTCCGG	3'
T18A/S22A_a	5'	CCGGAAAGACAGCGGAGCTTCTCGCGTTTGTGG	3'
T18A/S22A_b	5'	CCACAAACGCGAGAAGCTCCGCTGTCTTTCCGG	3'

3.2.3 Disulfide linkage experiments

Initially, purification of T18C/S22C and T18A/S22A was performed using

previously established protocols. Incomplete disulfide bond formation led to

troubleshooting for a different purification protocol. Reducing agent was added to the

purification buffers. In separate trials, the following reducing agents were tried at

concentrations ranging from 0-8 mM: Dithiothreitol (Acros Organics), 2-mercaptoethanol

(Fisher), and Tris(2-Carboxyethyl)Phosphine Hydrochloride (Pierce). Following the Ni-

NTA agarose chromatography, reducing agent was removed from the protein samples

using dialysis. Samples (~2 mg/ml) were loaded into Slide-A-Lyzer cassettes (MWCO:

10 kDa; Pierce, Rockford, Il) and dialyzed against 3 L of cell lysis buffer at 4 °C for 2

days. Buffer was exchanged once after 24 hours. To reduce the disulfide linker, reducing agent was added back to protein samples and incubated at ambient temperature for 3 days.

3.2.4 Enzyme kinetics

Thymidine and ATP kinetic constants for H53A and tryptophan mutants were measured at 37 °C using the coupled-enzyme spectrophotometric assay (Schelling, Folkers et al. 2001). Experiments were performed in triplicate and data were fit to the Michaelis-Menten equation with Origin software (OriginLab, Northhampton, MA). For the disulfide bond experiments (with T18C/S22C, T18A/S22A, and wild type), only maximal reaction velocity (v_{max}) were measured using 1 mM ATP and 20 μM thymidine.

3.2.5 Fluorescence spectroscopy

Tryptophan mutants (~8 μM) in assay buffer (50 mM Tris-HCl pH 8.0, 2.5 mM MgCl$_2$) were excited at 295 nm in a 1 cm path-length cuvette using a 0.5 s time integral, 0.2 nm increments, an excitation band slit width of 1 nm and an emission slit width of 5 nm. Emission data were collected at 10 °C from 310 – 390 nm in 0.2 nm increments. Each spectrum represents the mean of three scans. γ-thio ATP (Fluka, Switzerland) was added to protein samples at varying concentrations (from 1.6 – 160 μM) and incubated on ice for 2 min prior to spectrum acquisition. All measurements were performed in triplicate and data were analyzed with Origin software.

3.3 Results and discussion

3.3.1 Structural changes seen upon thymidine and ATP binding

Three TmTK structures were obtained from crystals that diffracted to high resolution: 1.95 Å for the apo form and the complex with thymidine, and 1.5 Å for the ternary complex. Crystals of the apo form had complete tetramers in the asymmetric unit while the binary and ternary complexes were present as dimers. Using a two-fold crystallographic symmetry operator, the binary and ternary complexes could be recreated as the presumed biological tetramer. Surprisingly for the dimeric ternary complex involving thymidine and the ATP analog, AppNHp, there appeared to be the substrate complex (thymidine and AppNHp) in one monomer and the product complex (TMP and ADP) in the other. This observation suggests the protein sample was catalytic even with the more stable amine linkage between the β and γ phosphates.

The overall fold for the monomeric structure is very similar amongst the three complexes (Fig. 3-1). The root mean square deviation (r.m.s.d.) for the overlay of the apo protein with the ternary complex (for 144 Cα out of 185 residues) and for the binary and ternary complexes (162 Cα atoms out of 162) is 0.4 Å. The structures suggest little alteration in the total structure over the course of substrate binding yet there are two regions that change conformation upon substrate binding. The first region is the lasso loop which upon thymidine binding goes from a region devoid of interpretable electron density to a defined structure (Fig. 3-1B) The second region (residues 40 – 58) is unstructured in both the apo and the binary complex, and ATP binding induces the formation of a β-hairpin structure, consisting of a short β strand (βc1) and β3. From previously solved structures of the binary complexes of CaTK and ADP, and BaTK with
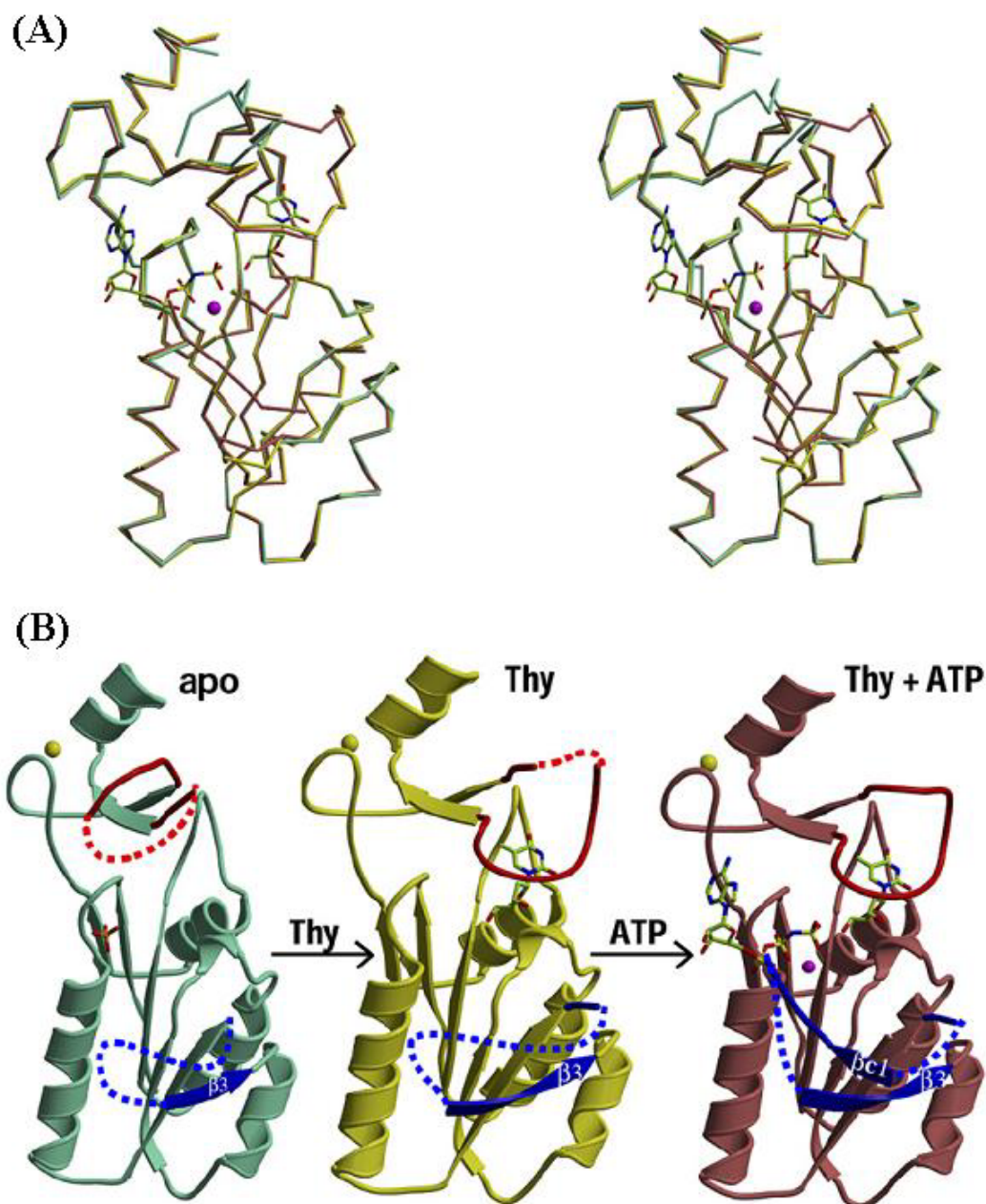
Figure 3-1: TmTK structures in apo, binary and ternary complex (A) Stereo view of an overlay of the three TmTK carbon backbones. The apo form in cyan, thymidine complex in yellow, and the ternary complex in magenta. Purple sphere represents Mg atom in the active site (B) Ribbon representation of the three individual structures. Same color scheme as in (A) with the addition of yellow spheres representing zinc atoms. Upon addition of thymidine the lasso loop (in red) forms almost to entirety. Upon addition of ATP, the lasso loop is completed and the $\beta c1$ hairpin forms (blue region)
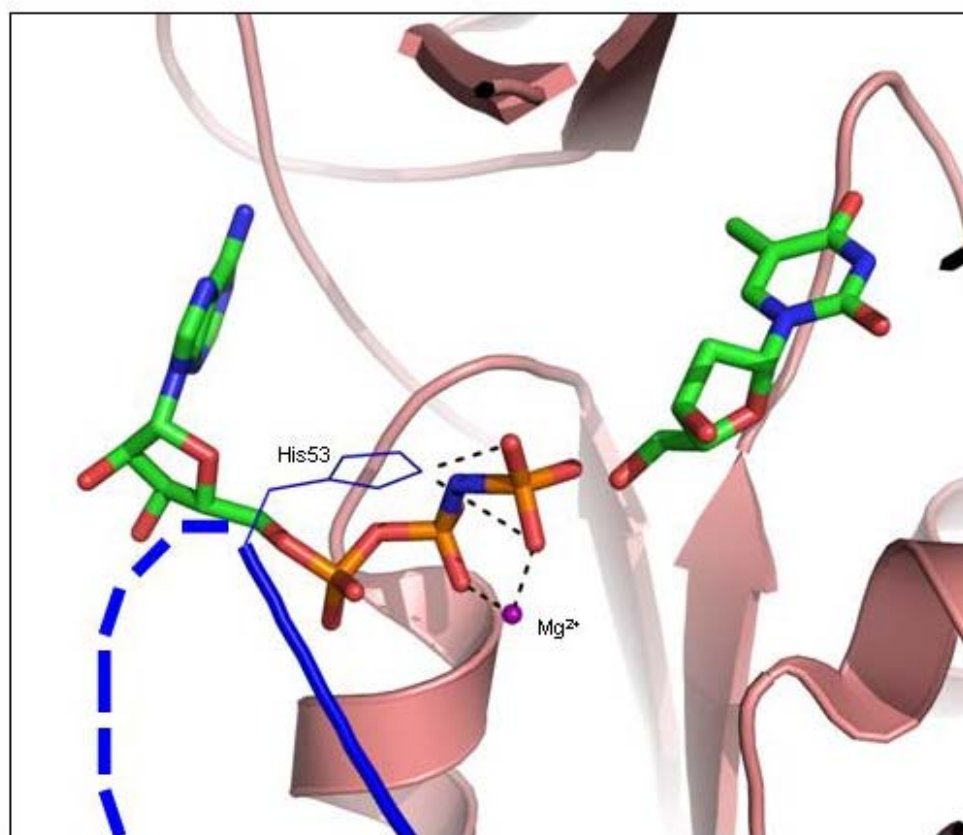
Figure 3-2: Role of histidine 53 in binding ATP. N3 of His53 makes potential hydrogen bonding contacts (pymol distance calculated = 2.6 and 3.5 Å) with the γ-phosphate from ATP in the ternary complex structure. This highly conserved histidine was suggested to play a role in catalysis. Shown in purple is the Mg^{2+} ion in the active site which also makes contacts with the β- and γ-phosphate (2.0 Å for both contacts shown)

TTP (bound at the ATP binding site), a similar organization of this region is seen, hinting

to the role of the phosphoryl donor in forming this conformation. A highly conserved

histidine at position 53, located at the tip of the β hairpin, forms hydrogen bonds with the

phosphates from the NTP donor, suggesting a role for the hairpin formation in catalysis

(Fig 3-2). To test this hypothesis, an H53A mutant was engineered and measured for

enzymatic activity, yet no change in ATP or thymidine kinetics were observed (Table 3-

2). Rather than being catalytically relevant, perhaps the loop functions as a sensor for

NTP binding, triggering other changes in the quaternary structure connected to the

opening at the dimer II interface. In the following section, further evidence suggesting

ATP's role in the conformational change of the β-hairpin movement is obtained through

fluorescence spectroscopy.

3.3.2 Tryptophan fluorescence monitors ATP induced β-hairpin movement

The suggested role of ATP inducing the formation of the β-hairpin region of

TmTK was investigated using tryptophan fluorescence. As mentioned in chapter 2,

tryptophan has strong fluorescence properties and is often used as a probe for measuring

conformational changes in proteins (Gorinstein, Goshev et al. 2000; Hagan, Worner-

Gibbs et al. 2005). With no tryptophans in the TmTK primary sequence, 5 separate

tryptophan mutants were engineered: three in the βc1/β3 region (V51W, G55W, V58W),

one proximal to the hairpin (V34W) that could provide an indirect probe for hairpin

movement, and one position far from the hairpin region (L129W, at the strong dimer

interface) serving as a control (Figure 3-3A). Following overexpression and purification,

the kinetic characterization for thymidine and ATP were measured for all 5 mutants and

compared to wild type, very little changes in catalytic properties were found (Table 3-2).

Other than L129W, all the tryptophan mutants had similar K_M values for thymidine with

small changes in turnover (k_{cat}). For ATP, comparable results were obtained for all

mutants except G55W, which is rationalized to have a 3-fold rise in apparent ATP

binding as a result of its proximity to the phosphoryl donor site. Our control L129W

shows a 6-fold increase in K_M and k_{cat} for thymidine, keeping the efficiency the same yet

appearing to have a weaker apparent binding constant and faster turnover. Initially we

rationalized this as being a result of the proximity to the thymidine binding site, thus only

seeing the increase in K_M for thymidine, however it might also be a result of the strong

dimer interface being disrupted. In chapter 4, the mutant L127R/V133R shows similar

kinetic values ($K_M = 5.2$ μM, $k_{cat} = 1.7$ s^{-1}) yet its migration on gel filtration is found to be

more similar to a monomer than a tetramer (or dimer). Considering that Leu129 is close

to these two residues and located on the alpha helix at the dimer I interface, there is a

possibility this mutation interferes with that interface leading to kinetics most closely

associated with a monomer TK. More on the interface mutations in chapter 4.

Table 3-2: Kinetic parameters for TmTK and mutants at 37 °C

Enzyme	Thymidine			ATP		
	K_M (μM)	k_{cat} (s^{-1})	k_{cat}/K_M (x 10^4 M^{-1}s^{-1})	K_M (μM)	k_{cat} (s^{-1})	k_{cat}/K_M (x 10^4 M^{-1}s^{-1})
Wild type	0.5 ± 0.2	0.3 ± 0.08	60	40 ± 12	0.4 ± 0.04	1.0
H53A	1.2 ± 0.2	0.51 ± 0.01	43	86 ± 7	0.52 ± 0.01	0.6
V34W	0.9 ± 0.2	0.59 ± 0.02	63	23 ± 4	0.35 ± 0.01	1.5
V51W	0.7 ± 0.1	0.25 ± 0.01	34	35 ± 5	0.20 ± 0.005	0.6
G55W	0.8 ± 0.1	0.62 ± 0.01	77	112 ± 10	0.45 ± 0.005	0.4
V58W	0.5 ± 0.1	0.47 ± 0.01	96	29 ± 3	0.38 ± 0.008	1.3
L129W	3.0 ± 0.3	1.91 ± 0.05	64	46 ± 5	1.49 ± 0.02	3.2

(A)

(B)
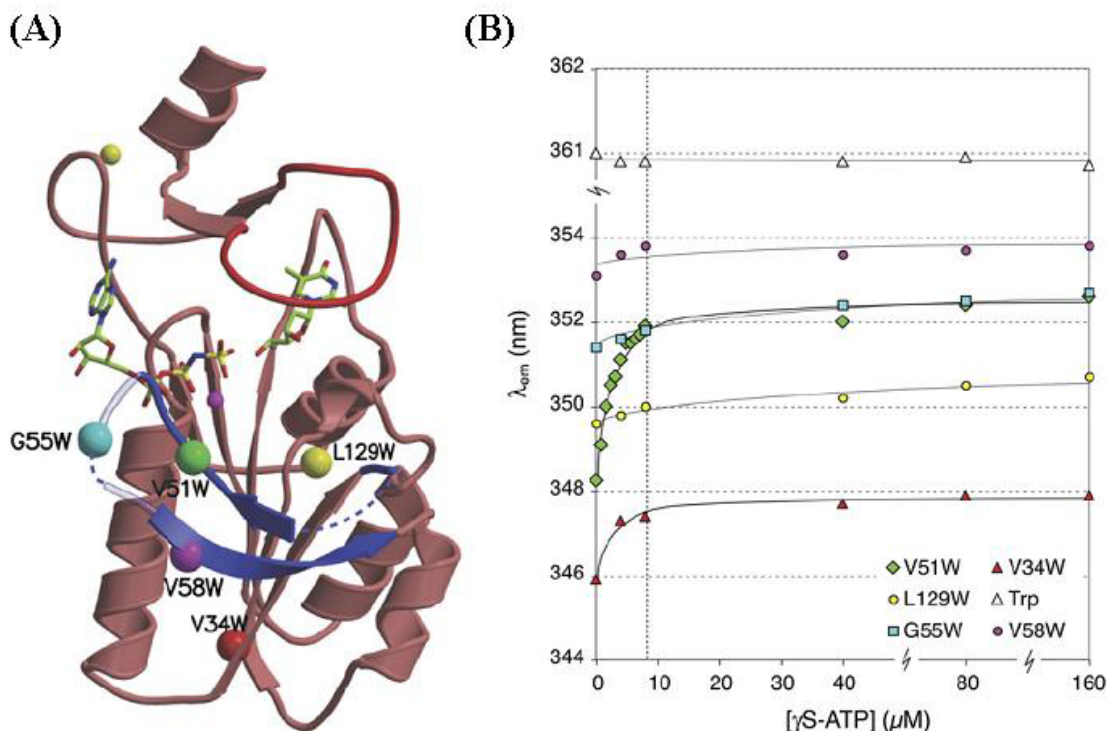
Figure 3-3: Tryptophan mutants and the fluorescence changes upon ATP binding. (A) Ribbon diagram of a TmTK monomer (in the ternary complex) with the tryptophan mutants labeled with colored spheres. (B) Changes in the fluorescence emission wavelength of TmTK tryptophan mutants during titration with γ-thio-ATP

The 5 tryptophan mutants were individually monitored using fluorescence upon titration with the non-hydrolyzable γ-thio-ATP. Initial experiments were done at 37 °C, to maintain the temperature used in the kinetic experiments. However, difficulties in reproducible results (over the set of 3 scans) was attributed to compromised stability of the mutants. Lowering the temperature for titration experiments to 10 °C increased the precision of the results. The ATP analog was titrated into TmTK solutions with and without thymidine present. No difference was seen when thymidine was present, consistent with the structural observation that the binding of the phosphoryl acceptor does not induce any changes to the βc1/β3 region. When titrating the ATP analog into the tryptophan mutants, distinct changes in fluorescence emission maximums (λ_{max}) are seen.

Initially, all five of the mutants have λ_{max} in the range of 346 to 354 nm. The blue shift in λ_{max} for the mutants as compared to free tryptophan (361 nm) is indicative of a more hydrophobic environment sensed by the indole moiety of the tryptophans. Upon titration with the ATP analog, λ_{max} for V34W and V51W red shifted 2 and 4 nm, respectively. At equimolar concentration of TmTK and γ-thio-ATP, a saturation level is reached. The data suggests a significant change in these tryptophan residues local environment as a result of ATP binding. For V34W, substrate binding causes an upward movement of the $\beta c1/\beta 3$ region, exposing the underlying position 34 to a more hydrophilic environment. In the case of V51W, the loop relocation likely changes the position of the tryptophan residue from a shielded interior position to the protein surface. The absence of similar wavelength shifts for G55W and V58W, which are also located in the same region, can be rationalized by small changes in the residues' local environments upon the organization of the hairpin. Consistent with this interpretation, the initial high λ_{max} prior to ATP analog titration suggest they are surface exposed prior to phosphoryl donor binding whereupon a shift in that region to the formed hairpin likely will not bury the residues and thereby minimal change is seen. For both G55W and V58W, the slight changes in λ_{max} are comparable to that of the control L129W. In summary, our fluorescence data are consistent with the structural observations of a conformational change in the $\beta c1/\beta 3$ region resulting from ATP binding.

3.3.3 ATP binding induces a conformational change in the quaternary structure

Along with tertiary structural changes, significant changes to the homotetramer's structure can be observed upon ATP binding. From the tetramers of all 3 complexes, the apo and the binary show similar dimensions across both the dimer I and dimer II interfaces dimensions while the ternary complex exhibits a 10% increase in the distance across the dimer II interface (from ~51 Å in the binary to ~56 Å in the ternary) (Fig 3-4). The expansion suggests that there exists a closed state (apo and binary) and an ATP induced open state (ternary). As a result of the interface widening, different contacts occur at the weak dimer interface for the two states. In the closed state, dimer II interface contacts are made up mainly of side chains from residues in helix α1 [19 Van der Waals (VdW) contacts, 3 salt bridges, and 3 polar interactions]. For the open state, the same interface is made up of 31 VdW contacts, 2 salt bridges, and 6 polar interactions. However in the open state, 20 out of the 31 VDW contacts and all 6 polar interactions involve the phosphoryl donor.

An analysis of the buried surface area at the dimer II interface helps to further illustrate the changes that takes place upon ATP binding. In the closed state the occluded surface area is ~900 $Å^2$ for the apo and 1030 $Å^2$ for the thymidine bound. The ternary complex has only 370 $Å^2$ of protein-protein surface contact area. When combining ATP interactions, the occluded surface area increases an additional 260 $Å^2$ to 630 $Å^2$, still significantly lower than the apo and binary complex. The same calculations at the dimer I interface show no significant change between the 3 states: 1070 $Å^2$ for apo, 1130 $Å^2$ for binary, and 1050 $Å^2$ for ternary.
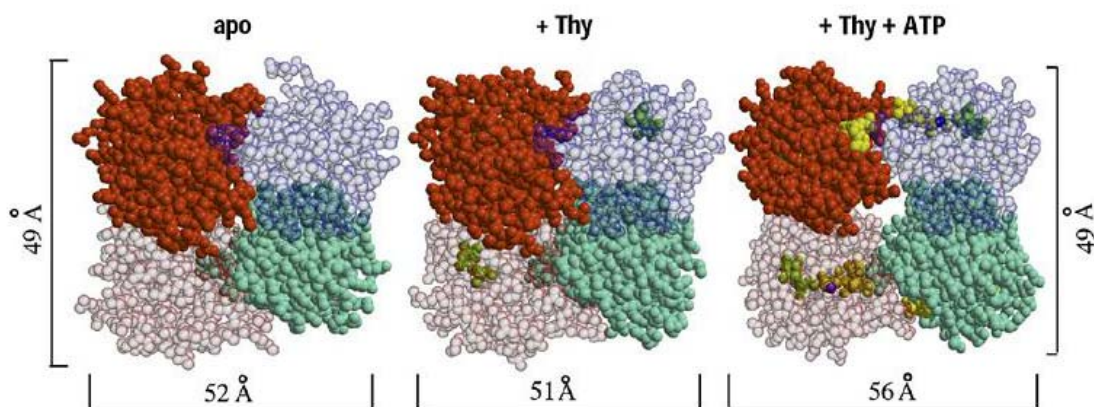
Figure 3-4: ATP induces dimer II expansion. Sphere representation of TmTK homotetramer in the 3 substrate-bound states. Individual monomers are shown in different colors. ATP and thymidine are shown in yellow and green, respectively. No change in the strong dimer interface (y-axis) noted with substrate binding. Upon ATP binding, the tetramer expands at the dimer II interface.

Due to greater number of protein-protein interactions and higher occluded surface area, it is suggested that the closed inactive conformation is the more stable. Interestingly, the structure of hTK1 with TP4A, indicated that the closed state is unable to accommodate the phosphoryl donor in the correct orientation (Segura-Pena, Lutz et al. 2007). In that structure there is no electron density for the adenosine portion of TP4A, due to its disordered orientation, indicative of incorrect or weak binding. This would suggest the closed state is unable to position the phosphoryl donor correctly and therefore can not catalyze phosphorylation. To experimentally validate that type-II TKs adopts a closed tetramer in solution and that this closed state is not active (or barely active compared to the open state), disulfide bridges were engineered at the dimer II interface to lock the interface closed.

3.3.4 Trapping the closed conformation by disulfide linkage

The TmTK structures in the closed state suggest that thiol side chains of cysteines at positions 18 and 22 along the α1 helix would be in close proximity to the corresponding residues of the neighboring subunit across the dimer II interface (Fig. 3-5). Under oxidizing conditions, the thiols are predicted to form two disulfide bridges, covalently linking the two subunits into the closed conformation. The locking of this interface will interfere with proper binding of ATP and should render the enzyme catalytically incompetent. Addition of a reducing agent should be able to reduce the disulfide bridges to –SH groups and re-open the interface, allowing for ATP binding and catalytic competency.

To test these predictions, the double cysteine mutant T18C/S22C was engineered, along with a double alanine mutant (T18A/S22A) used as a control to account for any possible effects of mutagenesis at these positions. Initially, these two mutants were overexpressed and purified similarly to previously described protocols (chapter 2). To validate the presence of the disulfide bonds, non reducing SDS-PAGE gels were run. From these gels, it appeared the T18C/S22C had a mixed population of proteins with 2 bands running at ~28 and ~45 kDa (Fig. 3-6). The higher band's MW corresponds to a disulfide linked dimer, while the lower band's monomeric size is comparable to that of wild type. The reason for two states of proteins is likely due to incomplete disulfide bond formation. It has been reported that the *E. coli* cytoplasm is too reducing for disulfide bonds to form (Poulsen and Ziegler 1977; Gilbert 1990) and as a result the glutaredoxin pathway in *E. coli* might cap the engineered cysteines with glutathione (Prinz, Aslund et al. 1997). The purification protocol was modified to include reducing agent in the
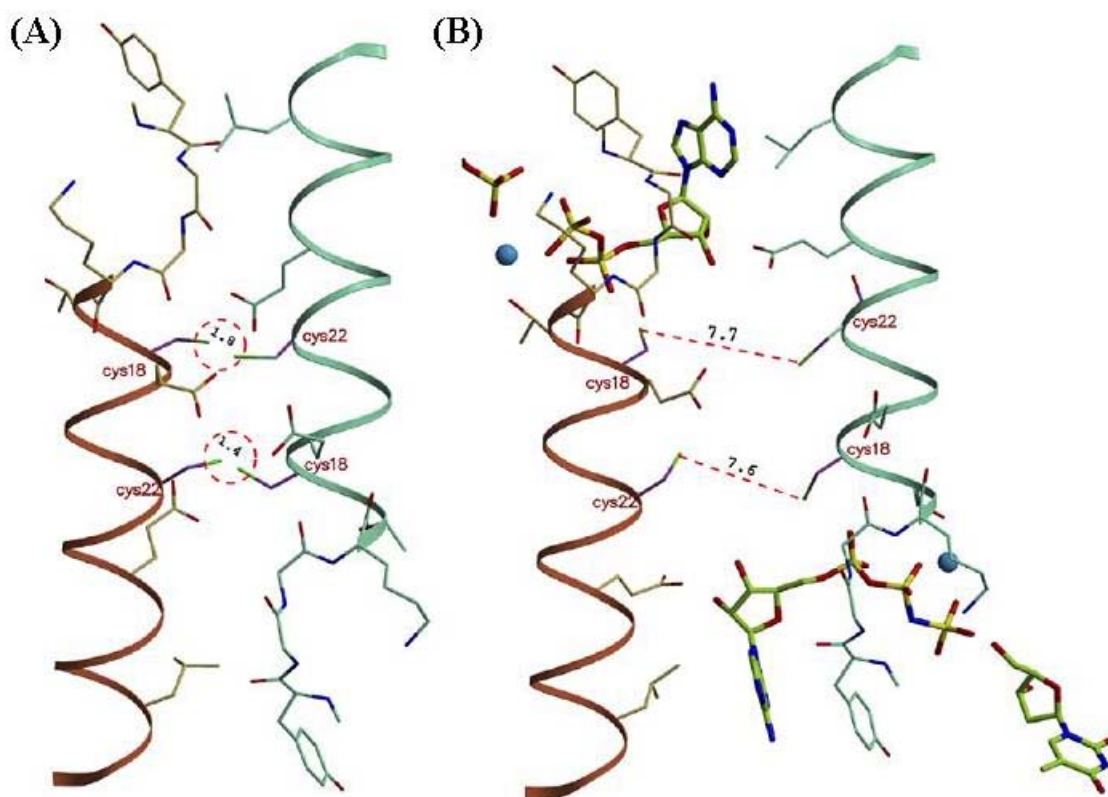
Figure 3-5: Disulfide bond modeling. (A) The closed state shows the close proximity of the α1 helices, specifically positions 18 and 22 where cysteines are modeled to have less than 2 Å between the –SH groups. (B) The open state shows the distance between positions 18 and 22 expands by 6 Å. The open state is therefore predicted to be unable to form a covalent linkage between engineered cysteines. These models were generated by Dr. Dario Segura-Pena using the program "O" (Segura-Pena, Lichter et al. 2007).
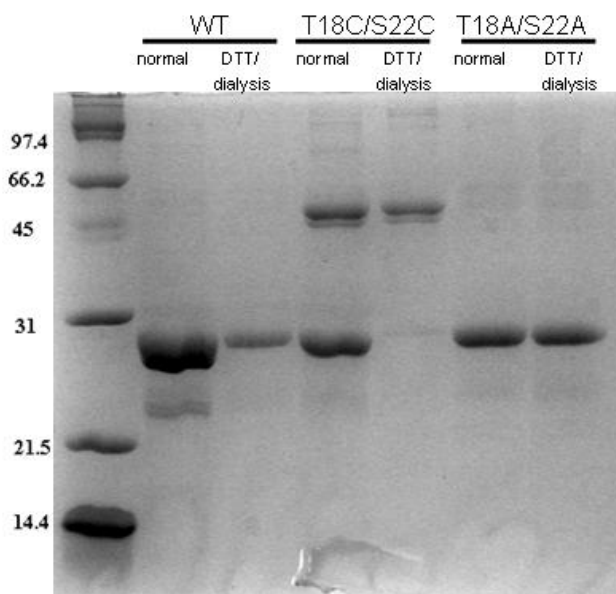
Figure 3-6: 12% SDS-PAGE gel of TmTK mutants purified normally and with DTT and dialysis. All samples were prepared in SDS buffer without β-mercaptoethanol, heated at 100 °C for 7 min, then cooled down to 4 °C for 5 min and then loaded on gel

purification buffers to maintain the reduced form of the sulfhydryl and eliminate capping or unspecific linkage. Upon elution from the Ni-NTA agarose column, protein samples were dialyzed against a protein storage buffer without reducing agent, thereby leaving the protein in an oxidizing environment and promoting the covalent linkage of the no longer reduced sulfhydryl groups. Initially, dithiothreitol (DTT) was used to reduce the protein. Experiments testing the affect of DTT on TmTK showed no effect when incubating the protein in up to 6 mM DTT for one day (at ambient temperature) yet a 40% lowering in catalytic activity when in 8 mM DTT. Therefore T18C/S22C was purified in the presence of 5 mM DTT then dialyzed for 3 days in protein storage buffer without reducing agent. After extracting the protein from the dialysis cassette, the protein formed one band at ~45

kDa (Figure 3-6), suggesting the complete formation of disulfide bound TmTK. The faint

appearance of two bands at 45 kDa is likely due to a potential disorientation of one of the

disulfides either from position 18 of one helix binding with position 18 on the other (as

opposed to the presumed correctly oriented position 22). Experiments using Ellman's

reagent [5,5'-Dithiobis(2-nitrobenzoic acid), Fluka] were done to test for free thiols

present in T18C/S22C (post dialysis), yet results were inconclusive mainly due to

incomplete reactivity.

Initial kinetic studies for the normally purified and the DTT purified/dialyzed

samples were done using saturating conditions for both ATP and thymidine. The results

show a small change in v_{max} for wild-type as a result of the new purification scheme, but

within margin of error (Table 3-3). Consistent with the hypothesis that a disulfide bound

protein will exist in the closed inactive conformation, the single population of disulfide

bound T18C/S22C retained only 1% of the activity of wild type. Interestingly, the mixed

population of protein seen in the normally purified T18C/S22C sample lost ~80% of

protein activity, likely due to the fraction of protein existing in the disulfide form. The

double alanine control showed a slight increase in activity suggesting that modifying

positions 18 and 22 to other amino acids does not confer a negative result.

Table 3-3: Max reaction velocities for TmTK disulfide mutant and controls (w/DTT)

enzyme	v_{max} (nmol mg $^{-1}$ min^{-1})	% relative activity
wt (normal)	1010 ± 90	100
wt (DTT/post dialysis)	930 ± 70	92
T18C/S22C (normal)	210 ± 10	21
T18C/S22C (DTT/post dialysis)	12 ± 1	1
T18A/S22A (normal)	1100 ± 100	109
T18A/S22A (DTT/post dialysis)	1220 ± 140	120

Experiments to reverse the disulfide bridges by adding reducing agent was undertaken. Protein samples were incubated with DTT (from 5 - 10 mM) for up to 3 days and found to be incapable of reducing the dimer band in SDS PAGE gels. Different reducing agents were then tried. Experiments were first sought with β-mercaptoethanol which was found to diminish the activity of wild type by 66% upon purification and dialysis. We therefore used TCEP, a common reducing agent that is not bi-functional, stable at most pH, and has been shown to be a more effective reducing agent than DTT (Han and Han 1994). Purification buffers were then supplemented with 5 mM TCEP and dialyzed for three days. Analysis of the non-reducing SDS PAGE gel indicates the majority of T18C/S22C mutant migrates as a dimer under these conditions (Fig 3-7).

Due to the TCEP treatment, v_{max} rates were compromised for wild type and T18A/S22A to roughly 70% and 50% respectively (Table 3-4). Yet still, the v_{max} for the T18C/S22C was measured to be only ~4% of the measured activity for wild type under the same conditions. More importantly, the reduction of the disulfide bonds was achieved in T18C/S22C, resulting in a 30-fold higher kinase activity. The recovered activity in T18C/S22C (reduced with 8 mM TCEP) is comparable to the WT treated with 8 mM TCEP, considering that only ~70 % of the double-cysteine mutant was reduced. The experiments with TCEP suggested that too long of an incubation or too high of TCEP concentration would interfere with enzymatic activity, which can be attributed to interference with the native cysteines that bind the structural zinc ion. In summary, the SDS PAGE analysis and kinetic measurements confirm that the double-cysteine mutant, T18C/S22C, can be locked in the catalytically incompetent, closed conformation under

oxidative conditions. The disulfide bridges can be reversed with the addition of a

reducing agent, allowing for resurgence of catalytic capability.
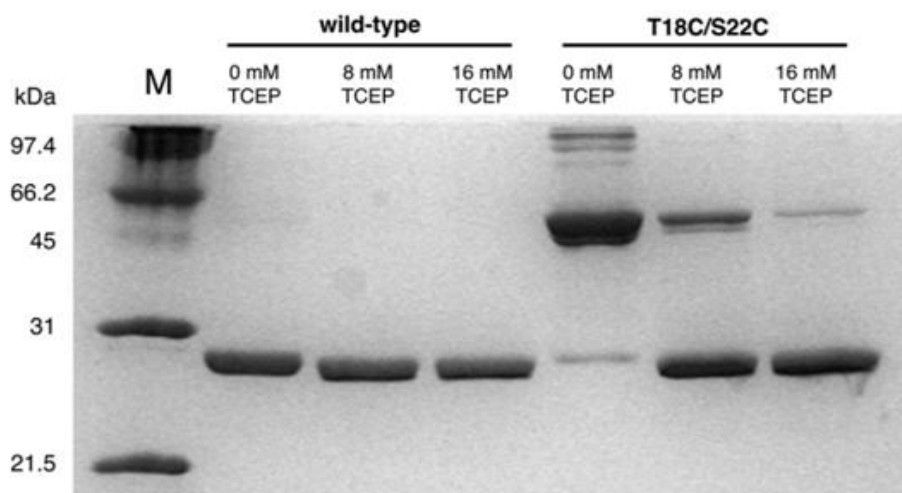
Figure 3-7: 12% SDS-PAGE analysis of the TCEP treated proteins (under non-reducing conditions). Shown in the gel were parallel experiments run with wild type and T18C/S22C. Protein samples purified in the presence of 5 mM TCEP and dialyzed for three days were then incubated with 0, 8, or 16 mM TCEP for 3 days. In the T18C/S22C sample un-incubated (0 mM TCEP) the presence of higher bands is likely due to unspecific disulfide linkages formed in the 3 days of dialysis.

Table 3-4: Max reaction velocities for TmTK disulfide mutant and controls w/TCEP

enzyme	Protein treatment	v_{max} (nmol mg^{-1} min^{-1})	% relative activity
WT TmTK	w/TCEP & dialysis	670 ± 30	100
T18A/S22A	w/TCEP & dialysis	620 ± 30	92
T18C/S22C	w/TCEP & dialysis	25 ± 0.1	3.7
WT TmTK	Postdialysis; 0 mM TCEP	670 ± 20	99
	Postdialysis; 8 mM TCEP	350 ± 25	52
	Postdialysis; 16 mM TCEP	76 ± 0.5	11
T18C/S22C	Postdialysis; 0 mM TCEP	7.6 ± 2	1.1
	Postdialysis; 8 mM TCEP	222 ± 5	33
	Postdialysis; 16 mM TCEP	86 ± 2	13

3.4 Conclusion

The crystal structures for TmTK in the apo, thymidine bound, and ternary complex support the hypothesis of conformational changes due to substrate binding as part of the catalytic cycle. The combination of crystallographic data and fluorescence measurements confirm the role of thymidine and ATP binding in ordering TmTK's structure. Thymidine binding organizes the lasso region, while ATP binding in the phosphoryl donor site induces the formation of an ordered β-hairpin structure in the βc1/β3 region and an expansion of the weak dimer interface by 4-5 Å. This elongation of the weak dimer interface allows for proper positioning of ATP and appears critical for TmTK's catalytic cycle. Consistent with this observation was the elimination of catalytic competency upon introduction of two disulfide bridges bridging the α1 helices at this interface.

Our observed quaternary structure changes can also explain the positive cooperativity measured for both hTK1 and TmTK with ATP (Hill coefficient ~ 2) (Munch-Petersen 1984; Lutz, Lichter et al. 2007). The allosteric nature can be rationalized by two proposed conformational states equivalent to the taut (T) state and relaxed (R) state proposed in the Monod, Wyman, and Changeaux (MWC) model (Monod, Wyman et al. 1965). Prior to the addition of ATP, a taut form is the more thermodynamically preferred state, yet it shows low substrate affinity due to the lack of space to accommodate the ATP. Upon one ATP binding, the tetramer must expand to accommodate the adenosine portion, and that expansion will increase the affinity for the other ATP molecules in a cooperative fashion (Fig. 3-8).
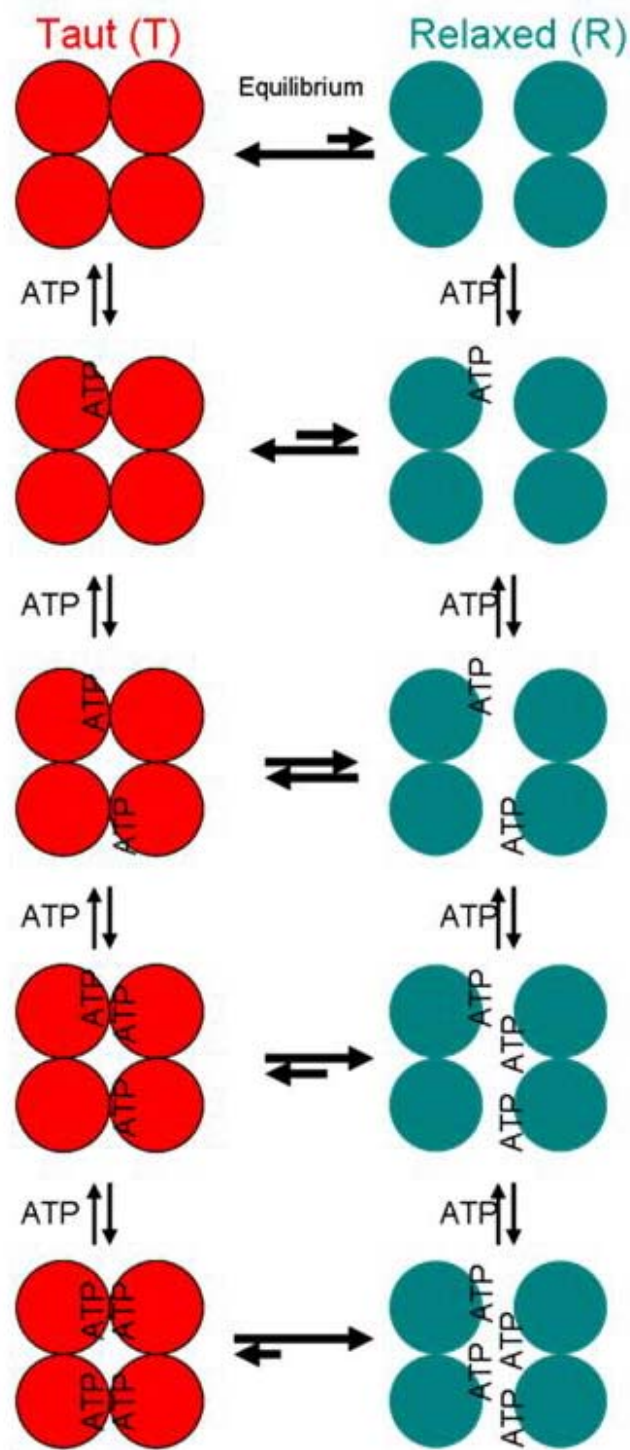
Figure 3-8: Proposed 2 state model for TmTK using the MWC model. The thermodynamically preferred closed inactive conformation (in red) is the taut (T) state, while the open active conformation (in green) is the relaxed (R) state. The addition of ATP will shift the equilibrium to the open conformation.

Thinking deeper into this 2-state model of TmTK, questions arise regarding the timing of catalysis in the enzyme complex. It is unclear whether the four reaction sites operate in a concerted manner or whether they work independently. The allosterism seen for TmTK at 82 °C suggests cooperativity between sites as a function of ATP binding. Yet, whether or not all 4 sites must be charged in order for proper orientation of substrates and a subsequent phosphorylation is unknown. Should a synchronized reaction utilizing all 4 sites be relevant to catalysis, then the apo-protein complex could result following one turnover, giving the closed conformation relevance as part of the reaction cycle. In contrast, a random catalysis would significantly lower the probability of all four sites being vacant, making the closed conformation a rare occurrence. Furthermore, a typical mammalian cell's ATP concentration is generally in the millimolar range making it highly unlikely that a TK will ever exist in an ATP-free state (Erecinska and Silver 1994).

Aside from its role in catalysis, the quaternary structure could be relevant as a regulatory mechanism. Evidence for this comes from other structures of type-II TKs. Despite attempts by other groups to isolate the apo form of the enzyme, the experiments consistently found the feedback inhibitor TTP in the phosphoryl acceptor binding site. In addition to blocking thymidine binding, the β and γ phosphates from TTP occupy the same positions generally held by a phosphoryl donor. TTP has been reported to have an inhibition constant (K_i) for hTK1 of 0.6 μM (Lee and Cheng 1976). With the TTP concentration reaching up to 20 μM at the end of the S-phase, ATP K_M values increase by 100-1000 times (Spyrou and Reichard 1988; Hu and Chang 2007). The feedback inhibitor's affect on ATP binding is dramatic considering that TTP binds in the acceptor

site with only the β and γ phosphate of both triphosphates binding in similar positions. A suggested reason for such a drastic effect by TTP is a conformational change induced by the feedback inhibitor, essentially pushing the protein into the closed inactive conformation. Upon TTP binding not only does the inhibitor occupy part of the active site, but it forces the enzyme complex into the closed conformation, dismantling ATP binding and shutting off catalysis.

In summary, this chapter presents the first structural and biochemical examination of a type-II TK along its catalytic cycle. Thymidine binding induces the formation of the lasso region while ATP binding forms the β-hairpin and an expansion along the weak dimer interface. Our proposed 2-state model (open and closed) for TmTK induced by ATP was consistent with our disulfide bond mutagenesis and could be critical for TmTK regulation and/or catalysis.

Chapter 4: Investigating the Oligomeric State of TmTK

4.1 Introduction

Four high resolution crystal structures for TmTK have been obtained: (1) the complex with the bisubstrate mimic TP4A (Segura-Pena, Lutz et al. 2007), (2) in the apo form, (3) with thymidine bound, and (4) in the ternary complex with thymidine and ATP (Segura-Pena, Lichter et al. 2007). Other than the apo protein which forms a tetramer in the asymmetric unit (space group $P2_1$), the TmTK structures crystallized in the asymmetric unit as a dimer (in the space group C2). Using crystallographic 2-fold symmetry, the presumed biologically active tetramer was built. The presumption that TmTK naturally exists as a tetramer is due to the presence of tetramers in the asymmetric unit of TmTK (apo form) crystals, as well as reports of other type-II TKs eluting as tetramers from size exclusion chromatography (Birringer, Perozzo et al. 2006) and crystallizing as tetramers (Welin, Kosinska et al. 2004). However, a closer look at the literature reveals that not all type-II TKs are tetramers. A 14 residue N-terminal truncated hTK1 (Birringer, Claus et al. 2005) and the TK from *Bacillus cereus* (Kosinska, Carnrot et al. 2007) exist as dimers. As well, an ATP-induced reversible transition in hTK1 from low-active dimer to highly active tetramer has been reported (Munch-Petersen, Tyrsted et al. 1993).

The two-state model for TmTK proposed in chapters 2 and 3 suggested the native tetramer expands along one interface as part of the catalytic cycle. The validity of this model depends upon whether the protein is a tetramer and whether or not that interface is

real. Furthermore, which of the dimer interfaces are present in the physiological TK is unclear. In TmTK structures with a dimer in the asymmetric unit, the dimer I ("strong") interface is always intact. The dimer II ("weak") interface is formed from crystallographic symmetry. The question then arises whether this weak interface is part of the native complex for TmTK. In reporting the structure for hTK1, Birringer et. al. found hTK1 eluted as a dimer and suggested the dimer II interface to be significant due to its role in positioning ATP (Birringer, Claus et al. 2005).

In this chapter, the oligomeric state and interfaces were studied for TmTK. First, the size exclusion chromatography (SEC) profile of TmTK was measured and compared to internal standards. SEC results show wild type TmTK elutes with a major peak corresponding to a molecular weight (MW) of 67 kDa, which does not fit with the predicted MW for a dimer (45 kDa) or a tetramer (91 kDa). A comparison of the SEC profile for wild type TmTK and hTK1 shows a difference in migration patterns, suggesting the unusual SEC migration is specific for TmTK. A comparison of SEC profiles for wild type and the mutant T18C/S22C, presents the possibility for both a monomer-dimer (M-D) and a monomer-dimer-tetramer (M-D-T) equilibrium.

To examine the relevance of the interfaces, mutagenesis studies were conducted whereby bulky amino acids were substituted in positions at each interfaces (separately) that could disrupt existing contacts. Two arginines were introduced in a hydrophobic pocket in the dimer I interface (L127R/V133R) and on the α1-helix at the dimer II interface (T18R/S22R). The dimer I mutant migrates in SEC predominantly as a monomer while still retaining catalytically activity. The mutagenesis suggests contacts at the dimer I interface are relevant in maintaining the native structure of TmTK. The dimer

II mutant shows no change in SEC profile or catalytic performance, suggesting either the

mutagenesis did not disrupt the presumed interface or the interface is not real (and

therefore TmTK is a dimer with the dimer I interface intact). Lastly, chemical

crosslinking experiments were employed with amine and sulfhydryl reactive crosslinkers,

to try to isolate the solution state oligomer. Sedimentation equilibrium experiments

conducted by colleague Dr. Ziad Eletr are included in the conclusion, further discussing

the possibility of both a monomer-dimer (M-D) and monomer-dimer-tetramer (M-D-T)

equilibrium .

4.2 Materials and Methods

4.2.1 Site directed mutagenesis

TmTK mutants were made using primer overlap extension PCR with pET-His-
tmtk as the template (Lutz, Lichter et al. 2007). The following single mutants were

constructed: T18R, S22R, L127R, V133R, S22C, and S128C. The primers used to design

each of these mutants are listed in table 4-1. Further mutagenesis to create the double

mutants T18R/S22R, L127R/V133R, and S22C/S128C was performed using a 2nd PCR

overlap protocol, where the newly created single mutant genes were used as DNA

template. Restriction sites for *Nde*I and *Spe*I were included in the primers and introduced

at the 5' and 3' position of the genes, respectively. Restriction digestion of the PCR

products was performed and the products were ligated into the vector pET14b. Ligated

gene-plasmid constructs were transformed into *E. coli* DH5α cells and plated on LB

plates ([Amp]=100 μg/ml). Mutations were confirmed via DNA sequencing.

Table 4-1: Primers used for site directed mutagenesis

T18R_a	5'	CCGGAAAGACACGCGAGCTTCTCTCC	3'
T18R_b	5'	GGAGAGAAGCTCGCGTGTCTTTCCGG	3'
S22R_a	5'	CGAGCTTCTCCGCTTTGTGG	3'
S22R_b	5'	CCACAAAGCGGAGAAGCTCG	3'
L127R_a	5'	GGCGAGACTGCGGAGCAGAGCGG	3'
L127R_b	5'	CCGCTCTGCTCCGCAGTCTCGCC	3'
S22C_a	5'	CCGAGCTTCTCTGCTTTGTGG	3'
S22C_b	5'	CCACAAAGCAGAGAAGCTCGG	3'
S128C_a	5'	CTGCTCCTCTGCCTCGCCGACACC	3'
S128C_b	5'	GGTGTCGGCGAGGCAGAGGAGCAG	3'

4.2.2 Protein overexpression and purification

Previously established protocols for TmTK overexpression and purification,

using the pET14b vector with an N-terminal $(His)_6$-tag system in BL21(DE3) cells were

used for both wild type and mutants (Lutz, Lichter et al. 2007). For SEC experiments

with wild type and T18C/S22C, the following protein storage buffer was used: 50 mM

Tris pH 8.0, 150 mM NaCl, 2.5 mM $MgCl_2$. For chemical crosslinking purposes, protein

storage buffers were supplemented with 50 mM potassium phosphate buffer pH 7.2

instead of Tris-HCl pH 8.0. Following protein purification, proteins were buffer

exchanged via ultrafiltration (Amicon Ultra-15, MWCO: 10 kDa, 4000 g at 4 °C) into

protein storage buffer, flash frozen in liquid N_2 and stored at -80°C. Protein

concentrations were quantified using A_{280} absorbance readings with molar extinction

coefficients calculated as follows: T18R/S22R and L127R/V133R: $\varepsilon_{280} = 9260$ $M^{-1}cm^{-1}$;

S22C, S128C : $\varepsilon_{280} = 9320$ $M^{-1}cm^{-1}$; S22C/S128C: $\varepsilon_{280} = 9380$ $M^{-1}cm^{-1}$ (Bio Workbench

3.2). Protein aliquots were stored at -80 °C after flash freezing in liquid nitrogen.

4.2.3   hTK1 gene isolation and protein overexpression/purification

hTK1 gene was isolated from human cDNA clones (clone# HSCD 00004059;

Harvard Institute of Proteomics) using gene specific primers containing unique restriction

sites. The gene was digested and ligated in pET14b with an N-terminal $(His)_6$-tag .

Protein overexpression was achieved by using the protocols published by Birringer et. al.

(Birringer, Perozzo et al. 2006). The buffer used during protein purification was switched

to 50 mM KP_i (pH 7.2) in place of 50 mM Tris (pH 8.0) for samples prepared for

crosslinking experiments. Protein purification was done with Ni-NTA agarose columns,

and elutions were analyzed via SDS PAGE gels. Fractions containing pure protein were

buffer exchanged via ultrafiltration (Amicon Ultra-15, MWCO: 10kDa, 4000 g at 4 °C, 4

cycles of 15 minutes) into protein storage buffer, flash frozen and stored at -80 °C .

Protein concentrations were quantified using A_{280} absorbance readings with a molar

extinction coefficient $\varepsilon_{280} = 7680$ $M^{-1}s^{-1}$

4.2.4 Enzyme kinetics

Enzymatic activity was determined using a pyruvate kinase-lactate dehydrogenase

coupled enzyme-assay (Schelling, Folkers et al. 2001; Lutz, Lichter et al. 2007). Kinetic

data for TmTK mutants were measured for thymidine (using 2 mM ATP as phosphoryl

donor) and ATP (using 60 μM thymidine as acceptor). For hTK1, only the kinetic

parameters for thymidine were determined. Assays were performed at 37 °C and done in

triplicate.

4.2.5 Size exclusion chromatography

SEC analysis was performed using a Superdex 200 10/300 GL FPLC column (GE Healthcare) pre-equilibrated with protein storage buffer. For wild type and T18C/S22C experiments, 100 µl of protein at varied concentrations was injected onto the column and eluted at a flow rate of 0.5 ml/min at ambient temperature. Elution profiles for the proteins were monitored by UV absorbance at 280 nm. hTK1 (~6 mg/ml, 100 µl) was injected and run with similar conditions. In the mutagenesis studies, 500 µl of T18R/S22R (~10 mg/ml), L127R/V133R (~10 mg/ml), and wild type (~10 mg/ml) were injected onto the column and eluted at a flow rate of 0.5 ml/min. Crosslinked wild type and L127R/V133R were injected at smaller volumes (50 µl) and monitored with absorbance at 220 nm. A calibration curve was established using a set of MW standards (Bio-Rad, Hercules, CA) that included the following reference proteins: gamma globulin (158 kDa), ovalbumin (44 kDa), and myoglobin (17 kDa).

4.2.6 Chemical crosslinking

Two sets of chemical crosslinking experiments were performed: using the amine reactive bis(sulfosuccinimidyl)suberate (BS^3) or the sulfhydryl reactive 1,8-bis(maleimido)diethylene glycol [BM(PEG)$_2$] (Pierce Biotechnologies). For experiments using BS^3, 50 µM protein was reacted with 400 µM BS^3 in 200 µl reaction volumes. After the addition of crosslinker, time points from 0-6 hours were taken by quenching 10 µl of the reaction mixture with 100 mM Tris pH 8.0. Time points were prepared in SDS PAGE running buffer (heated to 95 °C for 10 minutes, and cooled down to 4°C), run on 10%

SDS gels and visualized using coomassie staining. Separately, un-crosslinked and crosslinked protein samples were injected into the Superdex 200 10/300 GL column and analyzed for changes in their elution profiles.

Experiments with BM(PEG)$_2$ were performed using the cysteine mutants S22C, S128C, and S22C/S128C as well as with wild type TmTK (as a negative control). 100 μM protein was reacted with 200 μM BM(PEG)$_2$ in 200 μl reactions. Time points were taken from 0 – 24 hrs by quenching 10 μl with 100 mM DTT. Reactions were prepared without β-mercaptoethanol yet heated similarly to the samples prepared in the BS^3 experiments, run on 10% SDS gels and visualized with coomassie staining.

4.3   Results and discussion

4.3.1 Native TmTK elutes as a 67 kDa protein

In chapter 2, gel filtration was reported as a second step in the TmTK (without (His)$_6$-tag) purification process (Lutz, Lichter et al. 2007). While the protein elutes as one major peak, it consistently travels with a MW of approximately 70 kDa, which is ≈ 20 kDa less than expected for a tetramer. In this chapter, a further examination of the native state was conducted with higher selectivity and at different concentrations, using an analytical size exclusion chromatography column. SEC for TmTK shows a major peak corresponding to an estimated MW of 67 kDa with a second smaller peak of 24 kDa (Fig. 4-1, with calibration curve seen in Fig. 4-2). The primary sequence for TmTK (with a His$_6$-tag) is 23 kDa, suggesting the smaller peak is the monomer. Yet, the major peak does not fit the expected MW value of a tetramer and fits better as a trimer, which has not been seen in any of the existing TK structures deposited. Based on the symmetry seen in
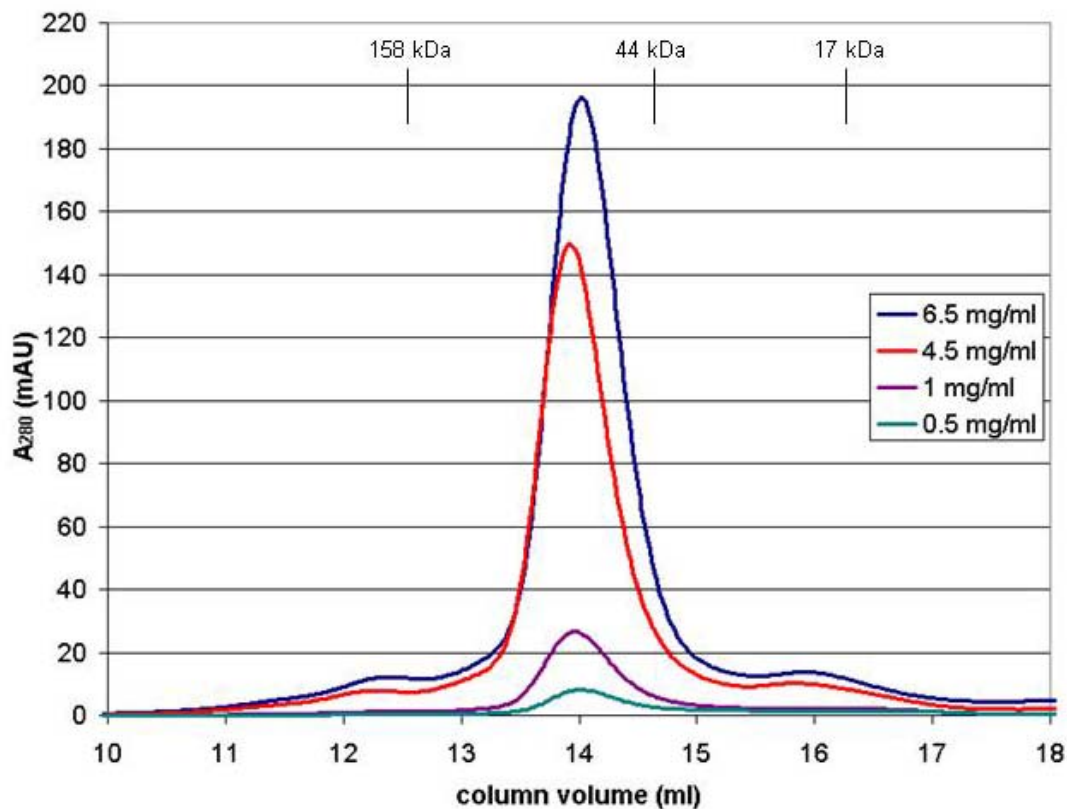
Figure 4-1: SEC for wild type TmTK. Range of concentrations measured from 0.5 -6 mg/ml (20 – 300 μM).
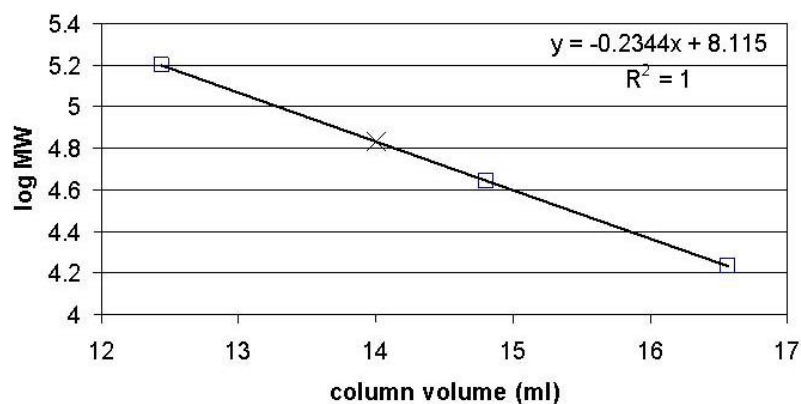

Figure 4-2: Calibration curve for wild type TmTK SEC data. Open squares represent the internal standards: gamma globulin (158 kDa), ovalbumin (44 kDa), myoglobin (17 kDa). X marks wild-type TmTK.

the TmTK structure, it is doubtful that the native protein exists as a trimer (Segura-Pena, Lichter et al. 2007; Segura-Pena, Lutz et al. 2007). Presumably, the migration of the protein is due to an irregular shape created by either a tightly compacted tetramer or a loose dimer. In an effort to look at any changes in the elution profile for wild-type TmTK as a function of concentration, samples of 0.5 - 6 mg/ml (20 - 300 μM) were investigated. No significant changes in the profile were seen in this concentration range. Dissociation constants (K_D) for type-II TK protein subunits have not been studied, however the K_D for M-D seen with the type-I HSV-1-TK has been reported to be 2.4 μM (Wurth, Thomas et al. 2001). Having examined TmTK's SEC profile in the range of 20 – 300 μM, it is possible that the K_D for TmTK M-D or M-D-T is similarly low as for HSV-1-TK. Experiments at lower and higher concentration ranges could be investigated to try to isolate the K_D for the M-D or M-D-T, yet in the range examined no changes are seen.

Proteins of similar fold could maintain similar volumes and therefore elute from SEC with comparable profiles. In order to test this hypothesis, the mesophilic homolog hTK1 was studied via SEC. The elution profile for hTK1 gave a major peak corresponding to a MW of 118 kDa which is 8 kDa greater then the predicted tetramer (110 kDa) (Fig. 4-3A). This estimated MW is consistent with literature reported SEC MW for hTK1 without N-terminal truncations (Birringer, Perozzo et al. 2006). There are two slight smaller peaks corresponding to 45 kDa and a shoulder peak at 24 kDa. Higher molecular weight material is seen at ~360 kDa, which is likely protein aggregates. The protein sample used was from elutions 3 and 4 from the purification to reduce the chance of contamination from co-purified proteins seen in the earlier elutions (Fig. 4-3B). MW
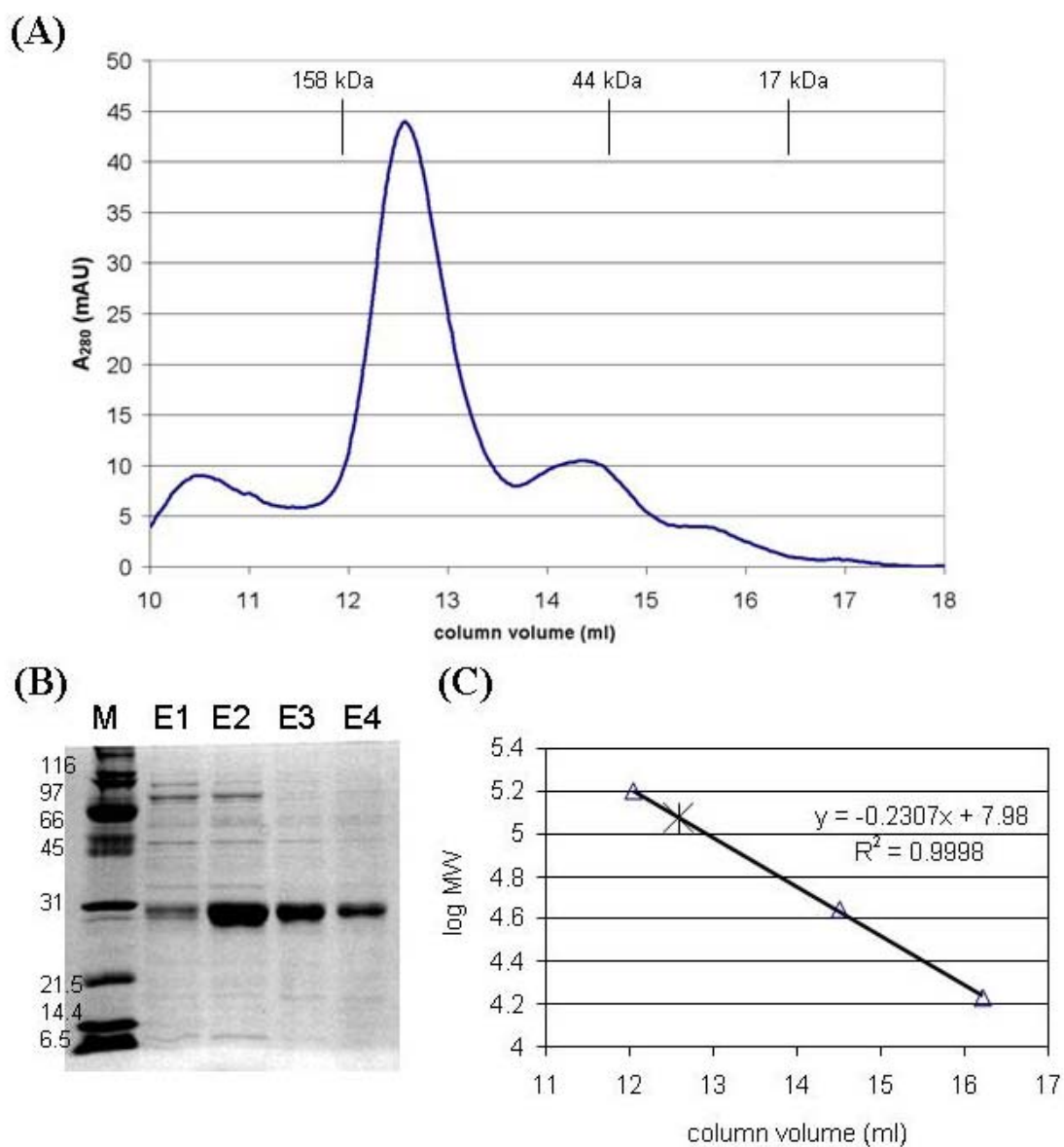
Figure 4-3: SEC for hTK1. (A) SEC profile of hTK1 (6 mg/ml). (B) Elutions from hTK1 purification. First 2 elutions had high background levels of co-purified protein bands, yet the E3 and E4 were relatively clean and therefore pooled and injected into SEC (B) Calibration curve done using internal standards. Open triangles are the standards, asterisk is the hTK1 major peak.

were estimated based on the same internal standards as before, run in the hTK1 protein buffer (Fig 4-3C).

In comparing SEC profiles for wild type TmTK with hTK1 it appears the hTK1 estimated MW is close to its predicted MW while TmTK has a main peak inconsistent with either a dimer or a tetramer MW. It has been reported that thermostability in *T. maritima* proteins is largely due to protein compactness (i.e. lower relative accessible surface area, and higher network of interacting residues) (Robinson-Rechavi, Alibes et al. 2006). Thus, it could be possible that the 67 kDa oligomer seen in the SEC data is a compact tetramer, traveling with a MW that is 25 kDa smaller than predicted. Similarly, the thermophilic TK from *Rhodothermus marinus* eluted from SEC with an estimated MW of 85 kDa, while the predicted tetramer size is 94 kDa (Blöndal, Thorbjarnardóttir et al. 1999). It is therefore plausible that thermophilic TKs are compact and elute with a smaller MW than predicted.

Wild type TmTK was next compared to the mutant T18C/S22C, previously shown to form disulfide bridges when prepared in oxidizing conditions (Segura-Pena, Lichter et al. 2007). To see how the disulfide linkages affects protein mobility on the SEC, we injected T18C/S22C (disulfide form) in the same column/same conditions as used for wild type. Concentrations of 2 - 8 mg/ml were investigated. Interestingly, the major peak for T18C/S22C eluted with a MW of 57 kDa, 10 kDa smaller than for wild type (Fig. 4-4). Smaller peaks were seen at 22 kDa and at 148 kDa. Judging from the SDS PAGE gel for the T18C/S22C sample (chapter 3, Fig. 3-7), the 148 kDa peak could be the higher order protein oligomerization caused from unspecific disulfide bond formation.
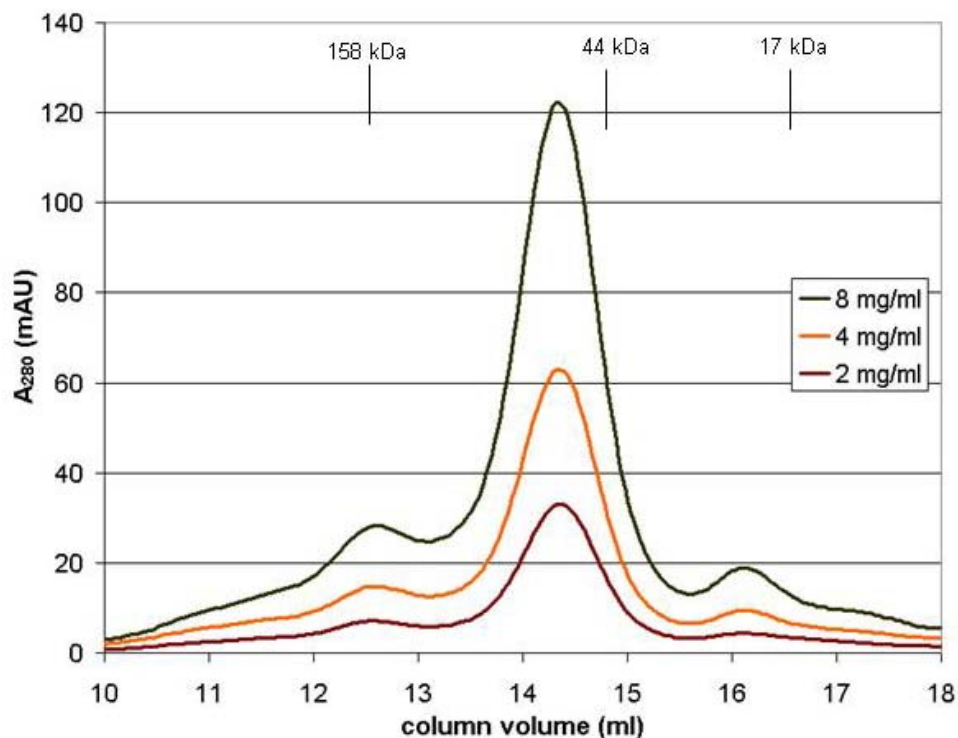
Figure 4-4: SEC for T18C/S22C. Range of concentrations measured from 2 -8 mg/ml (80 – 400 μM).

Three hypothesis are suggested for the 57 kDa peak for T18C/S22C. Firstly, engineering of disulfide bridges at the dimer II interface could bring two dimer units tightly together such that the protein elutes as a tightly packed tetramer corresponding to 57 kDa. While this is 34 kDa lower than the predicted MW for a tetramer, the MW for wild type was lower than a predicted tetramer to begin with. An alternative hypothesis is that TmTK is a native dimer along the dimer II interface. Engineering disulfides bridges along the α1-helices at the dimer II interface forms a covalently linked 57 kDa dimer, with the dimer II interface intact. An inconsistency with this hypothesis is the presence of the dimer I contacts in the asymmetric unit of protein crystals. Therefore a third

alternative hypothesis is that the dimer I interface is the relevant unit in solution, yet placing cysteines at surface exposed positions 18 and 22 could form disulfide bridges to the corresponding cysteines of another protein subunit. Creating new covalent linkages between TmTK subunits at these positions will create a new interface and could perturb the dimer I interface such that it can't stay intact. Thus what is formed is a covalent dimer at the dimer II interface, which is not relevant in the natural structure. The SEC data for T18C/S22C can be described by both a M-D or a M-D-T equilibrium. To further investigate, mutagenesis and crosslinking experiments are employed to identify the oligomeric state and the relevant interfaces.

4.3.2 Disruptional mutagenesis indicates the dimer I interface is crucial for oligomerization

The proposed model from chapters 2 and 3 suggests that the protein is a tetramer with 2 separate interfaces (Fig. 4-5A). The dimer I interface (Fig. 4-5B) is the "strong" dimer interface because of a large buried surface area (1228 Å). The other interface (dimer II, Fig 4-5C) is the "weak" interface because of its low level of occluded surface area (350 Å excluding ATP interactions, 760 Å including ATP) (Segura-Pena, Lutz et al. 2007). Double arginine mutants were engineered with intent to disrupt presumed interface contacts and force separation of subunits. To disrupt the dimer I interface, two arginines were engineered in place of residues Leu127 and Val133 which form a hydrophobic pocket (Fig. 4-6A). To disrupt the dimer II interface, two arginines were placed at residues Thr18 and Ser22 along the α1 helix, the same positions previously used to engineer cysteines to form disulfide bonds between the two helices (Fig 4-6B).
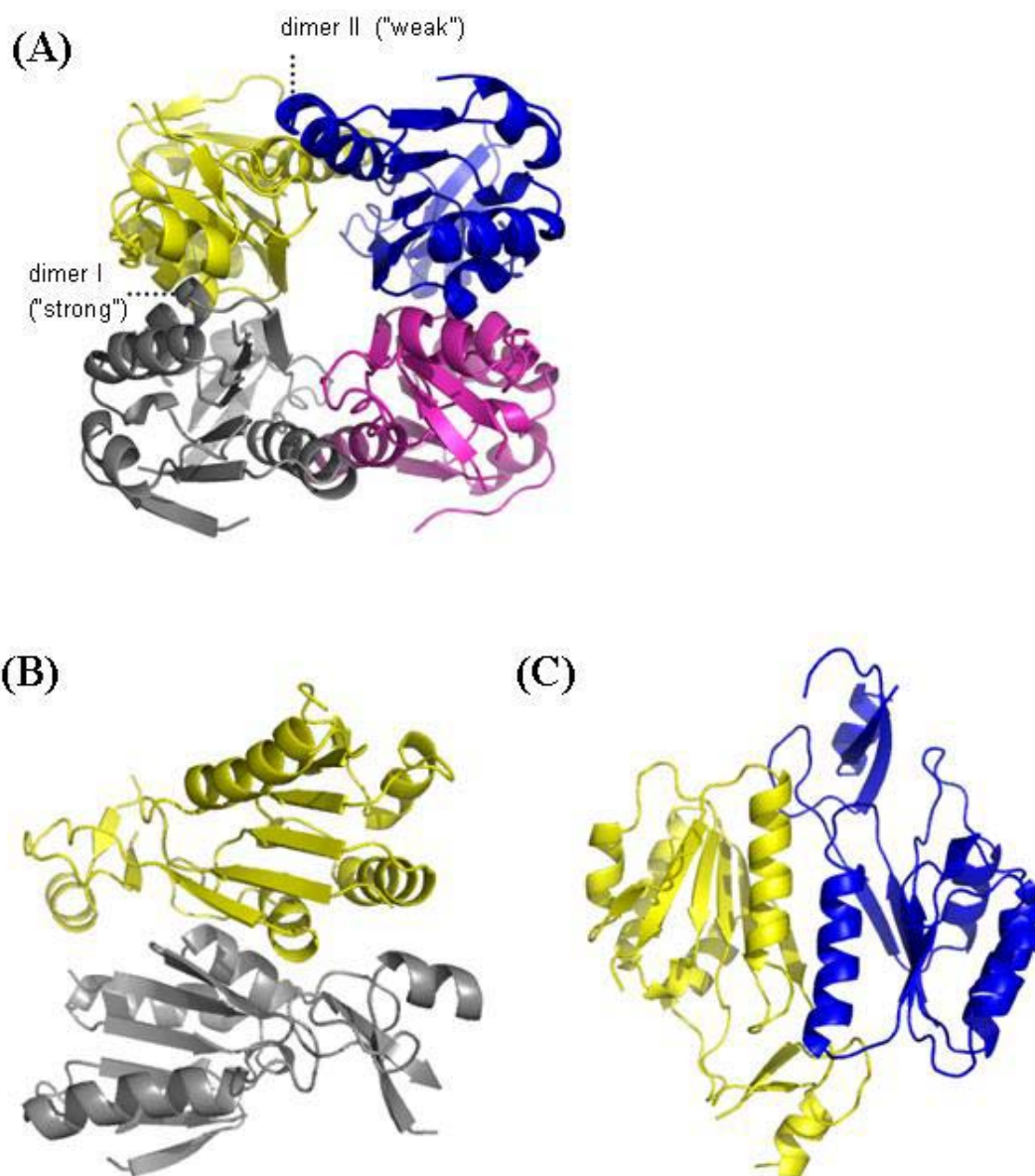
Figure 4-5: Crystal structure of TmTK (pdb # 2qp0) (A) Overall view of predicted tetrameric structure with 4 monomeric units colored differently. The weak and strong dimer interface are identified (B) View of the strong dimer (dimer I) interface, twisted 90°C to the right (as compared to a). (C) View of the weak dimer (dimer II) interface twisted 90°C downwards (as compared to a) (Segura-Pena, Lichter et al. 2007)
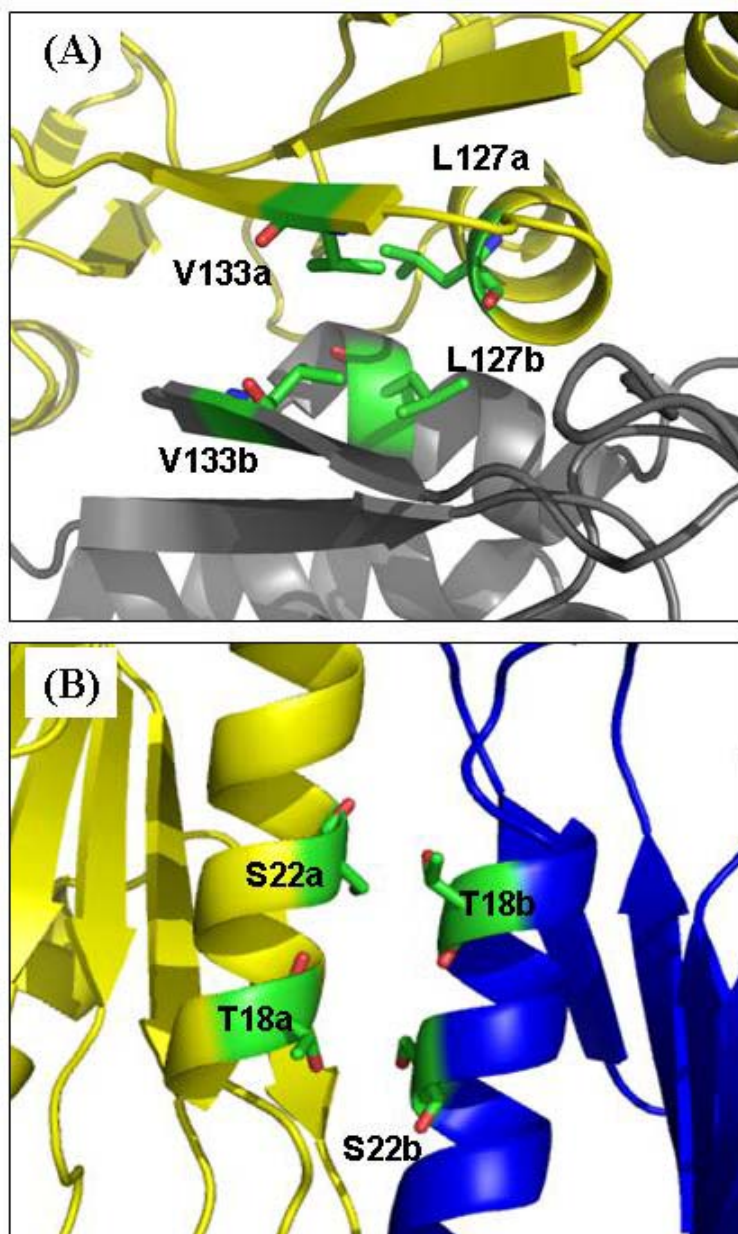
Figure 4-6: Positions for arginine mutagenesis to disrupt interfaces (A) Dimer I interface mutations. Leu127 and Val133 form a hydrophobic pocket at the interface. By placing arginines at these two positions, a disruption of the two units was attempted. (B) Dimer II interface mutation. Thr18 and Ser22 are located on α1 and previous work has shown the ability to mutate both to cysteines and form disulfide bridges. In this work, arginines were placed at these positions to interfere with that interface formation. Models were made with Pymol using structure pdb # 2qpo (Segura-Pena, Lichter et al. 2007)

The proteins were overexpressed and purified by the established protocols for wild type. Following the Ni-NTA column purification, both mutants were analyzed via SEC (Fig. 4-7). SEC data for T18R/S22R shows a major peak estimated at 61 kDa and a smaller peak at 28 kDa. The similarity in SEC profiles between wild type and T18R/S22R suggest mutagenesis done at the weak interface did not affect the overall native structure. One potential reason could be the arginines arrange themselves pointing away from the interface made by α1 contacts. The corresponding residue in hTK1 for Ser22 is Arg38, which orients itself towards the center of the protein. This suggests placing an arginine at the position in TmTK might not be sufficient for interfering with that interface. A secondary suggestion is that this interface is not present in the native state and therefore engineering mutants along the α1 helix will not disrupt any existing interface.

SEC results for the strong dimer interface mutant L127R/V133R provided a starkly different profile than wild type (Fig. 4-7). The major peak with ~70% of peak area corresponds to 26 kDa, likely a monomer. Other parts of the profile suggest higher molecular weight species, with a peak corresponding to 48 kDa and a slight shoulder peak estimated at 70 kDa. Introducing two mutations at this interface shifts the oligomeric state equilibrium almost completely to a monomer. This result negates the hypothesis that TmTK is a dimer at the dimer II interface only. However the question of whether it is a tetramer or a dimer (with the dimer I interface contacts) is not completely answered. Judging from the SEC profile, one could suggests the potential for a 3 state equilibrium, based on the three peaks: monomer (26 kDa), dimer (48 kDa) and tetramer

(70 kDa). Yet the third peak at 70 kDa is small and therefore a M-D equilibrium can be postulated as well from the two remaining peaks.
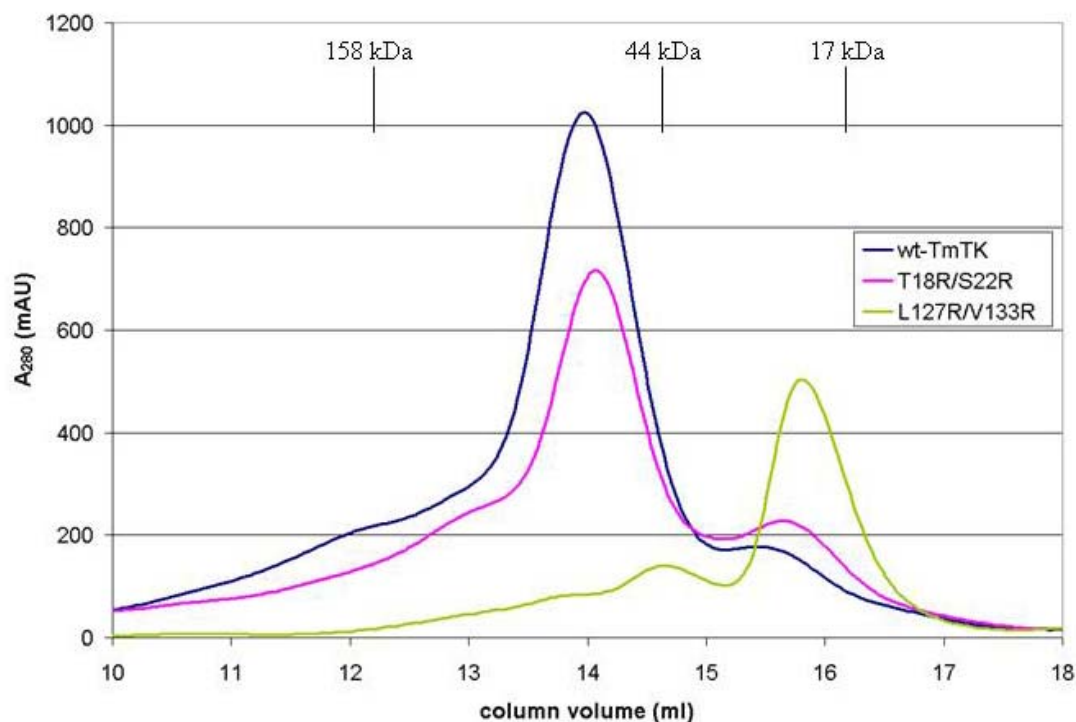
Figure 4-7: SEC profiles for T18R/S22R (light green) and L127R/V133R (magenta) and wild type (blue).

The double arginine mutants were examined for their catalytic properties. The kinetics for thymidine and ATP were measured using a coupled enzyme spectrophotometric assay (Schelling, Folkers et al. 2001). Table 4-1 shows the weak dimer interface mutant has little change in K_M and k_{cat} for both substrates. The monomeric strong dimer interface mutant not only retains catalytic activity but has a 6x faster turnover rate than wild type, suggesting that the enzyme functions faster in catalyzing the phosphoryl transfer when it is a monomer. Surprisingly there are some changes in the thymidine binding as evidenced in the 10x increase in K_M. This could be a

result of a rearrangement of the nearby loop formed by residues 112-120 where certain residues (i.e. Thr114) make hydrogen bonding contacts with the thymine base. This change in K_M lowers the overall catalytic efficiency but only by 2x. Interestingly, this is the first reported catalytic type II TK monomer.

Table 4-2: Kinetic parameters for TmTK arginine mutants

	Thymidine			ATP		
	K_M (μM)	k_{cat} (s^{-1})	k_{cat}/K_M (x 10^4 M-1s^{-1})	K_M (μM)	k_{cat} (s^{-1})	k_{cat}/K_M (x 10^4 M^{-1}s^{-1})
wild type	0.5 ± 0.2	0.3 ± 0.08	60	40 ± 12	0.4 ± 0.04	1
T18R/ S22R	1.3 ± 0.2	0.4 ± 0.01	28	50 ± 5	0.4 ± 0.01	0.7
L127R/ V133R	5.2 ± 0.2	1.7 ± 0.04	33	48 ± 8	1.5 ± 0.05	3.2

In summary, the mutagenesis work highlights the importance of the strong dimer interface. This is consistent with all TmTK structures, where the dimer I interface is intact in the asymmetric unit of the crystals. Two possible reasons for the monomeric TK as a result of disruption at the dimer I interface are (1) the protein is a dimer at the strong dimer interface or (2) the protein is a tetramer but the contacts at the weak interface are too few, in which case the mutations cause the protein to separate into monomers. The main conclusion drawn from the disruption mutagenesis experiments is the importance of the strong interface, and potentially its role in overall stabilization of the higher order oligomer. To complement the mutagenesis experiments, chemical crosslinking of wild type TmTK and L127R/V133R were conducted.

4.3.3 Amine reactive crosslinking produces 60 kDa product

Chemical crosslinking was employed to try and "fix" TmTK protein subunits in their solution state by reacting TmTK with bifunctional crosslinkers that react with specific functional groups in a protein. Bis(sulfosuccinimidyl)suberate (BS^3) is commonly used to study protein oligomeric states by reacting with primary amines (either lysines or the N-terminus) between proximal protein subunits (Handler, Eisenberg et al. 1996; Guo, Bandyopadhyay et al. 2008). BS^3 contains an 8-carbon spacer arm (11.4 Å) connected at both ends by *N*-hydroxysulfosuccinimide (NHS) esters, highly reactive to primary amines (i.e. lysines, and N-terminal –NH$_2$) at pH 7-9. TmTK's primary sequence contains 17 lysines, some at or near the interfaces within range of 6-11 Å, suitable distance for linking subunits via BS^3.

TmTK was incubated with BS^3 and the reaction was followed over time (Fig. 4-8). Upon adding the crosslinker, three bands form in the region of 45-60 kDa. The highest band at 60 kDa intensifies over the course of the reaction, while the other bands weaken. After 6 hrs, the 60 kDa band becomes most prominent, while some higher bands start to come into focus as a result of higher order crosslinking. TmTK sample was left to crosslink for 24 hours and the result was complete disappearance of the lower bands and the 60 kDa band maintained at strongest intensity. This 60 kDa band is inconsistent with either a tetramer or a dimer, and is smaller than the SEC estimated MW. The lower band or bands seen below the 60 kDa protein might be a result of some intermediary protein crosslinking or crosslinked protein that has undergone some proteolysis. Protein samples were prepared in phosphate buffer, and apparent complication in TmTK stability in phosphate buffer (i.e. degradation) has been noted (Z. Eletr, personal communication).

Figure 4-8: TmTK crosslinking experiments with BS³. 10% SDS gel shown. All samples were prepared in SDS buffer without mercaptoethanol, heated at 100°C for 7 min, then cooled down to 4°C for 5 min and then loaded on gel.

The positions of lysines in TmTK were reevaluated following the crosslinking with BS³. At the strong dimer interface there exists three pairs of lysines within 5 - 11 Å (4→137, 4→135, 97→116) and at the weak dimer interface three lysine pairs within 7 - 9 Å (31→168, 136→136, and 4→137 again). The sharing of Lys4 at both interfaces might pose a problem for linking at both interfaces and could therefore lead to dimer formation. Yet there still exists one Lys pair for each interface available for linkage, suggesting that both interfaces could link.

The L127R/V133R mutant was crosslinked with BS³, under the same conditions and time course as wild type (shown in Fig. 4-9). Throughout the course of the reaction,

the mutant mainly runs as a monomer. A small amount of crosslinking reaction might be

occurring as evidenced by a faint smearing at 45 – 50 kDa, but the band is not sharp and

it could only be visible through high contrast of the gel. This experiment further suggests

the strong dimer mutant is a monomer and therefore protein subunits are not close enough
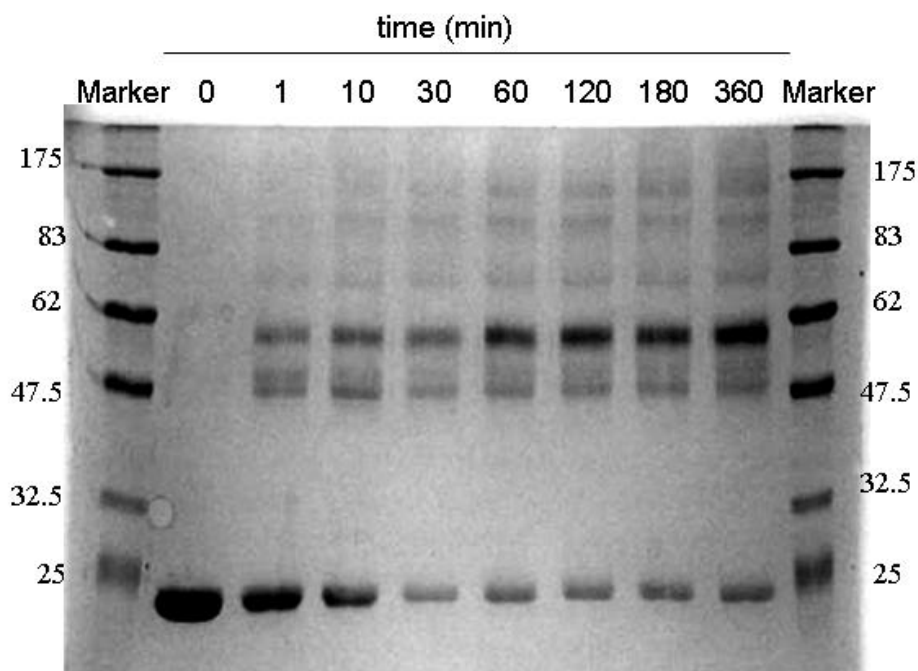
to react and form a crosslinked unit.
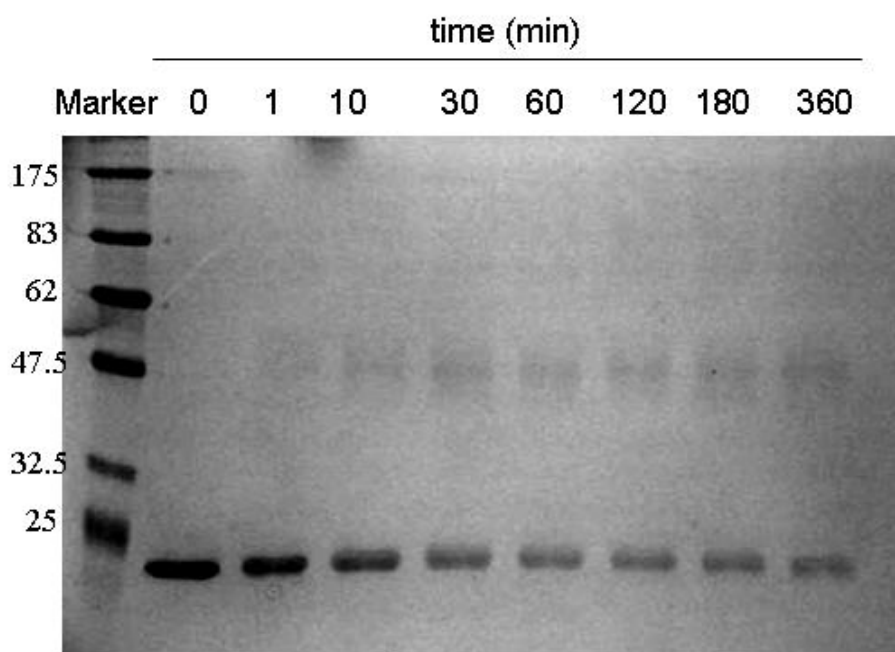
Figure 4-9: Crosslinking of L127R/V133R with BS^3. 10% SDS gel shown. All samples were prepared in SDS buffer without mercaptoethanol, heated at 100°C for 7 min, then cooled down to 4°C for 5 min and then loaded on gel.

The SDS gels of crosslinked wild-type and L127R/V133R were measured to

identify protein MW. However, ambiguities in MW specifically in the wild type gel

suggests the need for more experimentation. Therefore the crosslinked wild type TmTK

and L127R/V133R were injected in the SEC. Both the wild-type and L127R/V133R

(incubated with crosslinker for 6 hours) were injected into the SEC. Shown in Fig 4-10, wild type has one major peak with an estimated MW of 75 kDa. This shift of 8 kDa from uncrosslinked material suggests very little change. The strong dimer mutant on the other hand shows two peaks corresponding to 25 and 46 kDa, with a slight shoulder peak at a higher MW. These two peaks could correspond to the monomer and the small bit of dimer. Comparing the suggested dimer peak for L127R/V133R with wild type's major peak, they are inconsistent in MW. The reason could be that wild type is a higher order oligomer, likely a compact tetramer. Yet, the problems with BS^3 crosslinking (i.e. specificity, which interfaces linked, ambiguity in MW) led to the need for more experimentation.

Figure 4-10: SEC for crosslinked wild type and L127R/V133R. Samples that had been incubated with BS^3 for 6 hours were injected and absorbance at 220 nm was measured.

4.3.4 Sulfhydryl reactive crosslinking

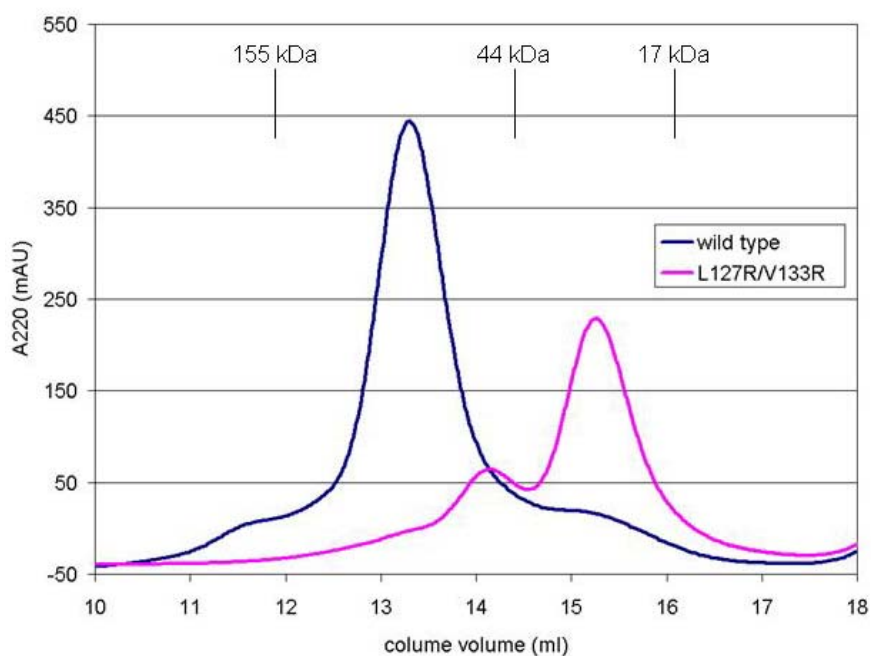When using BS^3 to study the interactions of the protein's subunits, there was no controlling the specificity of the crosslinking reaction. The potential for both weak dimer, and strong dimer linkages with BS^3 limits the ability of identifying which interfaces are crucial for crosslinking. Therefore, sulfhydryl specific crosslinking was employed with cysteine mutants engineered at each interface to examine whether each interface could be crosslinked separately.

Cysteine mutants were engineered at each interface. For the weak dimer interface, a cysteine was placed at position Ser22, one of the positions previously investigated for cysteine disulfide bond engineering (Fig. 4-11A). For the strong dimer a mutation at position Ser128 was introduced, which according to the crystal structure would be within 10 Å from the opposing residue (Fig. 4-11B). Lastly a double mutant containing both the weak and strong dimer cysteine mutants (S22C/S128C) was engineered with the presumption that this might be a way to visually lock all four units together. The sulfhydryl reactive crosslinker [BM(PEG)$_2$] has a spacer arm of ~15 Å, which should cover the distance measured for both sets of cysteine mutants.

The reactivity of BM(PEG)$_2$ with the cysteine mutants was low in efficiency, showing little changes in crosslinking until at least 6 hours of reactivity, likely due to the availability of only one cysteine at each interface to interact. Over a 24 hour reaction period, minimal crosslinking occurs at the weak dimer interface, appearing to form a ~ 47 kDa band in both the S22C and S22C/S128C mutants. Previous experiments with T18C/S22C suggests that the weak dimer mutant crosslinking by BM(PEG)$_2$ could work. However the S128C mutant did not show any crosslinking. It seems counterintuitive that

this interface would not link with the sulfhydryl crosslinker, due to the disruptional

mutagenesis results. Yet, it is possible the moderately hydrophilic polyethylene glycol

crosslinker was unable to position itself at that interface. It is also possible that the

introduction of a cysteine at position 128 might change the orientation of the residue

making it unsuitable for linkage. As the reaction was allowed to proceed, higher order

oligomerization can be seen with a dark band at the top of the gel increasing over time.

The double mutant had higher order oligomerization without crosslinking, suggesting that

the reactive cysteines were recombining unspecifically without crosslinker. In summary,

the sulfhydryl crosslinking experiments were inefficient demonstrating difficulties

linking at the strong interface, and little reactivity along the weak interface.
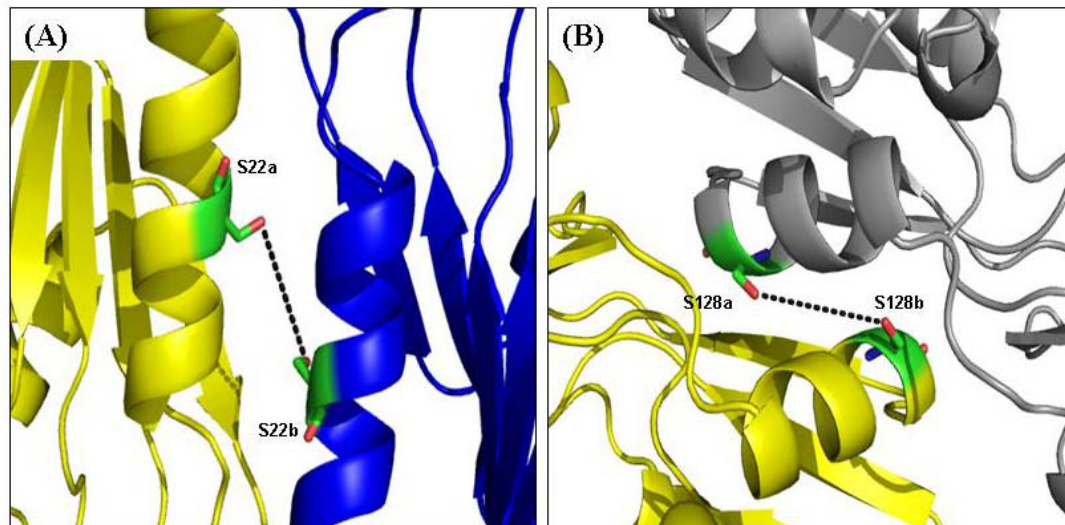
Figure 4-11: Cysteine mutants used in sulfhydryl reactive crosslinking (A) S22 is at the weak interface and the distance between the two hydroxyl groups is ~7 Å (B) S128 is at the strong dimer interface and the distance measured between the two hydroxyl groups is ~8 Å. (pdb # 2qp0)
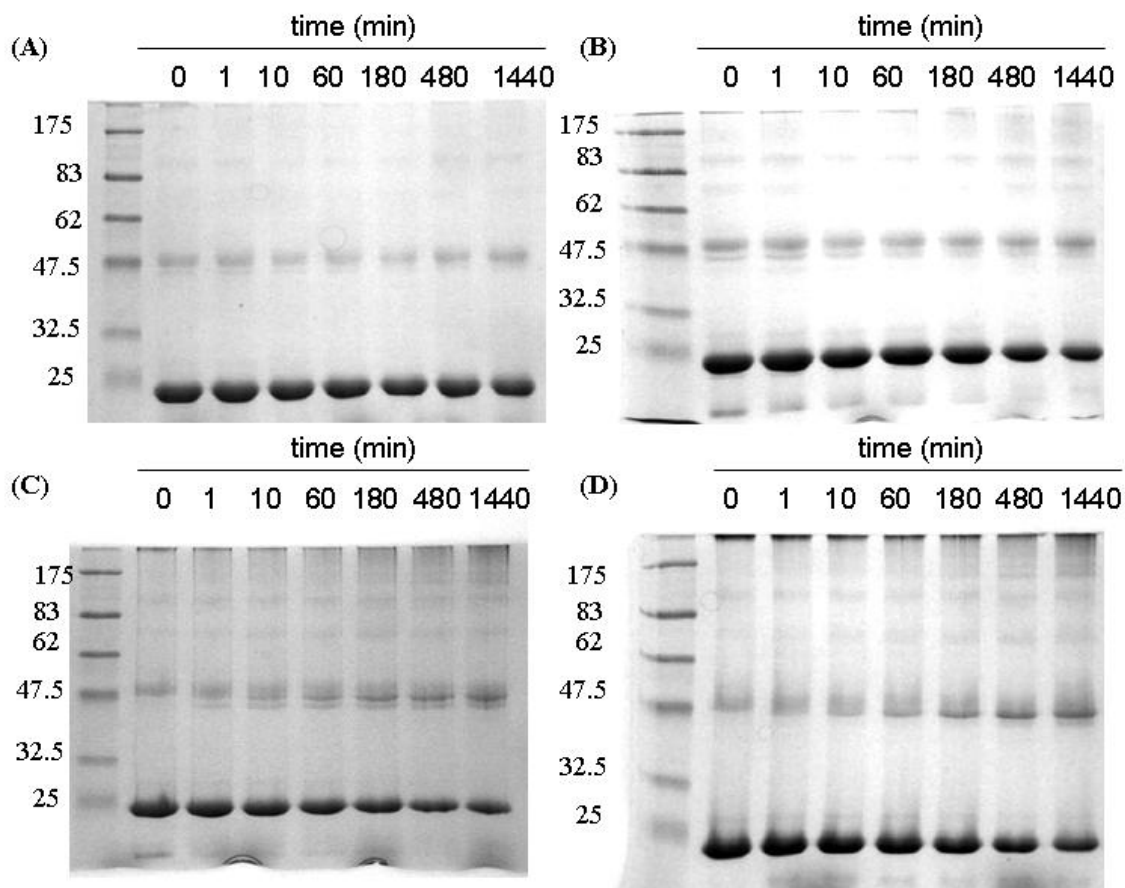
Figure 4-12: Sulfhydryl crosslinking of (A) wild type (B) S128C (C) S22C (D) S22C/S128C. 10% SDS gels shown. Protein samples were prepared without reducing agent. The thick protein bands and high background proteins is due to loading of 50 μg protein to ensure clear vision of any crosslinking. The background band seen for wild type suggests that there is some wild type protein that is not completely denatured by the SDS and heat. A distinct formation of a darker band at ~ 47 kDa over time is seen in the profile for S22C and S22C/S128C.

4.4 Conclusion

In this chapter, the oligomeric state for TmTK was investigated. The symmetry

seen in TmTK crystal structures suggests the protein is either a dimer or a tetramer.

Furthermore, evidence for the existence of both dimer and tetramer type-II TKs have

been reported (Lee and Cheng 1976; Black and Hruby 1990; Munch-Petersen, Tyrsted et

al. 1993; Birringer, Perozzo et al. 2006). The SEC data for wild type gives an estimated MW of 67 kDa, puzzlingly resembling either a loose dimer or a tight tetramer. Comparing this profile to the homolog hTK1 suggests the unusual migration is specific for TmTK. The SEC profile for the T18C/S22C mutant gave a major peak with a MW of 57 kDa. Hypotheses were formulated for both M-D and M-D-T equilibrium. In furthering the examination past wild type and the T18C/S22C mutant, mutants were constructed to potentially disrupt presumed interface contacts. The L127R/V133R mutant SEC results confirmed that the dimer I interface was relevant to the solution state. The presence of a peak with a MW of 22 kDa and two smaller peaks at 45 and 70 kDa suggested the possibility for an equilibrium for TmTK involving the three states of monomer-dimer-tetramer.

In separate work done by colleague Dr. Ziad Eletr, wild type and L127R/V133R were analyzed by sedimentation equilibrium experiments using analytical ultracentrifugation (AUC). In fitting the AUC results to a single species model, wild type TmTK gave a molecular weight of 32.5 kDa which does not correspond to either a homogeneous solution of monomers or dimers. The apparent MW indicates that only a small fraction of wild type TmTK exists as a dimer or a tetramer at the concentrations tested (43 - 64 μM). When the data was fit to M-D model, a better fit to the data was observed (reduced χ^2=3.14) and approximated a M-D dissociation constant (K_D) of 77 μM. Fitting to a M-D-T model, higher confidence in the fit was obtained (reduced χ^2= 1.91) and the K_D changed such that the dissociation constants for M-D is 475 μM and for D-T is 6 μM. Considering that the concentration range examined by SEC, indicated little change at around 77 μM, it seems unlikely that the M-D model is the correct one. This

would leave the suggested M-D-T equilibrium to be the preferred model, with mostly tetramer present and some monomer.

The question remains why should a native TmTK tetramer travel with a lower molecular weight than expected during SEC. In 2005, Robinson-Rechavi et. al. found protein compactness to be the leading factor for thermostability in *T. maritima* proteins as compared to oligomerization order, hydrogen bonds, and secondary structure (Robinson-Rechavi, Alibes et al. 2006). A compact structure could have a modified hydrodynamic volume, thereby making it elute with a smaller MW than expected and perhaps even change it from a globular protein to some different geometry.

Due to the catalytic abilities of the monomer mutant, it raises the question whether oligomerization is relevant strictly for structural integrity as opposed to any catalytic benefit. Beernink and Tolan reported mutagenesis experiments with the tetrameric protein fructose-1,6-bisphosphate aldolase, where less stable, yet catalytically active monomers were formed from the native tetramer form (Beernink and Tolan 1996). As compared to wild type, L127R/V133R showed a tendency towards aggregation at μM concentrations at 4 °C over the period of several days. Perhaps the compactness of the protein subunits rigidifies some of the flexible regions and protects the protein from degradation. It is also feasible that the compact structure eliminates cellular peptidases and proteases from targeting available digestion motifs.

In conclusion, an investigation of the oligomeric state was done using SEC, mutagenesis and crosslinking. While the data suggests the possibility for both M-D and M-D-T equilibrium, it is clear that the dimer I interface is relevant to the solution state structure. The dimer II interface is suggested to be relevant due to the T18C/S22C

disulfide linkages and the sulfhydryl crosslinking, yet the possibility that these residues are surface exposed is plausible as well. More evaluation of the oligomerization using sedimentation equilibrium, dynamic light scattering, or mass spectroscopy could be useful in identifying the oligomeric state.

Chapter 5: Conclusions and Future Perspectives

TKs are ubiquitous enzymes, relevant for the cellular production of the DNA precursor molecule TTP. Due to this biological function, TKs also play a medical role as the enzyme that activates NA pro-drugs, as a cancer diagnostic, a gene in combined suicide gene therapy with GCV, and as a target for newer cancer treatments including boron-neutron capture therapy (Barth, Yang et al. 2008) .

In this dissertation, a complete kinetic and biophysical characterization of the TK from *T. maritima* is described. This is the first isolated and fully characterized hyperthermophilic TK. At 37 °C, TmTK's catalytic efficiency for natural and unnatural nucleosides is quite similar to its mesophile homolog hTK1, yet suboptimal for its own performance as compared to 82 °C. Even more interesting is the higher specificity for the natural nucleoside thymidine than for the analog AZT when functioning at the physiological temperature for *T. maritima*. Attempts to identify potential causes for the change in substrate specificity led to the suggestion of a protein conformational change at 70 °C. The question of whether this type of behavior is specific to TmTK or applicable to other thermophilic TKs remains to be seen. The only other reported thermophilic TK from *R. marinus* was examined for its optimal temperature for catalytic activity but untested with nucleoside analogs (Blöndal, Thorbjarnardóttir et al. 1999). An investigation of RmTK and/or other thermophilic TKs such as the putative TK from *Thermoplasma acidophilum* (NCBI accession # CAC12339) could answer this question. With respect to the limits of radiolabeled NA pro-drugs, it would be advantageous to find

an assay which could test other nucleoside analogs besides AZT at elevated temperatures, providing a more comprehensive study of substrate specificity. The use of isothermal titration calorimetry (ITC) as a way of testing TK activity for nonradiolabeled material is currently being pursued (M. Trani, unpublished results).

Another novel element of this dissertation, was the systematic examination of a TK along its catalytic cycle. A two-state model was suggested whereby the protein expands at the weak dimer interface as a function of ATP binding. Fluorescence measurements of tryptophan mutants confirmed movement in the βc1/β3 region, and mutagenesis studies suggested the space between α1 of two subunits was crucial for positioning the phosphoryl donor. Judging from the way the feedback inhibitor TTP binds to type-II TKs, it can be inferred that the open and closed states are critical for TmTK regulation. However, the crux of the proposed opening and closing depends on whether or not the protein is indeed a native homotetramer.

In chapter 4, the migration pattern for TmTK via SEC could either be described as a tight tetramer or a loose dimer. Mutagenesis highlighted the importance of the strong dimer interface in keeping the oligomerization equilibrium shifted to the higher order oligomer. Similar studies with the weak dimer interface showed little change. Our initial presumption that the T18C/S22C mutant could form disulfide bonds due to the presence of a dimer II interface is plausible. Yet should the interface not exist, and positions 18 and 22 are surface exposed cysteines, then the promotion of intermolecular disulfide bond formation could occur (Woo, Lotz et al. 1991; Wootton and Yoo 2003). SEC data for the T18C/S22C presents one major peak with a MW of 57 kDa, ~35 kDa smaller than the predicted MW for a tetramer. Disulfide bounds at the presumed weak dimer interface

could form a dimer, still agreeing with the MW estimated from non-reducing SDS PAGE results. The L127R/V133R SEC profile showed two major peaks (three, if the shoulder is included) corresponding to both an M-D and an M-D-T equilibrium. Preliminary sedimentation equilibrium experiments provided good fits for both the M-D and M-D-T equilibrium but over a small range of concentrations. More in-depth sedimentation equilibrium experiments will be necessary to identify the oligomerization equilibrium. As well, reported differences in the use of Tris and phosphate buffers has been suggested to affect the protein stability for type-II TKs (Skovgaard and Munch-Petersen 2006) and could be a factor in the SEC data for TmTK (Z. Eletr, personal communication).

In principle, a two-state model could still exist if TmTK's preferred oligomeric state is a dimer. Even without a weak dimer expansion, fluorescence experiments suggested a shift in the $\beta c1/\beta 3$ hairpin region upon ATP binding. The structural reorganization of this region upon ATP binding could help to facilitate catalysis. While the H53A mutagenesis did not affect ATP or thymidine kinetics, an investigation of other residues in the region might be necessary to understand the reason for the $\beta c1/\beta 3$ region formation.

Lastly, the use of enzymes isolated from extremophiles have been studied for potential use in industrial and biotechnological purposes (Table 1-1). In terms of the ability to utilize TmTK for direct application, there has been interest in the engineering of a human TK for use in suicide gene therapy due to immunogenic responses by viral TKs (Warren, Song et al. 2002). Considering the similarities in structure and kinetics between the two proteins, TmTK can be used as a model from which to engineer changes into hTK1 or to study substrates meant to be used in a suicide gene therapy pair. The half-life

reported for hTK1 in phosphate buffer is 58 minutes, and measured to be even worse in Tris-buffers (Skovgaard and Munch-Petersen 2006; Zhu, Harlow et al. 2006). TmTK stability is greater, and could therefore be used as a first target for testing NA pro-drugs before investigating hTK1. As well, one could look at the sequence alignment for the two proteins and compare the structures to see which residues play an integral role in binding substrates. This method of sequence-based engineering might lead to enhancing specificity and activity for particular NA pro-drugs in hTK1.

References

Achenbach-Richter, L., R. Gupta, et al. (1987). "Were the original eubacteria thermophiles?" <u>Syst Appl Microbiol</u> **9**: 34-9.

Andrade, M. A., P. Chacon, et al. (1993). "Evaluation of secondary structure of proteins from UV circular dichroism spectra using an unsupervised learning neural network." <u>Protein Eng</u> **6**(4): 383-90.

Avery, O. T., MacLeod, C.M., McCarty, M (1944). "Studies on the Chemical Nature of the Substance Inducing Transformation of Pneumococcal Types: Induction of Transformation by a Desoxyribonucleic Acid Fraction Isolated from Pneumococcus Type III." <u>Journal of Experimental Medicine</u> **79**: 137-158.

Barth, R. F., W. Yang, et al. (2008). "Thymidine kinase 1 as a molecular target for boron neutron capture therapy of brain tumors." <u>Proc Natl Acad Sci U S A</u> **105**(45): 17493-7.

Barthel, H., M. C. Cleij, et al. (2003). "3'-Deoxy-3'-[18F]Fluorothymidine as a New Marker for Monitoring Tumor Response to Antiproliferative Therapy in Vivo with Positron Emission Tomography." <u>Cancer Res</u> **63**(13): 3791-3798.

Beernink, P. T. and D. R. Tolan (1996). "Disruption of the aldolase A tetramer into catalytically active monomers." <u>Proc Natl Acad Sci U S A</u> **93**(11): 5374-9.

Bello, L. J. (1974). "Regulation of thymidine kinase synthesis in human cells." <u>Exp Cell Res</u> **89**(2): 263-74.

Birringer, M. S., M. T. Claus, et al. (2005). "Structure of a type II thymidine kinase with bound dTTP." <u>FEBS Lett</u> **579**(6): 1376-82.

Birringer, M. S., R. Perozzo, et al. (2006). "High-level expression and purification of human thymidine kinase 1: quaternary structure, stability, and kinetics." Protein Expr Purif **47**(2): 506-15.

Black, M. E. and D. E. Hruby (1990). "Quaternary structure of vaccinia virus thymidine kinase." Biochem Biophys Res Commun **169**(3): 1080-6.

Blöndal, T., S. H. Thorbjarnardóttir, et al. (1999). "Cloning, sequence analysis and overexpression of a Rhodothermus marinus gene encoding a thermostable thymidine kinase." FEMS Microbiology Letters **179**(2): 311-316.

Bollum, F. J. and V. R. Potter (1958). "Incorporation of thymidine into deoxyribonucleic acid by enzymes from rat tissues." J Biol Chem **233**(2): 478-82.

Bradshaw, H. D., Jr. and P. L. Deininger (1984). "Human thymidine kinase gene: molecular cloning and nucleotide sequence of a cDNA expressible in mammalian cells." Mol Cell Biol **4**(11): 2316-20.

Cass, C. E., J. D. Young, et al. (1999). "Nucleoside transporters of mammalian cells." Pharm Biotechnol **12**: 313-52.

Chabes, A. and L. Thelander (2000). "Controlled protein degradation regulates ribonucleotide reductase activity in proliferating mammalian cells during the normal cell cycle and in response to DNA damage and replication blocks." J Biol Chem **275**(23): 17747-53.

Chen, M. S. and W. H. Prusoff (1978). "Association of thymidylate kinase activity with pyrimidine deoxyribonucleoside kinase induced by herpes simplex virus." J Biol Chem **253**(5): 1325-7.

Cheng, Y. C., B. Domin, et al. (1977). "Human deoxycytidine kinase. Purification and characterization of the cytoplasmic and mitochondrial isozymes derived from blast cells of acute myelocytic leukemia patients." Biochim Biophys Acta **481**(2): 481-92.

Coppock, D. L. and A. B. Pardee (1987). "Control of thymidine kinase mRNA during the cell cycle." Mol Cell Biol **7**(8): 2925-32.

CRC Handbook of Chemistry and Physics; 83rd ed.; Lide, D. R., Ed.; CRC Press LLC: Boca and F. Raton, 2002.

Dobrovolsky, V. N., T. Bucci, et al. (2003). "Mice deficient for cytosolic thymidine kinase gene develop fatal kidney disease." Mol Genet Metab **78**(1): 1-10.

Erecinska, M. and I. A. Silver (1994). "Ions and energy in mammalian brain." Prog Neurobiol **43**(1): 37-71.

Eriksson, M., U. Uhlin, et al. (1997). "Binding of allosteric effectors to ribonucleotide reductase protein R1: reduction of active-site cysteines promotes substrate binding." Structure **5**(8): 1077-92.

Eriksson, S., B. Kierdaszuk, et al. (1991). "Comparison of the substrate specificities of human thymidine kinase 1 and 2 and deoxycytidine kinase toward antiviral and cytostatic nucleoside analogs." Biochem Biophys Res Commun **176**(2): 586-92.

Eriksson, S., B. Munch-Petersen, et al. (1991). "Expression and substrate specificities of human thymidine kinase 1, thymidine kinase 2 and deoxycytidine kinase." Adv Exp Med Biol **309B**: 239-43.

Fillat, C., M. Carrio, et al. (2003). "Suicide gene therapy mediated by the Herpes Simplex virus thymidine kinase gene/Ganciclovir system: fifteen years of application." Curr Gene Ther **3**(1): 13-26.

Galmarini, C. M., L. Jordheim, et al. (2003). "Pyrimidine nucleoside analogs in cancer treatment." Expert Rev Anticancer Ther **3**(5): 717-28.

Ganter, C., Bock, A, Buckel, P, Mattes, R (1988). "Production of thermostable, recombinant alpha-galactosidase suitable for raffinose elimination from sugar beet syrup." Journal of Biotechnology **8**: 301-310.

Gerber, S. and G. Folkers (1996). "A new method for quantitative determination of tritium-labeled nucleoside kinase products adsorbed on DEAE-cellulose." Biochem Biophys Res Commun **225**(1): 263-7.

Gerth, M. L. and S. Lutz (2007). "Mutagenesis of non-conserved active site residues improves the activity and narrows the specificity of human thymidine kinase 2." Biochem Biophys Res Commun **354**(3): 802-7.

Gilbert, H. F. (1990). "Molecular and cellular aspects of thiol-disulfide exchange." Adv Enzymol Relat Areas Mol Biol **63**: 69-172.

Gill, S., R. R. Thomas, et al. (2003). "Review article: colorectal cancer chemotherapy." Aliment Pharmacol Ther **18**(7): 683-92.

Giuliano, M., C. Schiraldi, et al. (2004). "Expression of Sulfolobus solfataricus alpha-glucosidase in Lactococcus lactis." Appl Microbiol Biotechnol **64**(6): 829-32.

Gorinstein, S., I. Goshev, et al. (2000). "Intrinsic tryptophan fluorescence of human serum proteins and related conformational changes." J Protein Chem **19**(8): 637-42.

Guo, X., P. Bandyopadhyay, et al. (2008). "Partial acetylation of lysine residues improves intraprotein cross-linking." Anal Chem **80**(4): 951-60.

Hagan, R. M., J. Worner-Gibbs, et al. (2005). "Tryptophan insertion mutagenesis of liver fatty acid-binding protein: L28W mutant provides important insights into ligand binding and physiological function." J Biol Chem **280**(3): 1782-9.

Han, J. C. and G. Y. Han (1994). "A procedure for quantitative determination of tris(2-carboxyethyl)phosphine, an odorless reducing agent more stable and effective than dithiothreitol." Anal Biochem **220**(1): 5-10.

Handler, C. G., R. J. Eisenberg, et al. (1996). "Oligomeric structure of glycoproteins in herpes simplex virus type 1." J Virol **70**(9): 6067-70.

Hansen, T., B. Schlichting, et al. (2002). "Glucose-6-phosphate dehydrogenase from the hyperthermophilic bacterium Thermotoga maritima: expression of the g6pd gene and characterization of an extremely thermophilic enzyme." FEMS Microbiol Lett **216**(2): 249-53.

Hickey, A. M., L. Marle, et al. (2007). "Immobilization of thermophilic enzymes in miniaturized flow reactors." Biochem Soc Trans **35**(Pt 6): 1621-3.

Higuchi, R., B. Krummel, et al. (1988). "A general method of in vitro preparation and specific mutagenesis of DNA fragments: study of protein and DNA interactions." Nucleic Acids Res **16**(15): 7351-67.

Hiraga, S., K. Igarashi, et al. (1967). "A deoxythymidine kinase-deficient mutant of Escherichia coli. I. Isolation and some properties." Biochim Biophys Acta **145**(1): 41-51.

Hollaway, M. R. and M. J. Hardman (1973). "Evidence for a rate-limiting conformation change in the catalytic steps of the ficin and papain-catalysed hydrolyses of benzyloxycarbonyl-L-lysine p-nitrophenyl ester." Eur J Biochem **32**(3): 537-46.

Hu, C. M. and Z. F. Chang (2007). "Mitotic control of dTTP pool: a necessity or coincidence?" J Biomed Sci **14**(4): 491-7.

Huber, R., T. A. Langworthy, et al. (1986). "Thermotoga-Maritima Sp-Nov Represents a New Genus of Unique Extremely Thermophilic Eubacteria Growing up to 90-Degrees-C." Archives of Microbiology **144**(4): 324-333.

Ichikawa, E. and K. Kato (2001). "Sugar-modified nucleosides in past 10 years, a review." Curr Med Chem **8**(4): 385-423.

Ives, D. H. and S. Ikeda (1998). "Life on the salvage path: the deoxynucleoside kinase of Lactobacillus acidophilus R-26." Prog Nucleic Acid Res Mol Biol **59**: 205-55.

Johnson, H. A., W. E. Haymaker, et al. (1960). "A radioautographic study of a human brain and glioblastoma multiforme after the in vivo uptake of tritiated thymidine." Cancer **13**: 636-42.

Jordan, A., E. Torrents, et al. (1997). "B12-dependent ribonucleotide reductases from deeply rooted eubacteria are structurally related to the aerobic enzyme from Escherichia coli." Proc Natl Acad Sci U S A **94**(25): 13487-92.

Kaper, T., B. Talik, et al. (2005). "Amylomaltase of Pyrobaculum aerophilum IM2 produces thermoreversible starch gels." Appl Environ Microbiol **71**(9): 5098-106.

Karlstrom, H. O. (1970). "Inability of Escherichia coli B to incorporate added deoxycytidine, deoxyandenosine, and deoxyguanosine into DNA." Eur J Biochem **17**(1): 68-71.

Ke, P. Y. and Z. F. Chang (2004). "Mitotic degradation of human thymidine kinase 1 is dependent on the anaphase-promoting complex/cyclosome-CDH1-mediated pathway." Mol Cell Biol **24**(2): 514-26.

Keller, P. M., J. A. Fyfe, et al. (1981). "Enzymatic phosphorylation of acyclic nucleoside analogs and correlations with antiherpetic activities." Biochem Pharmacol **30**(22): 3071-7.

Knecht, W., G. E. Petersen, et al. (2002). "Deoxyribonucleoside kinases belonging to the thymidine kinase 2 (TK2)-like group vary significantly in substrate specificity, kinetics and feed-back regulation." Journal of Molecular Biology **315**(4): 529-540.

Kornberg, A. (1980). DNA replication, W.H. Freeman and company.

Kosinska, U., C. Carnrot, et al. (2007). "Structural studies of thymidine kinases from Bacillus anthracis and Bacillus cereus provide insights into quaternary structure and conformational changes upon substrate binding." Febs J **274**(3): 727-37.

Kuzin, A. P., Abashidze, M., Forouhar, F., Vorobiev, S.M., Acton, T.B., Ma, L.-C., Xiao, R., Montelione, G.T., Tong, L., Hunt, J.F. (2005). " X-ray structure of Clostridium acetobutylicum thymidine kinase with ADP.   ." Northeast Structural Genomics Target CAR26. .

Kuzin, A. P., Abashidze, M., Forouhar, F. Vorobiev, S.M., Acton, T.B., Ma, L.C., Xiao, R., Montelione, G.T., Tong, L. and Hunt, J.F. (2004). "X-ray structure of *Clostridium acetobutylicum* thymidine kinase with ADP. Northeast Structural Genomics Target Car *26*."

Lara, M. C., M. L. Valentino, et al. (2007). "Mitochondrial neurogastrointestinal encephalomyopathy (MNGIE): biochemical features and therapeutic approaches." Biosci Rep **27**(1-3): 151-63.

Leduc, D., S. Graziani, et al. (2004). "Two distinct pathways for thymidylate (dTMP) synthesis in (hyper)thermophilic Bacteria and Archaea." Biochem Soc Trans **32**(Pt 2): 231-5.

Lee, L. S. and Y. Cheng (1976). "Human deoxythymidine kinase II: substrate specificity and kinetic behavior of the cytoplasmic and mitochondrial isozymes derived from blast cells of acute myelocytic leukemia." Biochemistry **15**(17): 3686-90.

Lee, L. S. and Y. C. Cheng (1976). "Human deoxythymidine kinase. I. Purification and general properties of the cytoplasmic and mitochondrial isozymes derived from blast cells of acute myelocytic leukemia." J Biol Chem **251**(9): 2600-4.

Lehmann, M. and M. Wyss (2001). "Engineering proteins for thermostability: the use of sequence alignments versus rational design and directed evolution." Current Opinion in Biotechnology **12**(4): 371-375.

Liang, X., K. Jensen, et al. (2004). "Very efficient template/primer-independent DNA synthesis by thermophilic DNA polymerase in the presence of a thermophilic restriction endonuclease." Biochemistry **43**(42): 13459-66.

Lin, T. S., R. F. Schinazi, et al. (1987). "Potent and selective in vitro activity of 3'-deoxythymidin-2'-ene (3'-deoxy-2',3'-didehydrothymidine) against human immunodeficiency virus." Biochem Pharmacol **36**(17): 2713-8.

Lutz, S., J. Lichter, et al. (2007). "Exploiting temperature-dependent substrate promiscuity for nucleoside analogue activation by thymidine kinase from Thermotoga maritima." <u>J Am Chem Soc</u> **129**(28): 8714-5.

Lutz, S., M. Ostermeier, et al. (2001). "Rapid generation of incremental truncation libraries for protein engineering using alpha-phosphothioate nucleotides." <u>Nucleic Acids Res</u> **29**(4): E16.

Maltseva, T., E. Usova, et al. (2001). "The NMR conformation study of the complexes of deoxycytidine kinase (dCK) and 2'-deoxycytidine/2'-deoxyadenosine." <u>Nucleosides Nucleotides Nucleic Acids</u> **20**(4-7): 1225-8.

Marquez, V. E., T. Ben-Kasus, et al. (2004). "Experimental and structural evidence that herpes 1 kinase and cellular DNA polymerase(s) discriminate on the basis of sugar pucker." <u>J Am Chem Soc</u> **126**(2): 543-9.

Mathews, I. I., A. M. Deacon, et al. (2003). "Functional Analysis of Substrate and Cofactor Complex Structures of a Thymidylate Synthase-Complementing Protein." <u>Structure</u> **11**(6): 677-690.

McBreen, P., K. G. Orkwiszewski, et al. (1977). "Synteny of the genes for thymidine kinase and galactokinase in the mouse and their assignment to mouse chromosome 11." <u>Cytogenet Cell Genet</u> **19**(1): 7-13.

McDougall, J. K., R. Kucherlapati, et al. (1973). "Localization and induction of the human thymidine kinase gene by adenovirus 12." <u>Nat New Biol</u> **245**(145): 172-5.

Merrill, G. F., R. M. Harland, et al. (1984). "Genetic and physical analysis of the chicken tk gene." <u>Mol Cell Biol</u> **4**(9): 1769-76.

Mitsuya, H., K. J. Weinhold, et al. (1985). "3'-Azido-3'-deoxythymidine (BW A509U): an antiviral agent that inhibits the infectivity and cytopathic effect of human T-lymphotropic virus type III/lymphadenopathy-associated virus in vitro." Proc Natl Acad Sci U S A **82**(20): 7096-100.

Monod, J., J. Wyman, et al. (1965). "On the Nature of Allosteric Transitions: a Plausible Model." J Mol Biol **12**: 88-118.

Moolten, F. L. and J. M. Wells (1990). "Curability of tumors bearing herpes thymidine kinase genes transferred by retroviral vectors." J Natl Cancer Inst **82**(4): 297-300.

Morsomme, P., M. Chami, et al. (2002). "Characterization of a hyperthermophilic P-type ATPase from Methanococcus jannaschii expressed in yeast." J Biol Chem **277**(33): 29608-16.

Munch-Petersen, B. (1984). "Differences in the kinetic properties of thymidine kinase isoenzymes in unstimulated and phytohemagglutinin-stimulated human lymphocytes." Mol Cell Biochem **64**(2): 173-85.

Munch-Petersen, B., L. Cloos, et al. (1991). "Diverging substrate specificity of pure human thymidine kinases 1 and 2 against antiviral dideoxynucleosides." J Biol Chem **266**(14): 9032-8.

Munch-Petersen, B., W. Knecht, et al. (2000). "Functional expression of a multisubstrate deoxyribonucleoside kinase from Drosophila melanogaster and its C-terminal deletion mutants." J Biol Chem **275**(9): 6673-9.

Munch-Petersen, B., J. Piskur, et al. (1998). "Four deoxynucleoside kinase activities from Drosophila melanogaster are contained within a single monomeric enzyme, a new multifunctional deoxynucleoside kinase." J Biol Chem **273**(7): 3926-31.

Munch-Petersen, B., G. Tyrsted, et al. (1993). "Reversible ATP-dependent transition between two forms of human cytosolic thymidine kinase with different enzymatic properties." J Biol Chem **268**(21): 15621-5.

Munir, K. M., D. C. French, et al. (1992). "Permissible amino acid substitutions within the putative nucleoside binding site of herpes simplex virus type 1 encoded thymidine kinase established by random sequence mutagenesis [corrected]." J Biol Chem **267**(10): 6584-9.

Nelson, K. E., R. A. Clayton, et al. (1999). "Evidence for lateral gene transfer between Archaea and bacteria from genome sequence of Thermotoga maritima." Nature **399**(6734): 323-9.

Nishino, I., A. Spinazzola, et al. (1999). "Thymidine phosphorylase gene mutations in MNGIE, a human mitochondrial disorder." Science **283**(5402): 689-92.

Okazaki, R. and A. Kornberg (1964). "Deoxythymidine Kinase of Escherichia Coli. I. Purification and Some Properties of the Enzyme." J Biol Chem **239**: 269-74.

Okazaki, R. and A. Kornberg (1964). "Deoxythymidine Kinase of Escherichia Coli. Ii. Kinetics and Feedback Control." J Biol Chem **239**: 275-84.

Palomo, J. M., R. L. Segura, et al. (2004). "Improving the activity of lipases from thermophilic organisms at mesophilic temperatures for biotechnology applications." Biomacromolecules **5**(1): 249-54.

Perez-Perez, M. J., E. M. Priego, et al. (2008). "Structure, physiological role, and specific inhibitors of human thymidine kinase 2 (TK2): present and future." Med Res Rev **28**(5): 797-820.

Perutz, M. F. (1970). "Stereochemistry of cooperative effects in haemoglobin." <u>Nature</u> **228**(5273): 726-39.

Plagemann, P. G., R. M. Wohlhueter, et al. (1988). "Nucleoside and nucleobase transport in animal cells." <u>Biochim Biophys Acta</u> **947**(3): 405-43.

Pontarin, G., P. Ferraro, et al. (2006). "Mitochondrial DNA depletion and thymidine phosphate pool dynamics in a cellular model of mitochondrial neurogastrointestinal encephalomyopathy." <u>J Biol Chem</u> **281**(32): 22720-8.

Pontarin, G., L. Gallinaro, et al. (2003). "Origins of mitochondrial thymidine triphosphate: dynamic relations to cytosolic pools." <u>Proc Natl Acad Sci U S A</u> **100**(21): 12159-64.

Poulsen, L. L. and D. M. Ziegler (1977). "Microsomal mixed-function oxidase-dependent renaturation of reduced ribonuclease." <u>Arch Biochem Biophys</u> **183**(2): 563-70.

Prinz, W. A., F. Aslund, et al. (1997). "The role of the thioredoxin and glutaredoxin pathways in reducing protein disulfide bonds in the Escherichia coli cytoplasm." <u>J Biol Chem</u> **272**(25): 15661-7.

Robinson-Rechavi, M., A. Alibes, et al. (2006). "Contribution of electrostatic interactions, compactness and quaternary structure to protein thermostability: lessons from structural genomics of Thermotoga maritima." <u>J Mol Biol</u> **356**(2): 547-57.

Roth, D. G. and T. F. Deuel (1974). "Stability and regulation of phosphoribosyl pyrophosphate synthetase from rat liver." <u>J Biol Chem</u> **249**(1): 297-301.

Russell, R. J. M. and G. L. Taylor (1995). "Engineering thermostability: lessons from thermophilic proteins." <u>Current Opinion in Biotechnology</u> **6**(4): 370-374.

Sabini, E., S. Ort, et al. (2003). "Structure of human dCK suggests strategies to improve anticancer and antiviral therapy." Nat Struct Biol **10**(7): 513-9.

Saiki, R. K., D. H. Gelfand, et al. (1988). "Primer-directed enzymatic amplification of DNA with a thermostable DNA polymerase." Science **239**(4839): 487-91.

Samain, E., P. Debeire, et al. (1997). "High level production of a cellulase-free xylanase in glucose-limited fed batch cultures of a thermophilic Bacillus strain." J Biotechnol **58**(2): 71-8.

Sandrini, M. P., A. R. Clausen, et al. (2006). "Thymidine kinase diversity in bacteria." Nucleosides Nucleotides Nucleic Acids **25**(9-11): 1153-8.

Sandrini, M. P. and J. Piskur (2005). "Deoxyribonucleoside kinases: two enzyme families catalyze the same reaction." Trends Biochem Sci **30**(5): 225-8.

Schelling, P., G. Folkers, et al. (2001). "A spectrophotometric assay for quantitative determination of kcat of herpes simplex virus type 1 thymidine kinase substrates." Anal Biochem **295**(1): 82-7.

Segura-Pena, D., J. Lichter, et al. (2007). "Quaternary structure change as a mechanism for the regulation of thymidine kinase 1-like enzymes." Structure **15**(12): 1555-66.

Segura-Pena, D., S. Lutz, et al. (2007). "Binding of ATP to TK1-like enzymes is associated with a conformational change in the quaternary structure." J Mol Biol **369**(1): 129-41.

Skovgaard, T. and B. Munch-Petersen (2006). "Purification and characterization of wild-type and mutant TK1 type kinases from Caenorhabditis elegans." Nucleosides Nucleotides Nucleic Acids **25**(9-11): 1165-9.

Spinazzola, A., F. Invernizzi, et al. (2008). "Clinical and molecular features of mitochondrial DNA depletion syndromes." <u>J Inherit Metab Dis</u>.

Spyrou, G. and P. Reichard (1988). "Dynamics of the thymidine triphosphate pool during the cell cycle of synchronized 3T3 mouse fibroblasts." <u>Mutat Res</u> **200**(1-2): 37-43.

Ter-Pogossian, M. M., M. E. Phelps, et al. (1975). "A positron-emission transaxial tomograph for nuclear imaging (PETT)." <u>Radiology</u> **114**(1): 89-98.

Vernis, L., J. Piskur, et al. (2003). "Reconstitution of an efficient thymidine salvage pathway in Saccharomyces cerevisiae." <u>Nucleic Acids Res</u> **31**(19): e120.

Wang, J., D. Choudhury, et al. (1999). "Stereoisomeric selectivity of human deoxyribonucleoside kinases." <u>Biochemistry</u> **38**(51): 16993-9.

Wang, L., B. Munch-Petersen, et al. (1999). "Human thymidine kinase 2: molecular cloning and characterisation of the enzyme activity with antiviral and cytostatic nucleoside substrates." <u>FEBS Lett</u> **443**(2): 170-4.

Wang, S., W.-F. Liu, et al. (2008). "Multistate folding of a hyperthermostable Fe-superoxide dismutase (TcSOD) in guanidinium hydrochloride: The importance of the quaternary structure." <u>Biochimica et Biophysica Acta (BBA) - Proteins & Proteomics</u> **1784**(3): 445-454.

Warren, P., W. Song, et al. (2002). "Combined HSV-TK/GCV and secondary lymphoid tissue chemokine gene therapy inhibits tumor growth and elicits potent antitumor CTL response in tumor-bearing mice." <u>Anticancer Res</u> **22**(2A): 599-604.

Watson, J. D. and F. H. Crick (1953). "Molecular structure of nucleic acids; a structure for deoxyribose nucleic acid." <u>Nature</u> **171**(4356): 737-8.

Welin, M., U. Kosinska, et al. (2004). "Structures of thymidine kinase 1 of human and mycoplasmic origin." <u>Proc Natl Acad Sci U S A</u> **101**(52): 17970-5.

Willecke, K., T. Teber, et al. (1977). "Human mitochondrial thymidine kinase is coded for by a gene on chromosome 16 of the nucleus." <u>Somatic Cell Genet</u> **3**(3): 237-45.

Woo, H. J., M. M. Lotz, et al. (1991). "Carbohydrate-binding protein 35 (Mac-2), a laminin-binding lectin, forms functional dimers using cysteine 186." <u>J Biol Chem</u> **266**(28): 18419-22.

Wootton, S. K. and D. Yoo (2003). "Homo-oligomerization of the porcine reproductive and respiratory syndrome virus nucleocapsid protein and the role of disulfide linkages." <u>J Virol</u> **77**(8): 4546-57.

Wurth, C., R. M. Thomas, et al. (2001). "Folding and self-assembly of herpes simplex virus type 1 thymidine kinase." <u>J Mol Biol</u> **313**(3): 657-70.

Yang, S. Q., Q. J. Yan, et al. (2006). "High-level of xylanase production by the thermophilic Paecilomyces themophila J18 on wheat straw in solid-state fermentation." <u>Bioresour Technol</u> **97**(15): 1794-800.

Yengo, C. M., L. Chrin, et al. (1999). "Intrinsic tryptophan fluorescence identifies specific conformational changes at the actomyosin interface upon actin binding and ADP release." <u>Biochemistry</u> **38**(44): 14515-23.

Ying, X., A. M. Grunden, et al. (2008). "Molecular characterization of the recombinant iron-containing alcohol dehydrogenase from the hyperthermophilic Archaeon, Thermococcus strain ES1." <u>Extremophiles</u>.

Zhou, Y. H., X. P. Zhang, et al. (1991). "Random mutagenesis of gene-sized DNA

    molecules by use of PCR with Taq DNA polymerase." Nucleic Acids Res **19**(21):

    6052.

Zhu, C., L. S. Harlow, et al. (2006). "Effect of C-terminal of human cytosolic thymidine

    kinase (TK1) on in vitro stability and enzymatic properties." Nucleosides

    Nucleotides Nucleic Acids **25**(9-11): 1185-8.